Studies on the Protein Components of Biotin Synthase

Lisa McIver

PhD

The University of Edinburgh

2000

Declaration

I, Lisa McIver, hereby certify that this thesis has been composed by myself, that it is a record of my work, and that it has not been accepted in partial or complete fulfilment of any other degree or professional qualification.

Acknowledgements

I would like to acknowledge Dr Robert Baxter for the opportunity to carry out this PhD and I would like to thank him for his continued support and supervision. I would also like to thank both Dr Dominic Campopiano and Dr Andrew Munro for their guidance, encouragement and advice during the course of this work.

Without the following this work would not have been completed and I would like to thank them.

Professor Stephen Chapman for help and advice and in whose laboratory the experiments for chapter 3 were acomplished with the help of Dr Simon Daff.

Dr Scott Webster, Dr Lu Jiang and Brian Whigham who were responsible for the mass spectrometry.

The analytical ultracentrifugation work was done with Dr Olwyn Byron (Glasgow University).

The circular dichroism experiments were carried out with Dr Sharon Kelly (Stirling University).

Nicola Preston was responsible for the DNA sequencing and Andrew Cronshaw the N-terminal protein sequencing.

Dr Rhodri Thomas for the ICP-AES.

Finally, the Baxter group, the Chemistry department and KBH (past and present) especially Nik, P, Janet, Claire, Gill, Vern, Mikee, Tom, Donald, Jo, Mike and Mags.

Abstract

The genes encoding the *E. coli* flavodoxin $NADP^+$ oxidoreductase (FLDR) and flavodoxin (FLD) have been overexpressed in *E. coli* and the gene products purified to homogeneity. Physical characterisation of both proteins was carried out using steady-state and stopped flow kinetics, circular dichroism and fluorimetric studies. The molecular masses of the apoproteins were determined as 27648Da and 19606Da and the isolectric points as 4.8 and 3.5, respectively. The midpoint reduction potentials of the oxidised/semiquinone and semiquinone/hydroquinone couples of both FLDR (-308mV and -268mV) and FLD (-254mV and -433mV) were measured using redox potentiometry. This confirms the electron-transfer route as NADPH → FLDR → FLD. Binding of 2′ adenosine monophosphate increases the midpoint reduction potentials for both FLDR couples. These data highlight the strong stabilization of the flavodoxin semiquinone with respect to the hydroquinone state and indicate that FLD must act as a single electron shuttle from the semiquinone form in its support of cellular functions. FLDR and FLD were covalently crosslinked using 1-ethyl-3(dimethylamino-propyl) carodiimide. A single species was formed with an apparent molecular weight of 47kD. This complex was catalytically active in that it could reduce cytochrome *c* and potassium ferricyanide almost as efficiently as the individual proteins.

The gene encoding *E. coli* biotin synthase (*bio*B) has been expressed as a histidine-fusion protein and the protein purified in a single step using IMAC. The His_6-tagged protein was fully functional in *in vitro* and *in vivo* biotin production assays. Analysis of all the published *bio*B sequences identified a number of conserved residues. Single point mutations, to either serine or threonine, were carried out on the four conserved (Cys-53, Cys-57, Cys-60 and Cys-188) and one non-conserved (Cys-288) cysteine residues and the purified mutant proteins tested both for ability to reconstitute the [2Fe-2S] clusters of the native (oxidised) dimer and enzymatic activity. The C188S mutant was insoluble. The wild-type and four of the mutant proteins were characterised by UV-visible spectroscopy, metal and sulfide analysis and both *in vitro* and *in vivo* biotin production assays. The molecular masses of all proteins were verified using electrospray mass spectrometry. The results indicate that the His_6-tag and the C288T mutation have no effect on the activity of biotin synthase when compared to the wild-type protein. We conclude that three of the conserved cysteine residues (Cys-53, Cys-57 and Cys-60), all of which lie in the highly conserved 'cysteine-box' motif, are absolutely crucial for Fe-S cluster binding whereas Cys-188 plays a unknown structural role in biotin synthase.

Abbreviations

AB – ammonium bicarbonate buffer

ACP – acyl carrier protein

AgCl – silver chloride

AMP – adenosine monophosphate

AON – 8-amino 7-oxononanoate

AONS – 8-amino 7-oxononanoate synthase

ARR – anaerobic ribonucleotide reductase

ARR-AE – anaerobic ribonucleotide reductase activating enzyme

ATP – adenosine 5'-triphosphate

AUC – analytical ultracentrifugation

BCCP – biotin carboxyl carrier protein

bp - base pair

CD – circular dichroism

CO_2 – carbon dioxide

CoA – coenzyme A

CV - Column volume

Da – Daltons

DAN – 7,8-diaminononanoate

DANS – 7,8-diaminononanoate synthase

DNA – deoxyribonucleic acid

DOA – deoxyadenosyl

DOA$^{\bullet}$ - deoxyadenosy radical

DTB – dethiobiotin

DTBS – dethiobiotin synthase

DTT – Dithiothreitol

E_1' – oxidised / semiquinone redox couple

E_2' – semiquinone / hydroquinone redox couple

EDTA – ethylene diaminetetracetic acid

FAD – flavin adenine dinucleotide

Fe - iron

FLD - *E. coli* Flavodoxin

FLDR - *E. coli* Flavodoxin (ferredoxin) $NADP^+$ oxidoreductase

FMN – flavin mononucleotide

GdnHCl – Guanidine hydrochloride

His_6 - six consecutive histidine residues

HPLC – high pressure liquid chromatography

hq - hydroquinone

ICP-AES - Inductively coupled plasma - atomic emission spectroscopy

IMAC - Immobilised metal affinity chromatography

IPTG - Isopropyl - β, D - thiogalactopyranoside

LAM - lysine 2,3-aminomutase

LB – Luria Bertani medium

Mg - magnesium

NADPH – nicotinamide adenine dinucleotide phosphate

ox - oxidised

P450 – cytochrome P450 reductase

PCR – polymerase chain reaction

PEG – polyethylene glycol

PFL - pyruvate formate lyase

PFL-AE - pyruvate formate lyase activating enzyme

PLP – pyridoxal phosphate

Pt – platinum

RNA – ribonucleic acid

SAM - S -Adenosyl methionine

SDS PAGE - sodium dodecyl sulphate polyacrylamide gel electrophoresis

SE – sedimentation equilibrium

sq – semiquinone

SV – sedimentation velocity

TAE – Tris acetate EDTA

TB – transformation buffer

TCA - Trichloroacetic acid

TFA - Trifluoroacetic acid

Tris – Tris [hydroxymethyl] aminomethane

Table of Contents

List of Figures

Chapter 1: Introduction

Chapter 3: Characterisation of FLDR and FLD

Chapter 4: Characterisation of wild-type and mutant biotin synthases

List of Tables

Chapter 1: Introduction

Chapter 3: Characterisation of FLDR and FLD

Chapter 4: Characterisation of wild-type and mutant biotin synthases

Chapter 1: Introduction

1.1 An introduction to biotin

In 1901 Wildiers discovered that a substance obtained from beer wort, which he termed bios, stimulated the growth of yeasts (1). Over thirty years later Williams found that bios was a mixture of biotin, alanine, myoinositol and pantothenic acid (2). Biotin itself was found to be identical to "protective factor x" and "vitamin H" which had been previously isolated from mammalian livers (3). This factor was found to protect rats from the pathological effects of the ingestion of dried egg whites. Pure biotin was finally isolated, as its methyl ester from dried egg yolks by Kögl. Biotin has since been found to be an essential vitamin for all animals and humans. It is produced in minute quantities by bacteria, plants and yeast. Although, it is found in minute quantities in the majority of foodstuffs (egg yolk being the exception containing ~50μg/100g) and the recommended daily amount (*ca.* 300μg/day) is normally in a balanced diet and synthesised by intestinal microflora. Biotin has an extremely important role in animal nutrition and also in biotechnology.

1.1.1 Structure and properties

Kögl (4) established the empirical formula of biotin methyl ester as $C_{11}H_{18}O_3N_2S$ in 1936 but it was not until 1942 that the structure of biotin was elucidated by du Vigneaud *et al.* (5). The first of many chemical syntheses of the vitamin was described by Harris a year later (6). Biotin is a water soluble vitamin which X-ray studies have shown consists of an imidazolidone ring fused in the *cis* confirmation to a tetrahydrothiophene ring with a valeryl side chain (Figure 1-1). The molecule contains 3 asymmetric carbons and so has eight optically active forms. Only one form, D-(+)-biotin, is biologically active. Currently biotin is made using an expensive, laborious twelve step chemical synthesis originally developed by Roche (7) although significant improvements have been made by workers at Lonza AG (8). Demand for the vitamin is such that there is currently intense effort to develop a biotechnological route to the product.

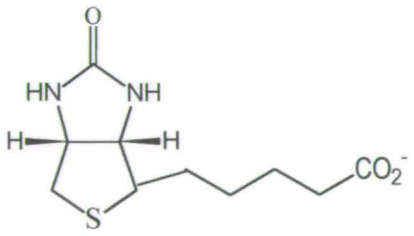

Figure 1-1

D-(+)-biotin consists of an imidazolidone ring fused in the *cis* configuration to a tetrahydrothiophene ring with a valeryl side chain.

1.1.2 The role of biotin as a coenzyme

Biotin is the cofactor in a number of enzymatic carboxylation reactions where it acts as a carrier of activated CO_2 (9). Enzymes which use biotin are involved in a variety of physiological processes such as fatty acid synthesis and gluconeogenesis. These enzymes fall into three categories shown in Table 1-1. Class I enzymes are carboxylases which transfer carbon dioxide as derived from hydrogen carbonate to acceptors. The substrate is carboxylated in two reversible steps. First, a carboxybiotin intermediate is formed at the expense of an adenosine 5′-triphosphate (ATP) molecule. The fact that N-1 was carboxylated in the enzyme-biotin complex presented an interesting mechanistic problem. A stepwise mechanism has been proposed where bicarbonate is phosphorylated by ATP to form carboxyphosphate. This is then attacked by the N-1 nitrogen to yield carboxybiotin (10) (11). The activated CO_2 is then transferred to the substrate to form the product (12). Substrates bind to the enzyme and are released in a specific sequence. The mechanism is "ping-pong", where one or more of the products are released before all the substrates are bound. Enzymes in class II are transcarboxylases and class III enzymes are decarboxylases which decarboxylate β-keto esters and their thioesters (13). In class II and III reactions ATP is not required and active CO_2 is transferred from either an acyl derivative or an α or β keto ester to the biotin enzyme (14). Pyruvate carboxylase, acetyl-CoA carboxylase, propionyl-CoA carboxylase and 3-methylmalonyl-CoA carboxylase are the only biotin enzymes so far found in human, animal and higher plant tissues.

Acetyl-CoA carboxylase from *E. coli* has been studied in detail and it has been found to consist of three subunits that catalyse the partial reactions (Figure 1-2) (15).

Subunit 1: The biotin carboxyl carrier protein (BCCP) is a 22kDa monomeric protein which contains the biotin molecule covalently linked to the ε-nitrogen atom of a lysine residue through an amide bond (16). This linkage has been found in all biotin enzymes studied to date.

Subunit 2: The 100kDa biotin carboxylase subunit catalyses the first step which is the ATP-dependent carboxylation of the N1 nitrogen atom of biotin to form carboxybiotin.

Subunit 3: The carboxy-transferase subunit (90kDa) which takes the carboxyl group from biotin to acetyl Coenzyme-A.

The length and flexibility of the link between biotin and its carrier protein enables the activated CO_2 group to move from one active site to another in the enzyme complex (15).

Table 1.1 The enzymes that use biotin

Class	Enzyme	Reaction catalysed	Biochemical role
I Carboxylases	Pyruvate carboxylase	Pyruvate to oxaloacetate	Gluconeogenesis, lipogenesis
	Acetyl Co-A carboxylase	Acetyl CoA to malonyl CoA	Fatty acid biosynthesis
	Propionyl-CoA carboxylase	Propionyl CoA to methylmalonyl CoA	Proprionate metabolism
	3-Methylcrotonyl-CoA carboxylase	3-Methylcrotonyl CoA to 3-methylglutaconyl CoA	Catabolism of leucine
	Geranyl-CoA carboxylase	Geranyl CoA to carboxygeranyl CoA	Microbial catabolism of isoprenoid compounds
	Urea carboxylase	Urea to N-carboxyurea	Bacterial catabolism of urea in microbes that lack urease and grow on urea as a sole source of carbon
II. Trancarboxylases	Methylmalonyl-CoA carboxyltransferase	Methylmalonyl CoA and pyruvate to oxaloacetate and propionyl CoA	Fermentation of certain carbohydrates to propionate in propionibacteria
III. Decarboxylases	Methylmalonyl-CoA decarboxylase	Methylmalonyl CoA to propionyl CoA and CO_2	Last step in lactate fermentation in *Micrococcus lactis*
	Oxaloacetate decarboxylase	Oxaloacetate to pyruvate a and CO_2	Inducible enzyme in *Aerobacter aerogenes* challenged to grow on citrate as a carbon source

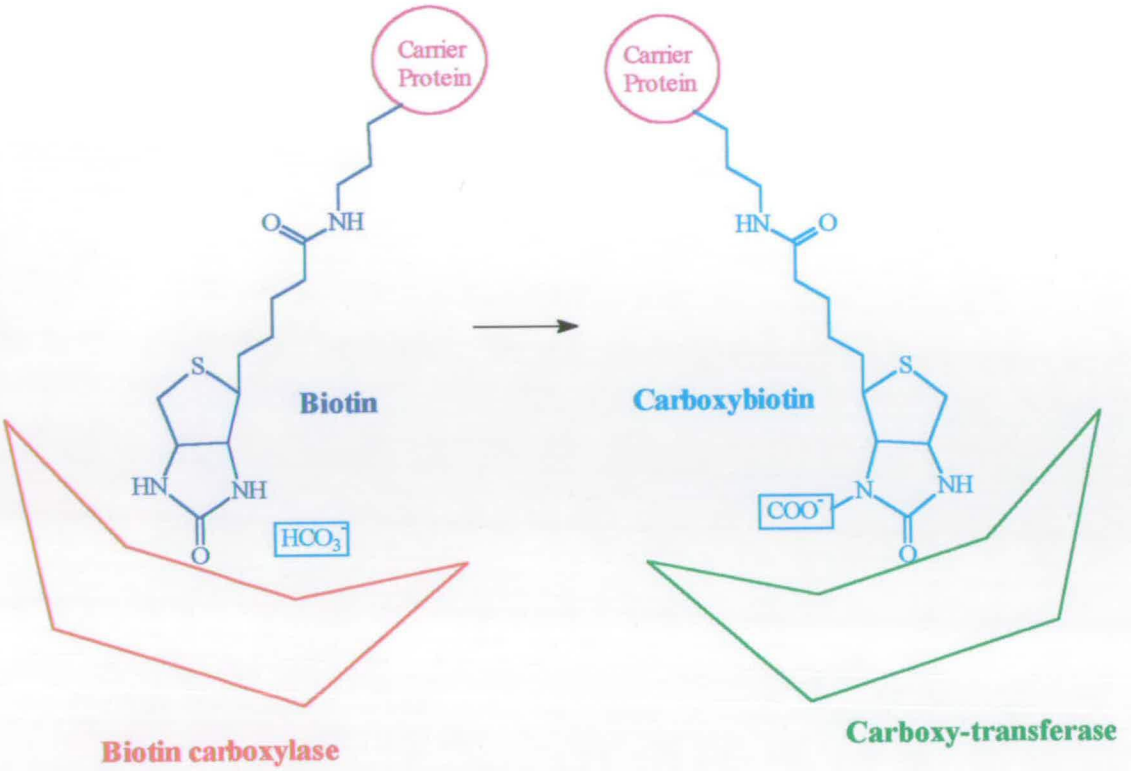

Figure 1-2

E.coli acetyl-CoA carboxylase consists of three subunits; the biotin carboxyl carrier protein subunit (22kDa) which links to the biotin molecule, the biotin carboxylase (100kDa) subunit which carboxylates biotin and the carboxyl-transferase (90kDa) subunit which transfers the carboxyl group from biotin to acetyl CoA (15).

1.1.3 Biotin binding proteins

Several proteins which bind to biotin have been identified with the most well known being the egg white glycoprotein, avidin (17) and streptavidin which has been isolated from *Streptomyces avidinii* (18). Avidin and streptavidin are 70kDa proteins which are tetramers of identical (17.5kDa) subunits, each of which is folded into an eight-stranded antiparallel β-barrel. Biotin binds at one end of this barrel in a pocket between two tryptophan residues (19). The interaction of biotin with avidin is one of the strongest protein-ligand complexes known with a $K_d = 10^{-15}$M. The binding is highly specific and can withstand extremes of pH, buffer salts and chaotrophic agents and has thus provided researchers with a unique tool for use in receptor studies, drug delivery, immunological staining and protein isolation. Avidin and streptavidin may also act as inhibitors of biotin uptake and of biotin requiring enzymes since they can complex both free and enzyme-bound biotin *in vivo* (3).

1.1.4 The biochemical and pathological effects of the deficiency of biotin

Biotin deficiency can result from long term antibiotic therapy which destroys the gut microflora leading to insufficient biotin being produced (20) and also from the excessive ingestion of raw eggs. A lack of biotin causes a reduction in all activites of biotin-dependent enzymes. Indirect effects include impairment of protein synthesis and inhibition of RNA synthesis. The resultant physiological effects in mammals include progressive ataxia, dermatitis, alopecia, skin lesions, nausea and metabolic acidosis. These symptoms can be readily relieved by supplementing the diet with biotin.

1.2 The Biosynthesis of Biotin

Current evidence suggests that the biosynthesis of biotin occurs by similar pathways in both microorganisms and higher plants (21) . However the majority of studies have been carried out in *Bacillus sphaericus* and *E. coli*.

1.2.1 The biotin operon

The biotin (*bio*) operon of *E. coli* has been extensively studied. Early work by del Campillo Campbell and Rolfe led to the discovery of the genes it encodes (22, 23). The 5.8 kilobase *bio* operon is located at 17 minutes on the *E. coli* genetic map between the attachment site of λ prophage (*attλ*) and the *uvrB* gene (24). Complementation analysis of biotin mutants indicated that the operon was composed of five genes *bioA, bioB, bioC, bioD* and *bioF* which code for the principal enzymes of biotin biosynthesis (25, 26). An unlinked gene *bio*H has also been discovered but as yet its function is unknown (27). Although current evidence suggests that it may be an acyl carrier protein (ACP) (28). Eisenberg subsequently identified two addition biotin genes; *bioP*, a permeability gene and *bioR*, a regulatory gene (29). Barker and Campbell also identified a gene known as *birA* and it is now known that this is the same as *bioR* which had previously been described by Eisenberg (30). The function of *birA*, now known to encode the *E. coli* biotin holoenzyme is described in section 1.2.2. Deletion mapping was used to determine the gene order of the operon (Figure 1-3) (25, 31). Guha *et al.* (32) determined the positions of the operator and the promoter and concluded that the operon was divergently transcribed. The four genes *bioB, F, C* and *D* are transcribed as a unit from left to right and the *bioA* gene from right to left, from a complex promoter/operator region located between *bioA* and *bioB*. Sequencing of this regulatory region has shown that the *bioA* and *bioB* promoters overlap and are situated face to face. An unusually large imperfect palindrome was identified as the single operator site and it was found to overlap the two

promoters. Both promoters have the typical Pribnow box and -35 sequences similar to those in other bacterial promoter sequences (33).

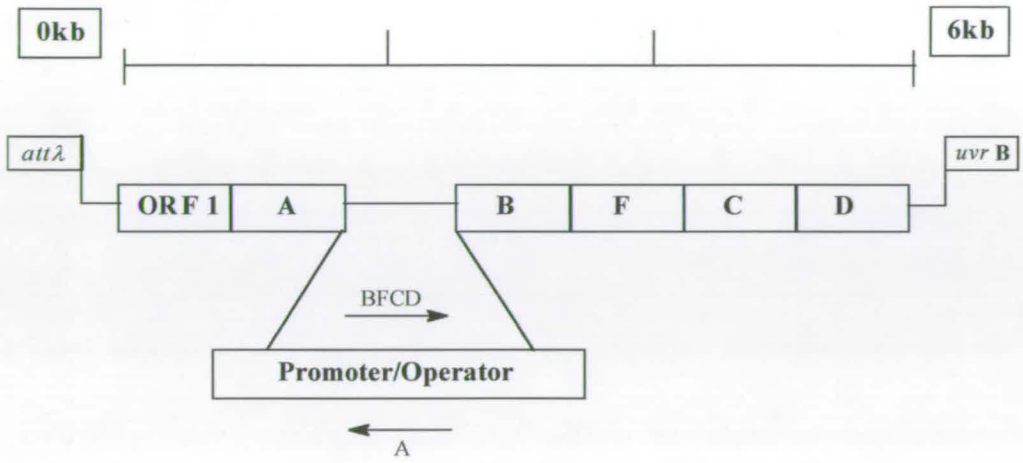

Figure 1-3

The *E.coli* bio operon is divergently transcribed with the *BioB*, *BioF*, *BioC* and *BioD* genes being transcribed from left to right and the *BioA* gene from right to left; the function of ORF1 is not known.

Another biotin gene has been described in *Sinorhizobium meliloti* which is a N_2-fixing root bacteria. *BioS* is a biotin-inducible gene which encodes a 35kDa protein. The BioS protein has predicted structural motifs similar to that of the LysR- type regulators and this indicates that it may have a regulatory role (34).

1.2.2 Regulation of biotin biosynthesis

The earliest evidence for control of biotin biosynthesis in *E. coli* was discovered by Pai and Lichstein who noted that biotin production decreased with the increased biotin concentration in the growth media (35). The nature of this inhibition was found to be repression rather than feedback inhibition (36). Thus, the classic model of Jacob and Monod for regulation of an operon by repression can be applied to the biotin operon (37). Regulation of gene expression is now known to involve the protein BirA which is a 321 amino acid protein with a molecular weight of *ca.* 35.3kDa. BirA is a bifunctional protein serving both as the biotin activating enzyme and as a transcriptional regulator (38). It converts biotin to biotinoyl-AMP (using ATP) and biotinoyl-AMP is the activated form required for ligation of biotin to the BCCP. The intermediate in this reaction, the BirA-biotinoyl-AMP complex functions as a co-repressor. It binds to the 40 base pair *bio* operator, repressing transcription of the biotin biosynthetic genes. Thus BirA synthesises its own co-repressor ligand, a unique property

among DNA binding proteins. Howard *et al.* sequenced the *birA* gene and suggested that it has a helix-loop-helix domain similar to other DNA binding proteins (39). The crystal structure of BirA was published in 1992 by Wilson *et al* (40) and confirmed this proposal. The expression of biosynthetic enzymes and the *de novo* synthesis of biotin is thus dependant on the intracellular biotin concentration and the concentration of unbiotinylated carrier protein. When the concentration of biotin in the cell is low, no BirA-biotinoyl-AMP can accumulate because biotinoyl-AMP is being consumed in the biotinylation of the acceptor protein. In this case transcription of the biotin genes is maximal. When the cellular concentration of biotin is high, the BirA-biotinoyl-AMP complex concentration is increased and this binds to the operator preventing transcription.

1.3 The Biotin Biosynthetic Pathway in Eukaryotes

Biotin is synthesised in higher plants and the pathway appears to involve similar enzymes to those found in bacteria. Baldet has described the presence of free and bound plant derived biotin in green peas (41). The bound biotin appears to be associated with the soluble fractions of the chloroplasts and mitochondria as would be expected from its function as a "CO_2 carrier". Baldet *et al.* also investigated and identified the intermediates of biotin biosynthesis in lavender cells (21). They found that an unknown stable intermediate accumulated and when this was analysed it was found to coelute with 9-mercaptodethiobiotin on HPLC. They suggest that dethiobiotin (DTB) may be converted to biotin *via* this intermediate. Baldet and Weaver (42) have isolated the cDNA which encodes the *Arabadopsis thaliana bioB* gene. The predicted *bioB* gene product (from cDNA sequencing) shows specific homology with the *bioB* gene products of numerous bacteria. In 1997 this protein was overexpressed and purified. It was found to be reddish in colour, dimeric (100kDa) and had the spectral characteristics of a 2Fe-2S protein (43). Although this data and the recent identification of the *bioB* gene in *Saccharomyces cerevisiae* (44) indicates that a functional eukaryotic pathway similar to the bacterial pathway exists, little more is known of the eukaryotic synthesis of biotin.

1.4 The Biotin Biosynthetic Pathway in Prokaryotes

The currently accepted pathway for the biosynthesis of biotin in *E. coli* was proposed by Eisenberg (13) (Figure 1-4). It now appears that the main steps in this pathway are ubiquitous in bacteria (45).

1.4.1 The first step

Pimelic acid was identified as the first biotin precursor and in *B. sphaericus* this is converted to pimeloyl CoA by pimeloyl-CoA synthase in the presence of HSCoA, ATP and Mg^{2+} (46). This is not the case in *E. coli* where ^{13}C labelling studies by the groups of Ifuku and Sanyal have suggested that pimeloyl-CoA is produced directly from a malonyl-CoA starter unit by a pathway similar to that of fatty acid and polyketide synthesis (47, 48). Lemoine *et al.* have suggested that in *E. coli* BioC catalyses the stepwise condensation of the malonyl-CoA starter by the addition of acetate units from malonyl groups in a similar way to that of chalcone synthase (49). They also propose a role for BioH in that it can transfer pimeloyl from the active cysteinyl residue of BioC directly to CoA, preventing the accumulation of free pimelate inside the cells. Studies in our laboratory have found that when BioH is overexpressed and purified 99% of the protein has the expected molecular weight of 28505Da and 1% has a molecular weight that is 340Da higher. We think that this is a phosphopantothein molecule that has been added as a post translational modification (28). However, the function of the *E. coli* bioC gene, thought to encode a pimeloyl CoA synthase, is unknown. Attempts to express this protein give only insoluble products.

1.4.2 8-Amino-7-oxononanoate synthase

The next step in the pathway is the condensation of L-alanine with pimeloyl-CoA to give 8-amino-7-oxononanoate (AON). This reaction is catalysed by 8-amino-7-oxononanoate synthase (AONS) which is the product of the *bioF* gene. The predicted size of the *E. coli* enzyme is 41599Da (384 amino acids). This enzyme has an absolute requirement for pyridoxal phosphate (PLP) as a cofactor. The *bio*F gene from *B. sphaericus* has been cloned and the AONS overexpressed in *E. coli* (50). Recently the structure of *E.coli* AONS (PDB 1BSO) has been determined by Alexeev *et al.* (Figure 1-5) (51). The enzyme is a homodimer and its structure is typical of a type II aminotransferase. The dimer has two active sites whose identical residues are contributed from each monomer. Each monomeric unit has three domains, the N-terminal domain which wraps around the opposing monomers, a large central domain and the C-terminal domain. The active site is a cleft between the two latter domains with PLP attached to lysine 236.

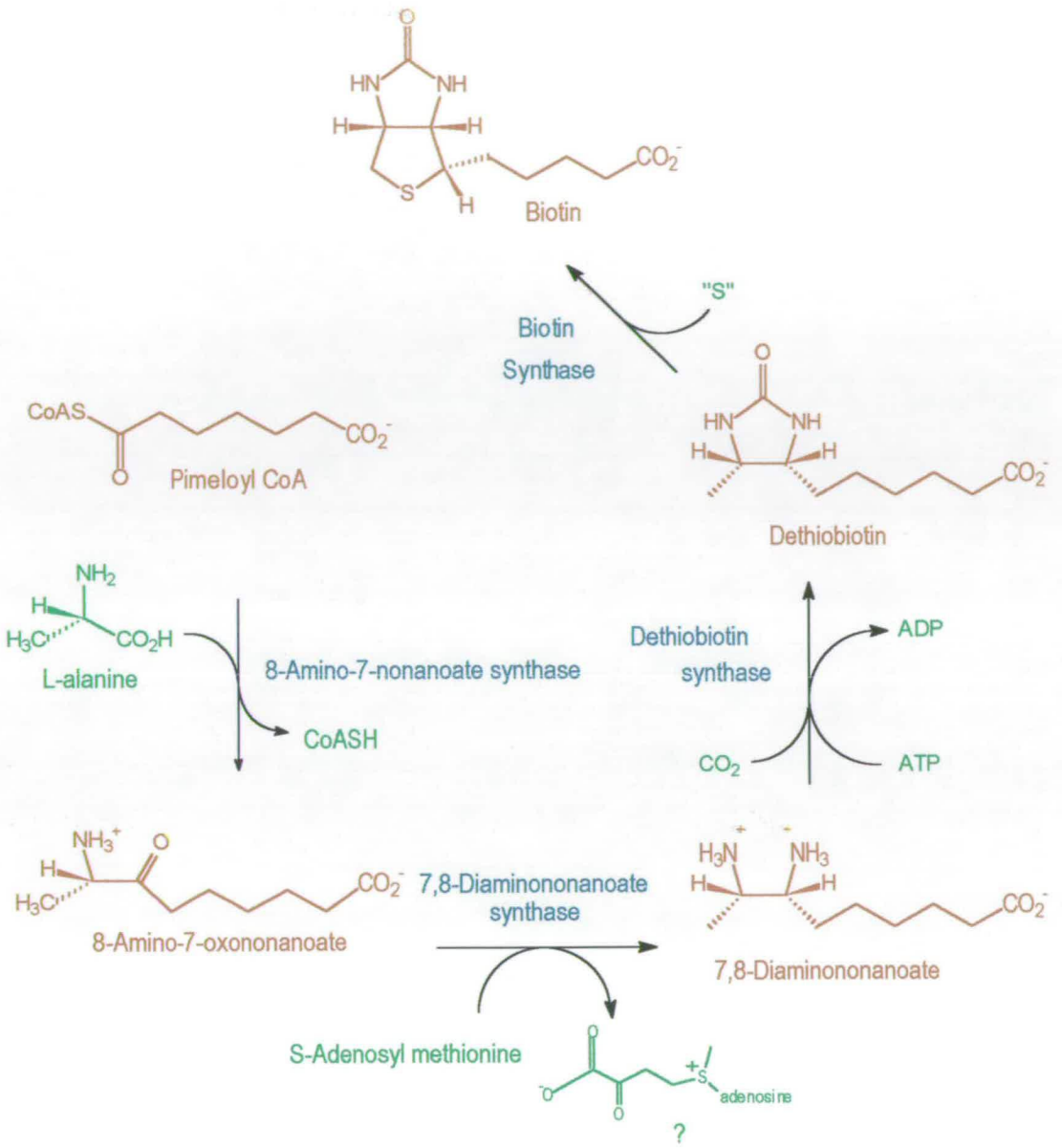

Figure 1-4

The *E.coli* biotin biosynthetic pathway; 8-Amino-7-oxononanoate (41599Da) is the product of the *BioF* gene, 7,8-diaminononanoate (47403Da) is the *BioA* gene product, dethiobiotin synthase (23917kDa) is the *BioD* gene product and biotin synthase (38648Da) is the *BioB* gene product.

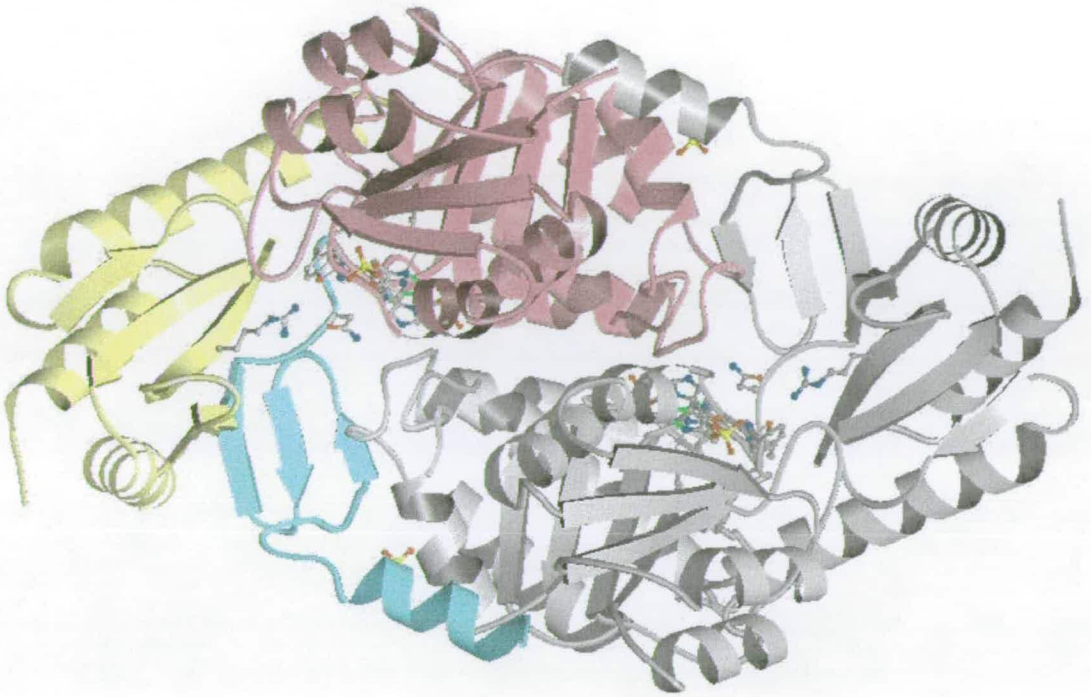

Figure 1-5

The structure of 8-amino-7-oxononanoate synthase (PBD 1BSO). The enzyme fold (dimer shown) is similar to that of a type II aminotransferase. The N-terminal domain (turquoise) wraps around the opposing monomer. The active site cleft is between the large domain (purple) and the C-terminal domain (yellow) (51).

1.4.3 7,8-Diamononanoate synthase

Transamination of AON by the enzyme 7,8-diamononanoate synthase (DANS), the product of the *bio*A gene, then leads to the formation of 7,8-diamononanoate (DAN). Studies by Pai showed that ATP, Mg^{2+} and PLP are required for this reaction. Methionine was originally suggested to be the amino donor (52) but it was subsequently shown that S-adenosyl methionine (SAM) is the actual substrate. DANS has been purified and has been shown to be a dimer with each subunit being 430 amino acids (47403Da) and it is unique in its absolute requirement for SAM as an amino donor. The structure of DANS has recently been solved both by Lindqvist (53) and Alexeev (54) at the University of Edinburgh (Figure 1-6). The

structure of DANS is very similar to that of AONS in that it is also similar to a type II aminotransferase with three domains in each monomer. The PLP is attached to lysine 274 and there are two structural sodium atoms on the surface of each monmer.

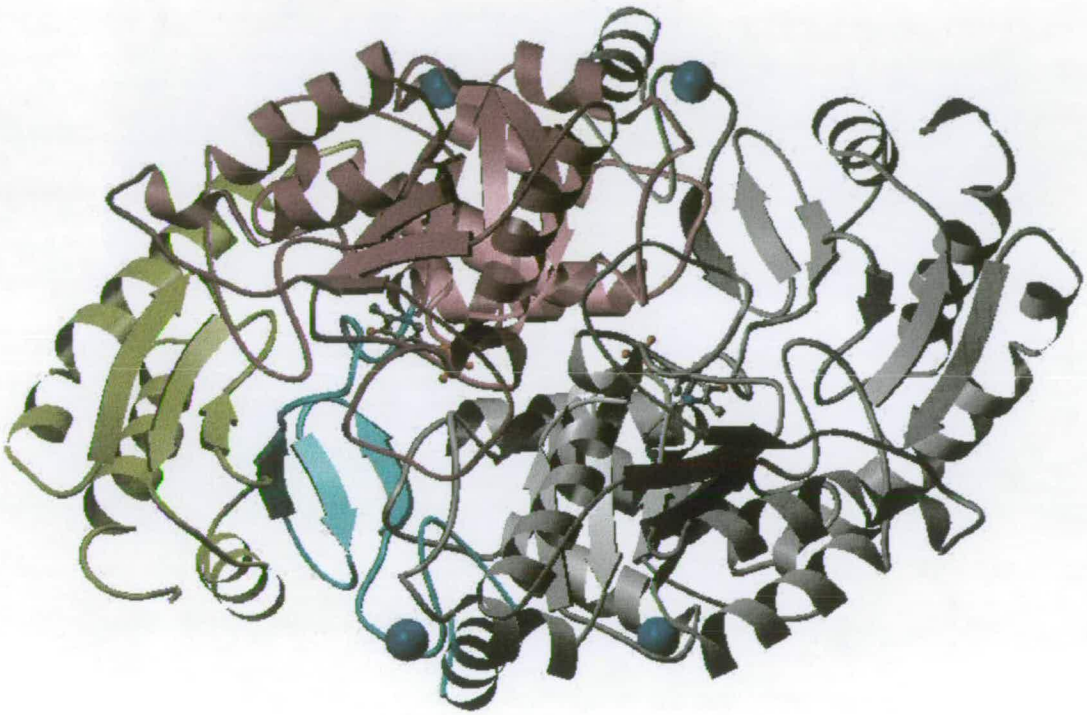

Figure 1-6

The atomic structure of 7,8-diaminononanoate synthase. The enzyme structure (dimer shown) is typical of that of a type II aminotransferase. The N-terminal domain (turquoise) wraps around the opposing monomer. The active site cleft is between the large domain (purple) and the C-terminal domain (yellow). Two structural sodium atoms are present in each monomer (shown in blue). The structure shown is that determined by Alexeev (54).

1.4.4 Dethiobiotin synthetase

The next step in the biosynthesis involves CO_2 insertion into DAN catalysed by the *bioD* gene product, DTB synthetase (DTBS), to produce DTB. This reaction requires ATP and Mg^{2+} (55). Paradoxically, DTBS is a virtually unique CO_2 utilising enzyme in that it does not involve biotin as a prosthetic group. The gene sequence was first deduced by Otsuka *et al.*

(56) and was later corrected by Alexeev *et al.* (57). This encodes a 224 amino acid protein, the N-terminal methionine being cleaved by a post-translational process. The sequence has now been verified by C- and N-terminal sequencing of the protein and confirmed by laser desorption mass spectrometry. The native enzyme has been purified and has been shown to be a homodimer with a monomeric molecular weight of 238917Da (55). DTBS shows little homology with other proteins with the exception of the related proteins from *Serratia marcescens* (58) and *B. sphaericus* (59) with which it shares 70.2% and 49% amino acid sequence identity respectively, assuming conservative substitutions. The crystallisation and structure of cloned *E. coli* DTBS has been reported (Figure 1-7) (60, 61). The 3D structure of the enzyme has been solved to 1.6 Å resolution (PDB 1DAD). Each monomer subunit has a seven stranded parallel β-sheet surrounde by helices. This sheet contains the classic mononucleotide binding motif with the fingerprint peptide Gly, X_5, Gly, Lys, Thr. The sequence of steps in its catalytic mechanism have been examined in depth by both mechanistic and structural studies (62-64) and the roles of catalytic residues examined by mutation studies.

1.4.5 The final step

The final step in the biotin biosynthetic pathway is the insertion of sulfur into the carbon skeleton of DTB to yield biotin. Little is known about the reaction mechanism or the actual source of the sulfur atom. Sequence similarity searches reveal that there are twenty six known species of bacteria, yeast and plants which contain genes encoding amino acid sequences similar to that of *E.coli* biotin synthase. The entire sequences of twenty four species are known and only the first five N-terminal residues are known for the *Citrobacter freundii and Salmonella typhimurium* proteins. To date, biotin synthase from *B. sphaericus* (65), *A. thaliana* (43), *S. cerevisiae* (44), and *E. coli* (66) have been cloned, overexpressed and purified. However, sufficient complementation analysis has been carried out on *Methylobacillus, B. flavum* (67), *B. subtilis* (68) *E. herbicola* (69) and *S. marcescens* (70) to verify that these genes encode active biotin synthases. The alignment of all the sequences shows that there are a number of highly conserved regions of the protein. Four residues in the known proteins are completely conserved and a number of others are almost completely conserved. Three of these residues are cysteine which occur in the following motif Cys, X_3, Cys, X_2, Cys. This motif is also found in anaerobic ribonucleotide reductase activating enzyme (ARR-AE, Swissprot accession number P39329) (71), benzylsuccinate synthase activating enzyme (CAA05050) (72), lipoic acid synthase (P25845) (73), lysine aminomutase LAM (74), the nitrogen fixation B gene product (P11067) (75), FNR protein (P03019) (76), pyrrolo-quinoline-quinone synthase (Q01060) (77), pyruvate formate lyase activating protein (PFL-AE) (P09374) (78), spore photoproduct lyase (P37956) (79), molybdenum cofactor

synthase (MOAA) (O27593) (80), NARA protein (P39757) (81) and the *thiH* gene product (P30140) (79). It has been speculated that this motif is involved in the binding of iron as all of these proteins are known to contain Fe-S clusters.

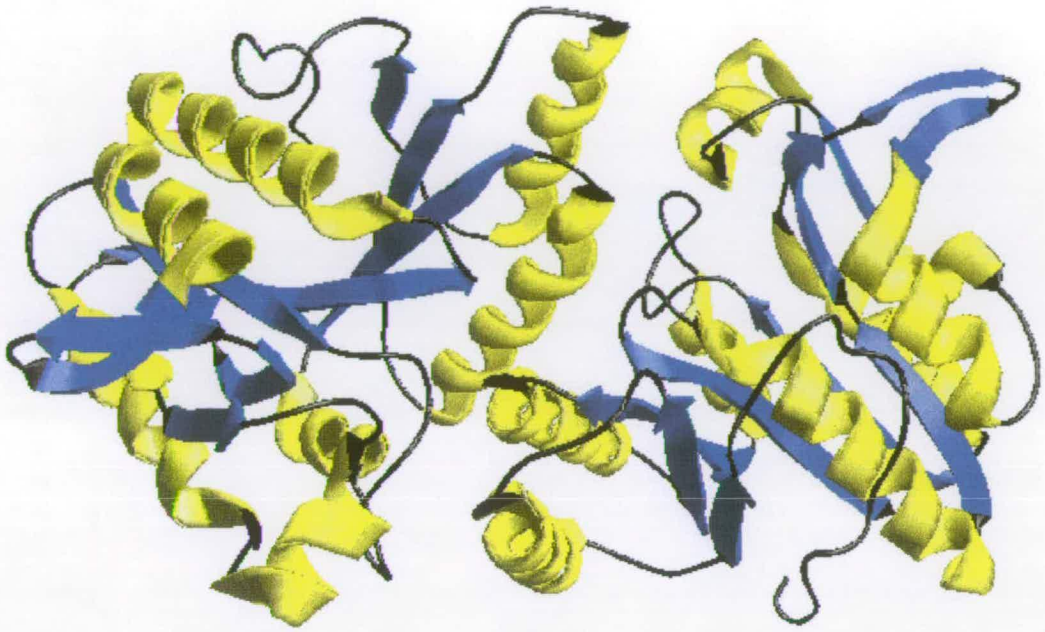

Figure 1-7

Dethiobiotin synthase 1.6Å (PBD 1DAD). The seven stranded parallel β-sheet (blue) is surrounded by six helices (yellow).

1.5 The Components of the *E.coli* Biotin Synthase System

Prior to 1992 little was known about the conversion of DTB to biotin. The reaction was originally thought to be catalysed solely by the *bioB* gene product, biotin synthase. It is now known that the reaction is extremely complex and involves a number of other proteins along with biotin synthase. In this work we will refer to the *bioB* gene product as biotin synthase.

1.5.1 *E. coli* biotin synthase is an Fe-S protein

Fe-S clusters are found in numerous proteins where they perform a number of important roles. However, the mechanism by which they are formed *in vivo* is not yet fully understood. In catalytic reactions Fe-S clusters can act as Lewis acids during dehydration. They are also involved in electron tranport, the stabilisation of protein structure, the formation of protein-bound radicals, DNA recognition and in the regulation of metabolic pathways. A further function of Fe-S clusters is that they can act as biological sensors of oxygen and iron (82).

The *E. coli* biotin synthase protein is a 346 amino acid protein with a predicted weight of 38665Da (56) which contains a Fe-S cluster (48). Sanyal *et al.* cloned, overexpressed and purified the *bioB* gene product from *E. coli* (66). Two protein species were found which had molecular weights of *ca.* 82kDa and *ca.* 104kDa based on native gel electrophoresis. Both species ran on SDS gels with the expected molecular weight of *ca.*39kDa. The 82kDa protein was found to be a homodimer which contains one [2Fe-2S] cluster per protein monomer and the 104kDa species a homodimer that contains a single [2Fe-2S] cluster per dimer. The 104 kDa species can be converted to the 82kDa species (one [2Fe-2S] cluster per monomer) on incubation with Fe^{3+}, S^{2-} and 2-mercaptoethanol. Both proteins species are red in colour and have UV-visible absorbance spectra typical of that of other Fe-S proteins with peaks at 324nm and 419nm. Anaerobic dithionite reduction of the protein resulted in a gradual bleaching of colour indicating some degradation of the Fe-S cluster. Three years later it was reported that during the purification of biotin synthase, yet another species of biotin synthase which had a molecular weight of *ca.*160kD had been discovered during purification (44). Flint *et al.* have reported EPR work on the Fe-S cluster of the 82kDa protein (83). Their results confirm the presence of one [2Fe-2S] cluster in each subunit of the homodimer in aerobically purified samples. One iron ion has two sulfur ligands while the other has one cysteine ligand and an oxygenic terminal ligand. In contrast after anaerobic dithionite reduction it appears that the two [2Fe-2S] clusters in each monomer convert to form a single [4Fe-4S] cluster at the subunit interface *via* reductive dimerisation (Figure 1-8). This form of the Fe-S cluster has each iron ion coordinated to a cysteine. Reoxidisation of the reduced sample leads to a degradation of the [4Fe-4S] cluster and a partial reformation of the [2Fe-2S] cluster. It is thought that the formation of the [2Fe-2S] cluster is a consequence of aerobic purification.

A redox role for the cluster seems unlikely and a more likely role for the [4Fe-4S] cluster lies in the initiation of the radical mechanism by facilitating reductive one-electron cleavage of SAM to form methionine and a 5'-deoxyadenosyl radical ($DOA^{\bullet}$) (Figure 1-9). It has also been suggested that the [4Fe-4S]↔[2Fe-2S] cluster interconversion may play a further role *in vivo* in radical enzymes by providing a method of regulating enzyme activity in response to oxidative stress, without irreversible cluster degradation (84).

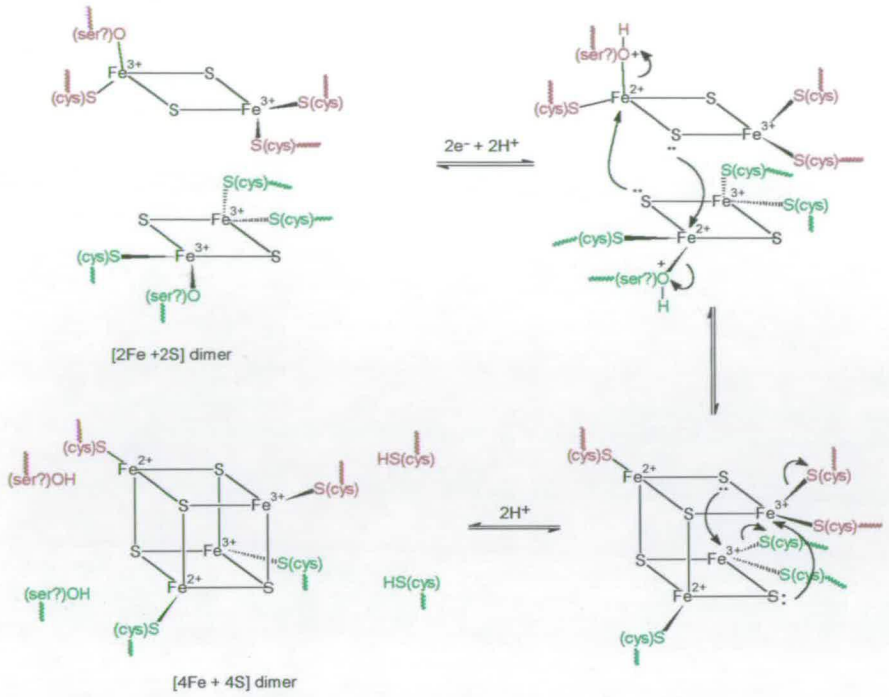

Figure 1-8

Proposed scheme for the reductive dimerisation of two [2Fe-2S] clusters to form a single [4Fe-4S] cluster at the dimer interface. Reproduced from Johnson *et al* (83).

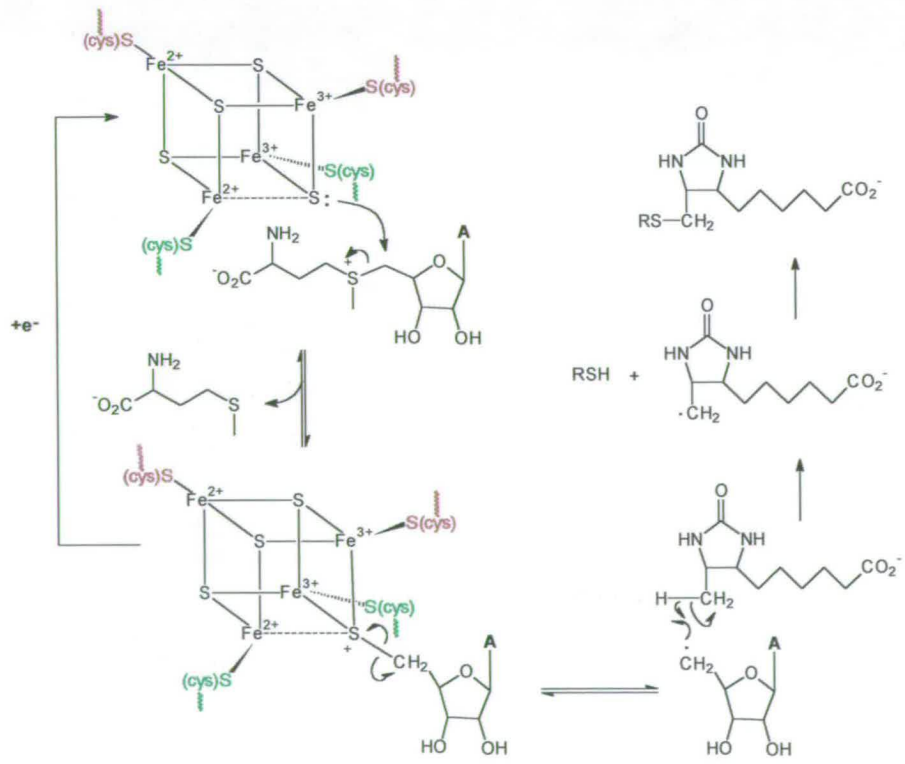

Figure 1-9

Proposed mechanism for the reductive cleavage of SAM by a [4Fe-4S] cluster. Reproduced from Johnson, M. K. *et al* (83).

1.5.2 The stimulatory cofactors

In 1992 it was reported that in crude cell free extracts of *E. coli* clones which carried a plasmid encoding the *bioB* gene, the convertion of DTB to biotin was stimulated by certain stimulatory cofactors (85). The cofactors reported by these authors were fructose-1,6-bisphosphate, SAM, Fe^{2+}, reduced nicotinamide adenine dinucleotide phosphate (NADPH) and potassium chloride. The function of fructose-1,6-bisphosphate, which is a glycolytic intermediate, is unknown but it has been postulated that it could be a cofactor, although a role as an enzyme activator seems likely. It was also suggested that other as yet unidentified enzymes may be required and within the next two years it was discovered that *E. coli* flavodoxin (FLD) (86) and *E. coli* flavodoxin $NADP^+$ oxidoreductase (FLDR) (87) were necessary for the reaction. The purified biotin synthase alone is unable to convert DTB to biotin. Only when fructose-1,6-bisphosphate, SAM, Fe^{2+}, NADPH and potassium chloride, dithiothreitol (DTT) and the cell free extract of a *bio*B$^-$ strain, were added did biotin production occur. The turnover number was very low (*ca.* $1h^{-1}$) possibly due to the fact that the concentration of biotin synthase was greater than all the other required cofactors. Sanyal *et al* also reported a K_m for DTB of 2μM and a k_{cat}/K_m equal to $103M^{-1}s^{-1}$ based on the 82kDa species (48). Several other authors have also tried to define the absolute requirements for biotin synthase activity. Birch *et al.* have suggested that there is a thiamine pyrophosphate-dependent protein required for the reaction and also one of the following amino acids: asparagine, aspartate, glutamine or serine (88). They also developed a more sensitive assay system which is based on the conversion of radiochemical DTB to produced labelled biotin. The reaction products are then separated using thin layer chromatography and analysed using HPLC and autoradiography. It should be noted that in their experiments they were not working with pure samples of biotin synthase. The most recent (and most complete) cocktail of ingredients required for biotin synthase activity is derived from the work of Sanyal *et al.* (89). They report that pure biotin synthase was only active if the following cofactors were added - FLD, FLDR, SAM, Fe^{2+}, fructose-1,6-bisphosphate, cysteine and DTT. They also noted that the addition of a labile low molecular weight product from the DANS reaction stimulated the biotin reaction. A further finding was that fructose-1,6-bisphosphate can be replaced by asparagine (44). However, the biotin synthase preparations still have a poor turnover with an upper limit of 2 molecules of biotin per monomer. It seems likely that the reaction mixtures still do not contain all the physiological factors needed as the enzyme is obviously not functioning very efficiently. It is also possible that the biotin synthase may become modified after one turnover to an unactive form or that only a small fraction of the pure biotin synthase is active.

Biotin synthase from *B. sphaericus* has been found to be able to transform DTB to biotin, in the presence of SAM and photoreduced deazaflavin which substitutes for FLD, FLDR and NADPH (90).

1.5.3 The cysteine desulfurase protein NifS

In 1991 Jacobson *et al.* discovered the nitrogenase gene cluster of *Azotobacter vinelandii (A. vinelandii)* (91). Two years later it was found that the protein product of the *nifS* gene, NifS, was able to catalyse the desulfuration of cysteine to alanine and sulfide. The physiological role of this reaction appears to be the production of S^{2-} for the regeneration of the Fe-S cluster of the nitrogenase Fe-protein. The NifS protein is a homodimer, with a monomeric weight of 44kDa, which utilises PLP as a cofactor. The mechanism of the NifS reaction starts with the formation of a cysteine–PLP Schiffs' base adduct and H-2 abstraction to form a quinioid. Nucleophilic attack then occurs by an enzyme thiolate anion at the sulfur of the substrate cysteine (Cys 325). This results in the cleavage of the C-S bond to form a PLP-bound alanine enamine and formation of an enzyme-bound cysteinyl persulfide, which is a likely candidate for a sulfur donor (92). *In vitro* experiments to confirm the role of NifS have been carried out. In the nitrogenase Fe-protein the [4Fe-4S] cluster was removed *via* a metal chelator and and the apo-protein was then incubated with NifS, cysteine, DTT, Fe and MgATP. The [4Fe-4S] cluster was found to have been reformed (93).

This experiment has also been carried out on SoxR a dimeric transcription factor of the *soxrs* regulon of *E. coli* which contains two [2Fe-2S] clusters per monomer which were chemically removed with EDTA. The Fe-S was regenerated in two ways both non-enzymatically (six hours) using Fe, S and a reducing system, and enzymatically using NifS from *A.vinelandii* (two minutes). A mutant SoxR protein, which had one out of its four cysteine residues substituted for an alanine residue did not have cluster reformation (94).

In 1996 Flint reported that he had found a protein in *E. coli* with a similar sequence and molecular weight to NifS. He called this protein the *E. coli* NifS-like protein, as it contains PLP and can catalyse the conversion of cysteine to alanine and sulfur (95). He speculated that this protein could be involved in the regeneration of Fe-S cluster in *E. coli* Fe-S-proteins but so far this has not been verified.

1.6 The Flavoprotein Components of the Biotin Synthase System

Flavoproteins are proteins which contain a flavin as a prosthetic group. The name derives from the Latin flavus meaning yellow and this refers to the chromophore of the water soluble vitamin, riboflavin (vitamin B_2). Riboflavin is the precursor for flavin mononucleotide (FMN) and flavin adenine dinucleotide (FAD). In the production of FMN, riboflavin is phosphorylated by ATP. FMN is then derivatised by ATP to yield FAD (Figure 1-10).

Flavoproteins catalyse redox reactions and the reactive part of the flavin molecule is the isoalloxazine ring which can accept two electrons, and in doing so it can take up a proton and a hydride ion. When the flavin accepts one electron it is converted from its oxidised form to its semiquinone. When another electron is added to the semiquinone, the flavin is in its hydroquinone or fully reduced state. There are two types of semiquinones observed in flavoproteins, red anionic semiquinones or blue neutral semiquinones.

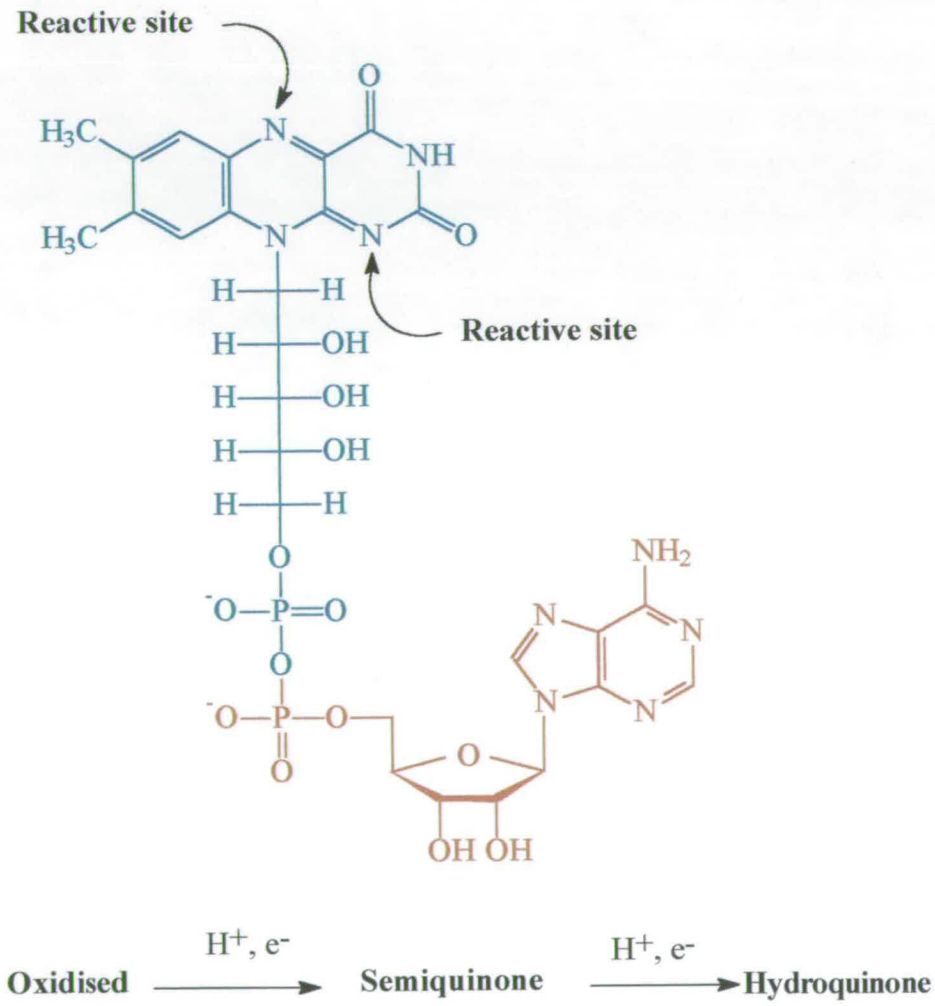

Figure 1-10

The structure of the oxidised form of flavin adenine dinucleotide (FAD). This made up of flavin mononucleotide (FMN) unit (shown in blue) and AMP (shown in red).

1.6.1 *Escherichia coli* flavodoxin

E. coli FLD was discovered in 1971 where it was described as an acidic protein with a molecular weight of around 20 kDa (96). Three years later it was discovered that two flavoproteins, R and F, were required to activate cobalamin-dependent methionine synthase, which catayses the formation of methionine from homocysteine and methyltetrahydrofolate. The reaction involves two methyl transfers where cobalamin is both the methyl donor and acceptor. The reaction requires FLDR, FLD and SAM (97). The enzyme contains zinc which becomes ligated to the homocysteine (98).

Both of these *E.coli* proteins, R and F, were purified and it was found that they needed a reduced triphosphate nucleotide to facilitate electron transfer (99). Protein R proved to be a FAD-containing protein with a molecular weight of *ca.* 27kDa. When it was incubated with NADPH, the FAD was rapidly reduced to its hydroquinone form, with no semiquione species being observed. Protein F contained FMN and had a molecular weight of *ca.* 19.4kDa, it was inert to NADPH but on reduction with dithionite a neutral blue semiquinone was formed (100).

In 1982 Blachowski reported that both FLD and ferredoxins became reduced in *E. coli* by oxidoreductase reactions, and that this reduced FLD was required to activate pyruvate formate-lyase (PFL) (101). PFL catalyses the CoA-dependent formation of pyruvate from acetyl-CoA and formate (102). In 1991 Rowena Matthews' group in Michigan discovered that the R and F factors which were needed for the activation of cobalamin-dependent methionine synthase were in fact FLDR and FLD. They cloned, expressed, purified and determined the amino acid sequence of FLD from *E.coli*. They found that it had a molecular weight of 19606 Da after N-terminal methionine removal and its amino acid sequence was similar to that of other flavodoxins (103).

In 1993 they found that FLD was required to activate anaerobic ribonucleotide reductase (ARR), which is the enzyme responsible for the production of deoxyribonucleotides for anaerobic DNA synthesis (104). Subsequently they cloned and crystallised *E. coli* FLD and using *Aspergillus nidulans* FLD as a model, they were able to solve the three dimensional structure to 3.0Å. FLD has five parallel β-sheets which are flanked by helices, this is similar to other flavodoxins (PDB 1AG9). Four tyrosine residues (Y58, Y59, Y94, Y97) and a single tryptophan residue (W57) form a box which surrounds the flavin, with residues W57 and Y94 as the top and bottom of this box (105). Two years later they had managed to refine the structure to 1.8Å (Figure 1-11) (106, 107).

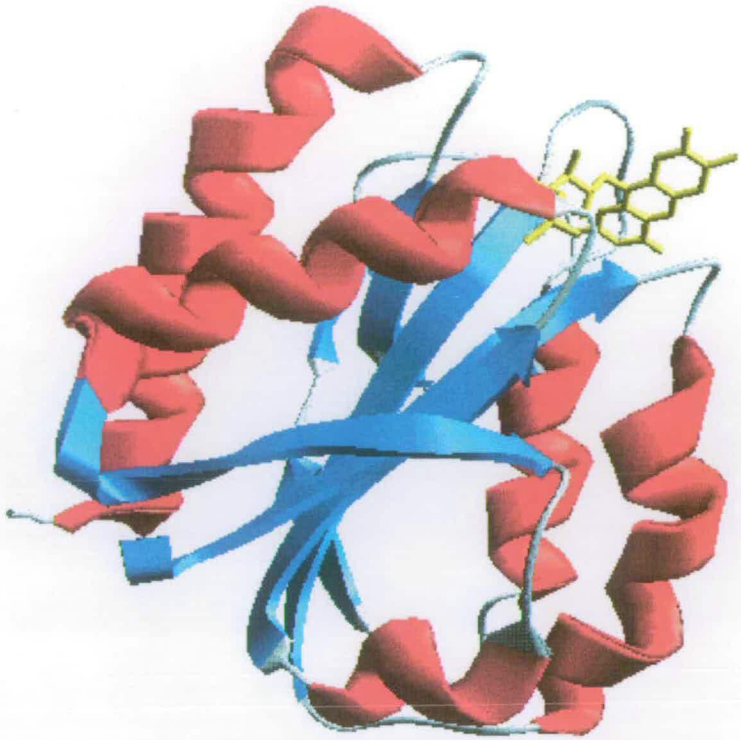

Figure 1-12

The 3-D structure of *E.coli* Flavodoxin at 1.8 Å (PDB 1AG9)

FLD has five parallel β-sheets (blue) which are flanked by helices (red), the flavin (yellow) is surrounded by tyrosines (Y58, Y59, Y94, Y97) and a tryptophan (W57).

1.6.2 *Escherichia coli* flavodoxin NADP$^+$ oxidoreductase

In *E.coli* FLDR can use either FLD or ferredoxin as an electron acceptor but it appears to favour FLD as its redox partner. NADPH is FLDR's electron donor and FAD mediates electron transfer to FLD. In 1993 the FLDR gene was cloned and the protein overexpressed for use in the activation of ARR (108). The synthesis of FLDR was found to be under the control of the *soxrs* regulon, which may be an adaptive response against superoxide. Thus, FLDR may be involved in the protection of bacteria from damage by oxygen radicals since the absence of FLDR does not affect anaerobic growth. In bacteria, pyruvate:ferredoxin oxidoreductase can substitute for FLDR and mutants which lack FLDR have an increased sensitivity to paraquat (109). In 1997 the structure of FLDR was solved to 1.7Å resolution (Figure 1-12) (PDB 1FDR) (110). The structure was found to be similar to other reductases such as nitrate reductase and cytochrome b_5 reductase. It contains two distinct domains which are joined by a single covalent connection. The FAD-binding domain is a double sandwich structure with six strands. The NADPH-binding region is an open α/β structure with a central parallel pleated sheet and six strands surrounded by helices. The *E.coli* FLDR has not been

co-crystallised with NADPH or FLD, so the residues involved in substrate binding and protein-protein interaction are unknown. However, the structure of other reductases with the NADPH mimic 2'-AMP have been solved. By analogy with these three arginine residues (R144, R174 and R184) are thought to interact with NADPH. In all these reductases residue R174 is completely conserved and R144 is conserved in four out of five structures. The results of site-directed mutagenesis studies in our laboratory where each arginine was changed to alanine, indicates that all three residues are definitely involved in the binding of NADPH (111).

In the atomic structure it can be clearly seen that there is a depression in FLDR where it seems logical to assume that FLD would bind. In modelling studies, FLD from *Anabena sp* was successfully docked into this depression. In this region there are also three arginine residues (R236, R237 and R238) and work in our laboratory to investigate their role in FLD binding is currently underway.

In 1998 we reported on the biophysical studies of *E. coli* FLD and FLDR, analysing the interactions between these two proteins, and determined the redox properties of the flavin cofactors (112). In 1994 it was discovered that FLD and FLDR could support the function of 17α–hydroxylase activities of bovine cytochrome P-450 (113). It has also been shown that FLD and FLDR support the activity of cytochrome P-450BM3 and that the reduction mechanism is a 'ping pong', with FLD acting as a shuttle rather than participating in a ternary complex between the FLD, FLDR and the P-450 (112).

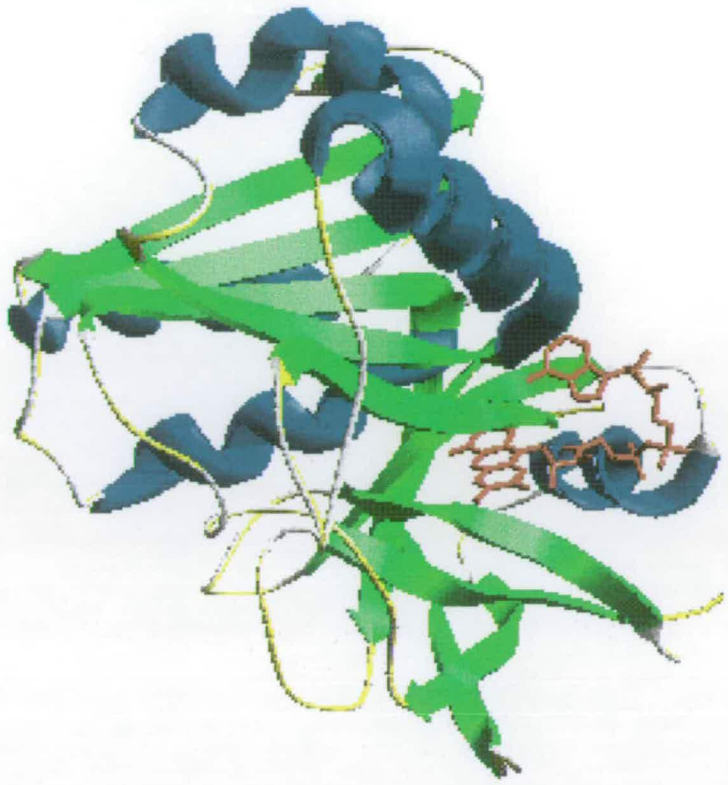

Figure 1.-12

The atomic structure of *E.coli* ferredoxin (flavodoxin) $NADP^+$ oxidoreductase at 1.7 Å (PDB 1FDR). The FAD(red) binds in a double sandwich domain with six strands surrounded by helices (blue). The NADPH-binding region is an open α/β structure with a central parallel β-sheet (green).

1.7 The Mechanism of the Biotin Synthase Reaction

The biotin synthase reaction has proven to be extremely complex and efforts to elucidate its mechanism have led to complex and confusing results. The first problem is the source of the sulfur atom which is inserted into two saturated carbon atoms of dethiobiotin to form the thiophene ring of biotin. Early work on the identity of the sulfur donor proved inconclusive and it has only recently that evidence has shown it to be derived from cysteine. In *B. sphaericus* crude cell free extracts, sulfur from [^{35}S] cysteine was incorporated into biotin. However, this was not the case in the asssay where pure biotin synthase was activated by deazaflavin (90). In *E. coli* crude cell-free extracts incorporation of ^{35}S from [^{35}S]cysteine and [^{35}S]cystine have been reported (88). In defined mixtures, there is no evidence of incorporation of ^{35}S from either [^{35}S] cysteine or [^{35}S] SAM (89). The fact that there is no sulfur incorporation in defined mixtures but incorporation occurs in cell free extracts points to

there being a component in cell free extracts which can convert the sulfur atom from cysteine into a form that can eventually be incorporated into biotin. In the currently defined cell free catalytic mixtures there are three possible sources of sulfur; the Fe-S cluster, an as yet unidentified sulfur-containing species associated with biotin synthase, (although this has never been observed, it would be consistent with the one turnover) and DTT. If DTT was the sulfur donor *in vitro* then the lack of the correct physiological donor would again explain the above results (44).

Shaw *et al.* found that sulfur from [^{35}S]-cysteine was incorporated into a reaction intermediate which could then produce labelled biotin and this strengthens the case for cysteine being the sulfur donor or a precursor to the sulfur donor (114). Whether it was just the sulfur atom or the entire amino acid that was attached to the intermediate remains to be verified.

Marquet and coworkers found that biotin production in *B.sphaericus* increased 3-4 fold when $FeCl_3$ and Na_2S were added to the assay mixture. They proposed that this was due to the reconstitution of the Fe-S cluster. They repeated the experiment using $Na_2{}^{34}S$ and found that ^{34}S-biotin was produced indicating that the sulfide could be utilised by the enzyme and incorporated into biotin. To verify whether or not the Fe-S cluster is involved in sulfur donation they reconstituted the apoenzyme with $FeCl_3$ and $Na_2{}^{34}S$. When this enzyme was used in the assay ^{34}S-biotin was produced indicating that the Fe-S cluster is the sulfur donor. They repeated the experiment with *E.coli* biotin synthase (without the addition of cysteine to the assay medium) and got very similar results. This appears to be a function for Fe-S clusters in that they can in fact provide sulfide for use in reactions. The most recent work on the sulfur donor has been carried out by Gibson in collaboration with Flint. In their assays however they had gone back to working with impure biotin synthase as further purification of the enzyme reduces its activity. They suggest that the biotin synthase acts as an "assay reagent" rather than a catalyst. In *in vitro* experiments using ^{35}S cysteine and ^{35}S methionine they produced ^{35}S biotin only when the labelled cysteine was present in the reaction mixture. They suggest that the sulfur is from either the Fe-S cluster or from a cysteine residue on the protein. They carried out mass spectrometry analyses on the enzyme looking for covalent interations and detected two species which they termed "naïve" and "experienced". The "naïve" enzyme gave a narrow peak with a mass of 38514.4Da and the "experienced" enzyme gave a broad peak with a mass of 38518.4Da. They suggest that if sulfur was lost from the "experienced" enzyme then something must be gained to account for the increase in mass. They make no suggestions as to the nature of the chemical change (115).

The second problem of the biotin synthase reaction is the mechanism of C-H to C-S bond formation. Many groups have investigated this and as early as 1968 Wright *et al.* fed randomly tritiated DTB to cells of *Aspergillus niger* (116). Their results indicated that there was a loss of 4 hydrogen atoms. Eight years later Parry fed specifically titrated DTB to *A.*

niger and his results showed that only two hydrogens were lost - one from C6 and the other from C9. There was no loss of hydrogen at C5, C6 or C7 (117). Parry produced results, again using *A. niger,* that indicated that there was loss of the 6-pro-S-hydrogen at C6 (but not the 6-pro-R hydrogen). Since the absolute configuration at C6 is S then sulfur is inserted with retention of configuration (118). Arigoni and Marti investigated the stereochemistry at the C9 methyl group of DTB. They chirally labelled the methyl group with tritium, deuterium and hydrogen and it was found that "scrambling" of chirality occurred. The logical conclusion to this is that there is an intermediate between DTB and biotin that has a labile methylene radical (119). A number of authors have speculated as to whether there is a thiol intermediate involved in the reaction. Marquet (120) and Baxter (121) have both suggested that 9-mercaptodethiobiotin could be this intermediate but they also note that 9-mercaptoDTB could be an abnormal precursor of DTB *in vitro.*

Recent work by Shaw *et al.* has proved that SAM is directly involved in the biotin synthase reaction (114). Radiochemical assays involving [^{14}C]-DTB resulted in the formation of an enzyme-generated intermediate. Formation of this intermediate was SAM-dependent and it was definitely derived from DTB, as it was radioactively labelled. The [^{14}C]-intermediate was purified and then assayed. It in turn produced labelled biotin by a mechanism which again required SAM. Characterisation of this intermediate was not possible due to the fact that only nanogram quantities were produced. It is known however that it is not 9-mercaptodethiobiotin, as it does not coelute with this compound on HPLC. It is possible that this intermediate is 9-hydroxydethiobiotin (capture of H_2O or O_2) or arises by reaction of a DTB radical with cysteine to give the thioether adduct although 9-OH DTB was shown not to be an intermediate in whole cell work. In assays using [^{14}C-*methyl*]-SAM a labelled product was formed which was found to be [^{14}C]-methionine. This result supports the hypothesis that SAM is cleaved to produce methionine and a 5′-deoxyadenosyl radical (DOA$^{\bullet}$). Shaw and co-workers have proposed a mechanism where two molecules of SAM are required for each molecule of biotin produced. In this they propose that the conversion of DTB to the intermediate involves the generation of either a substrate-bound or enzyme-bound radical from the reductive cleavage of SAM, as does the intermediate to biotin step. If the radicals are both formed on the substrate, then one molecule of SAM would be needed to activate the methyl carbon and another to activate the methylene carbon of DTB. They did note however that over time it appeared that almost three molecules of SAM were used per biotin molecule produced and this has been supported by the work Guianvarc'h and co-workers on *B.sphaericus* biotin synthase who report a stoichiometry of 3:1 for SAM : biotin and that methionine and DOA are produced in equal amounts (122). In the case of enzyme radicals such as lysine 2,3-aminomutase (LAM) SAM consumption is catalytic with respect to substrate, although it can be increased during the reaction due to abortive processes.

However, for a direct radical formation on DTB SAM would be a substrate infering a 2:1 stoichiometry.

Studies on the biotin synthase reaction are in their infancy, but the fact that it cleaves SAM and probably uses a radical mechanism means that is could be a member of a group of enzymes which use SAM to form enzyme-bound (ARR, PFL) or substrate-bound radicals (LAM) which uses a B_{12} -like mechanism where the homolytic cleavage of a C-H bond on the substrate lysine is mediated by DOA, as shown by the reversible transfer of ^{3}H from the substrate to DOA (123). It should also be noted that the glycyl radical amino acid sequence (RVS(C)GY) which is found in ARR-AE and PFL-AE is not present in biotin synthase (84)

Recent work by the Marquet group has further examined the role of SAM in the biotin synthase reaction. In order to find out if DOA directly abstracts the substrate hydrogen as in the LAM reaction they synthesised 6,9-[$^{2}H_5$]DTB, 9-[$^{2}H_3$]DTB, 6(*S*)-[$^{2}H_1$],9-[$^{2}H_1$]DTB and 6(*R*)-[$^{2}H_1$],9-[$^{2}H_1$]DTB and incubated them in the biotin synthase reaction. Mass spectrometry analysis of the products revealed that ^{2}H from both the 9-methyl and the 6-pro-R position are definitely transferred from DTB to DOA (84). Mass spectrometry results reveal that deuterium transferred to DOA but whether it is at position 4' or 5' is unknown. The results also confirmed that in fact two molecules of SAM are required for the reaction (124)

While the results are not entirely unambiguous in that mass spectrometry analysis of the mono deuterated DOA formed did not enable distinction between 5' and 4' deuterated species a point which may be immaterial since Frey (Southampton Biochemical Society meeting) has pointed out that C4 to C5 hydrogen transfer can occur in DOA radicals. This data strongly supports the DOA radical hypothesis and the proposals of the Marquet and Shaw groups are consistant enough to be combined in the scheme shown in Figure 1-13.

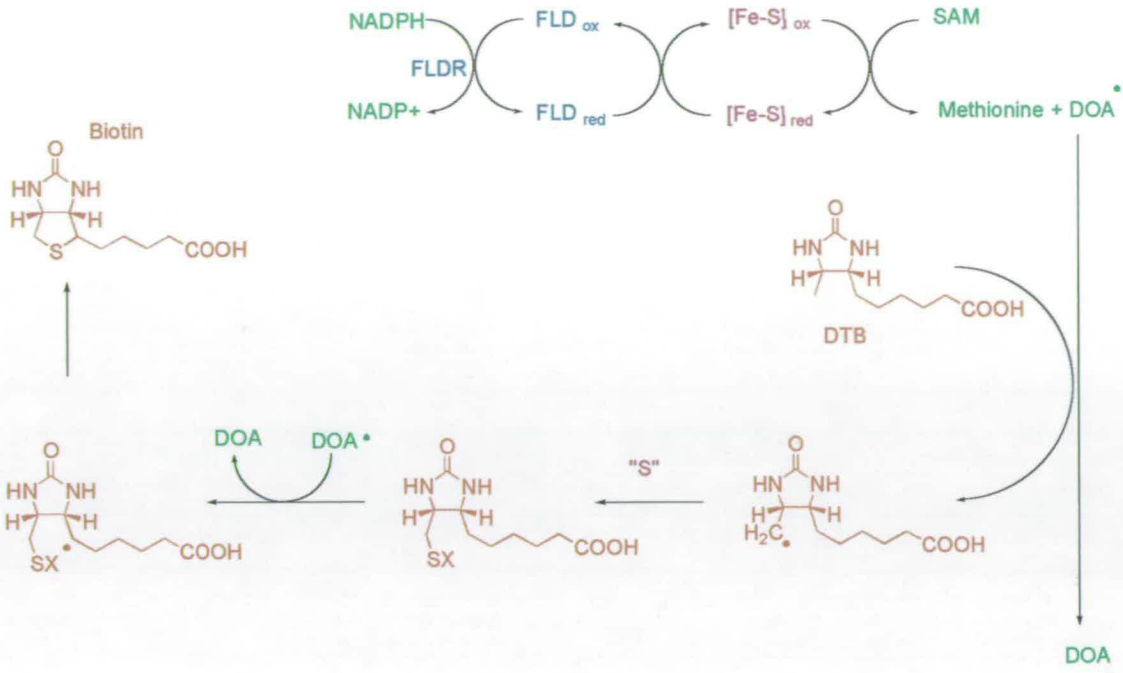

Figure 1-13

The proposed mechanism for the conversion of DTB to biotin.

1.8 Fe-S cluster enzymes

The fact that biotin synthase is based on a core [2Fe-2S] protein with a requirement for NADPH, a FLD/FLDR redox couple and SAM as a radical generator suggests that it belongs to a growing family of enzymes which use Fe-S clusters. Four of these, anaerobic ribonucleotide reductase activating enzyme (ARR-AE) lipoic acid synthase (LIPA), lysine 2,3-aminomutase (LAM) and pyruvate formate lyase activating enzyme (PFL-AE) have been studied in recents years. However, even within this small group there appears to be subtle differences with regard to subunit composition and chemical function.

ARR was discovered in 1989 and was found to be an $\alpha_2\beta_2$ heterotetramer (125, 126). Like biotin synthase it also requires potassium, SAM and DTT, FLD and FLDR (104). Its reaction involves formation of a glycyl radical on the α subunit of the enzyme and is oxygen-sensitive. The β subunit is required for catalytic activity and contains a [4Fe-4S] cluster which joins the two β subunits together (127). SAM binds to the β subunits with a stoichiometry of 1:1 and it then is reduced by the Fe-S cluster during enzyme activation (128, 129). In 1993 a mechanism was proposed where FLDR is reduced by NADPH and this reduced FLDR then reduces FLD. The Fe-S cluster is in turn reduced by FLD. SAM then binds to the Fe-S cluster and is reduced. After this it dismutates into methionine and a primary DOA radical. The glycyl radical is then fomed *via* proton abstraction at the α-carbon of glycine 681 (130). More recent

work on characterisation of this cluster reveals that the β2 protein actually contains two [2Fe-2S] clusters per chain which are converted to a single [4Fe-4S] cluster on reduction with dithionite (131).

LAM from *Clostridium substerminale* catalyses the interconversion of L-lysine and L-β-lysine and it is a hexameric Fe-S protein with a molecular weight of 285kDa (subunit weight is 47kDa). It is a PLP-containing enzyme which requires SAM. The Fe-S cluster of LAM exists as three different forms, one of which directly interacts with SAM. It is proposed that SAM is cleaved by reaction at the Fe-S centre to reversibly form methionine and a (hypothetical) DOA radical at the enzymes active site. This radical could then initiate the formation of a radical on the substrate, lysine (132).

Lipoic acid synthase, the *lipA* gene product, inserts a sulfur atom into octanoic acid to form lipoic acid. Lipoic acid is a cofactor in oxidative carboxylations of α-keto acids and in glycine cleavage. In these reactions lipoic acid is, like biotin, joined to the enzymes *via* an amide bond to a ε-amino group of a lysine residue. The *E. coli lipA* gene has been cloned and sequenced and it has a 36% sequence similarity to the *E. coli* biotin synthase (133) (134). The enzyme has been shown to be a dimer which contains a [2Fe-2S] cluster in each monomer. On reduction these two cluster converts to a single [4Fe-4S] cluster (73). Both lipoic acid synthase and biotin synthase contain a Y (F) N H N motif that may be part of the enzymes active site. The similarity in the chemistry of the dithiolane ring of lipoic acid and the tetrahydrothiophene ring of biotin suggests that the two enzymes may have similar mechanisms of action (135). This type of oxidative cluster rearrangement has only been observed for the subunit bridging [4Fe-4S] cluster in the nitrogenase Fe-protein, ARR lipoic acid synthase and in biotin synthase (83).

PFL is a homodimer with a monomeric weight of 85kDa whose structure has recently been solved (136, 137). It has many similarities to ARR in that it also requires an Fe-dependent activating enzyme (a monomer of 28kDa) which contains a [4Fe-4S] cluster (PFL-AE) and SAM, DTT, NADPH and the FLD/FLDR couple (101) for activation (138, 139). In its active form, PFL contains a single stable glycyl radical (Gly-734) which is necessary for catalysis (140). The radical is thought to be produced by a mechanism similar to that of ARR. Single point cysteine to serine mutants in the PFL-AE have proven that three cysteine residues are absolutely essential for activity (Cys 29, 33 and 36). Direct interaction of SAM with the Fe-S cluster is possible (141). The spectroscopic data shows that the [4Fe-4S] cluster in the PFL-AE cluster undergoes facile oxidative degradation to [2Fe-2S] clusters as a result of exposure to oxygen during isolation (78).

Other enzymes which are involved in sulfur incorporation such as the enzymes of thiamine and molydopterin biosynthesis have been documented in the literature. In the *E. coli* thiamine

biosynthetic pathway, a thiazole and a pyrimidine are synthesised and then coupled to give thiamine. The mechanism of sulfur insertion to form the thiazole is not fully understood, but it is conjectured that the source of sulfur is cysteine and that the *thiS* gene product is the sulfur carrier (142, 143). Little is known about molbydopterin biosynthesis other than it requires a three enzyme system for sulfur transfer (143). The enzymes which insert sulfur into into amino acids in *E.coli* are serine acetyl transferase which activates serine and acetyl-CoA and forms O-acetyl-L-serine and O-acetyl-L-serine (thiol) lyase which converts this to cysteine (144).

The mechanism of biotin synthase remains an enigma and before a mechanistic understanding can be reached a large number of questions still have to be answered with respect to the biotin synthase reaction. The factors limiting catalysis by biotin synthase need to be identified. The mechanism of sulfur transfer from the Fe-S cluster to the dethiobiotin radical needs to be investigated. The mechanism of the reductive cleavage of SAM by reduced Fe-S clusters needs to be elucidated.

1.9 Aims

The main aim of this work was to characterise the protein components of the *E. coli* biotin synthase system. The electron transfer proteins FLD and FLDR were characterised and then mutational analysis of the Fe-S cluster of biotin synthase was carried out. In normal cells these proteins are expressed at low levels so expression systems had to be developed which would allow the large scale production of milligram quantities.

Chapter 2: Materials and Methods

2.1 General Reagents

Chemicals and solvents were of the appropriate quality and were purchased from Pharmacia, Promega, Sigma, Biorad, Gibco BRL, Amicon, New England Biolabs, Waters Millipore or Invitrogen unless otherwise stated.

2.2 Solutions and Buffers

AB buffer - ammonium bicarbonate (50mM, pH7.9) and zwittergent 3-16 (0.05%)

Ampicillin - a stock solution (100mg/ml) was sterilised by filtration (0.45 μM) and used at a final concentration of 100μg/ml. The solution was stored at 4°C.

Buffer A - Tris-HCl (50mM, pH 7.5)

Buffer B - Sodium phosphate (100mM, pH 7.5)

Buffer C - Sodium acetate (100mM, pH 5.0)

Buffer D - Imidazole (5mM), sodium chloride (0.5M), Tris-HCl (20mM, pH 7.9)

Buffer E - Imidazole (1M), sodium chloride (0.5M), Tris-HCl (20mM, pH 7.9)

Electroblot buffer – 3-[cyclohexlamino]-1-propanesulfonic acid (10mM, pH11.0), methanol (10%)

Ethidium bromide - a stock solution (10mg/ml) was made and used at a final concentration of 5 μg/ml. The solution was stored at 4°C in a dark bottle.

IPTG - a stock solution of isopropyl - β, D - thiogalactopyranoside (100mM) was sterilised by filtration (0.45 μM filter) and stored at 4°C.

SDS running buffer - Tris-HCl (25mM, pH8.3), glycine (192mM), SDS (1 % (w/v))

SDS sample buffer - Tris-HCl (0.5 M, pH 6.8, 1.0ml), Glycerol (2.0ml), SDS (10% (w/v), 1.6 ml), 2-β-mercaptoethanol (0.4 ml), bromophenol blue (0.05% (w/v), 2.0ml)

TAE - Tris-HCl (40mM, pH8.0), acetic acid (57.1 ml), EDTA (0.5 M, pH 8.0, 100ml)

Tetracycline - a stock solution (12.5mg/ml) was used at a final concentration of 12.5μg/ml. The solution was stored at -20°C.

Transformation buffer (TB) - Calcium chloride (50mM), Tris-HCl (10mM, pH 8.0)

2.3 Media

Agar plates - bacto-agar (15g/l) was added to specified media to prepare agar plates.

MRS modified - proteose peptone (15g), yeast extract (5g), sodium acetate (5g), ammonium citrate (2g), tween 80(1ml), di-potassium hydrogen orthophosphate (2.4g), magnesium sulphate (0.2g), manganese sulphate (0.02g), the pH of the solution was adjusted to 6.4 with acetic acid, made up to 900ml and then autoclaved (121°C, 15psi, 15min). Glucose (20g) was dissolved in water (100ml) and filter sterilised into the medium once it had cooled.

Resuspension medium - 12% reconstituted milk solution (5 ml), MRS modified medium (2.5ml) and glycerol (2.5ml). This media was then autoclaved (121°C, 15 min, 15 psi).

Luria Bertani (LB) - bacto - tryptone (10g), bacto - yeast extract (5 g), sodium chloride (10g) were dissolved in distilled water (1 litre) and then adjusted to pH 7.5 with sodium hydroxide.

Minimal (M9) - di-sodium orthophosphate (6 g), potassium di-hydrogen orthophosphate (3 g), sodium chloride (0.5 g), ammonium hydrogen chloride (1 g). This was adjusted to pH 7.4, made up to 1 l with distilled water and autoclaved (121°C, 15 min, 15 psi). The media was allowed to cool and then the following filtered (0.45 μM) solutions were added - magnesium sulphate (1M, 2ml), glucose (20%, 10ml) and calcium chloride (1M, 0.1ml).

Minimal casamino acids (M9 CA)- Identical to M9 but with casamino acids (2 g/l).

2YT - bacto - tryptone (16 g), bacto - yeast extract (10g), sodium chloride (5 g) were dissolved in distilled water (1 litre) and then adjusted to pH 7.5 with sodium hydroxide.

2.4 Bacterial Cell Lines

JM101, JM109 and TOP10™ cell lines were used for the storage of genes and also for the initial transformation of ligation products. PCOi was used to prepare a *bio*$^-$ cell free extract. Hyperproduction of proteins was carried out using B834 (DE3) HMS 174 (DE3) DH5αF' and JM101. *Lactobacillus plantarum* (ATCC 8014) was used in the microbial biotin assay.

Cell Line	Genotype	Reference
JM101	F' traD36 lacI^q Δ(lacZ) M15 proA$^+$B$^+$/ supE thi Δ(lac-proAB)	(145)
JM109	F' traD36 lacI^q Δ(lacZ) M15 proA$^+$ B$^+$ /e14$^-$ (McrA$^-$) Δ(lac-proAB) thi gyrA96 (Nal^r) endA1 hsdR17 ($r_k^-m_k^+$) relA1 supE44 recA1	(145)
Top 10™	F'mcrA D(mrr-hsdRMS-mcrBC) Φ80lacZΔM15 ΔlacX74 deoR recA1 araD139 Δ(ara-leu)7697 gal/U gal/K rpsL endA1 nupG	(146)
PCOi	bio$^-$Δ(attλ, bio uvrB) thr, leu, thi, placi which confers tetracycline resistance	
B834 (DE3)	F$^-$ ompT hsdS$_B$ ($r_B^-m_B^-$; an E. *coli* B strain) gal dcm met with DE3, a λ prophage carrying the T7 RNA polymerase gene	(147)
HMS174 (DE3)	F$^-$, recA, hsdR [$r_{K12}^-m_{K12}^+$] Rif^r with DE3, a λ prophage carrying the T7 RNA polymerase gene	(147)
DH5αF'	F/endA1 hsdR17 (r_k^- m_k^-) supE44 thi1 recA1 gyrA (Nal^r) relA1Δ9lacIZYA-argF) u169 deoR (Φ80dlacA (lacZ) M15)	(148)

2.5 DNA Vectors and Plasmids

Vectors used for the initial cloning and storage of genes were pUC18/RBS, a derivative of pUC18 that contains a *Nco*I cloning site, and pEE1010. Plasmids used for the cloning and overexpression of proteins were pET16b, pET6H (his-tagged proteins), pCL21 (FLDR), pD551 (NIFS), pDH1 (FLD), pET16b/bioB (wild-type biotin synthase), pHis$_6$B (His$_6$-tagged

biotin synthase), pC53S, pC57S, pC60S, pC188S and pC288T (His_6-tagged biotin synthase mutants).

2.6 Oligonucleotide Primers

The following oligonucleotide primers were used (restriction sites are in bold and codon changes are underlined).

BIOB PCR 5' - GGTAAAA**CCATGG**CTCACCGCCCA - 3'

BMUTFOR 5' - GTAAAAGCGATGGGG**CTCGAG**GCGTGTATG - 3'

BXHO I 5' - CGCCGA**CTCGAG**CACCTG - 3'

C53S 5' - AAGACCGGAGCTTCCCCGGAA - 3'

C57S 5' - CCGGAAGATTCTAAATACTGCCCG - 3'

C60S 5' - AAATACTCTCCGCAAACGTCGCGC - 3'

C188S 5' - GGGATCAAAGTCTCTTCTGGC - 3'

C288T 5' - GGTCAGCAGTTT**GGTACC**GTA - 3'

M13 5' - CGCCAGGGTTTTCCCAGTCACG - 3'

NEW REV 5' - GTTGTGTGGAATTGTGAGCGG - 3'

RED FOR 5' - CAGGAGAATT**CCATGG**CTGATTGGGTAACAGGC - 3'

RED REV 5' - ATAA**GGATCC**GCTTACCAGTAATGCTCCGCTGTCAT - 3'

BIOB PCR contains an *Nco*I site and it was used for sequencing and amplification of the *bio*B gene. BMUT FOR and BXHO I incorporated a *Xho*I site in the *bio*B gene by changing a single base pair at two different sites (G375C and G246C). C53S, C57S, C60S, C188S and C288T caused single point, cysteine to either serine or threonine, mutations in the *bio*B gene.

M13 and NEW REV are pUC18 vector primers and were used for the PCR and sequencing of genes cloned into pUC18. RED FOR and RED REV were used to PCR the *fldr* gene from pEE1010.

2.7 Equipment

Electrophoresis was carried out using a Biorad Protean II minigel system (protein) and a Gibco BRL H5 system (DNA). Denley BR401, Sorvall RC-5B and DuPont Micrcospin 12 centrifuges were used for centrifugations A Pharmacia FPLC system and various columns were used for chromatographic separations of proteins.

2.8 Storage of Bacterial Stocks

LB or 2YT medium containing the appropriate antibiotics were used for the short-term storage of *E. coli*. Colonies of bacteria were stored on inverted parafilm sealed agar plates at 4°C for up to four weeks. For long term storage strains were frozen (-80°C) in LB or 2YT media containing glycerol (15%) (149).

2.9 Preparation of *E. coli* Competent Cells

LB or 2YT media (10ml) was inoculated with a single bacterial colony from a fresh agar plate or from frozen stocks and grown overnight (37°C, shaking at 250rpm). Fresh LB or 2YT (10ml) containing magnesium chloride (1M, 0.2ml) was seeded with some of the overnight culture (0.2ml). The cells were grown to OD_{600nm} = 0.2 and then chilled on ice (5min). Centrifugation (3000rpm, 15min, 4°C) was used to pellet the cells. The supernatant was discarded and the pellet resuspended in cold TB (4 ml). The cells were then placed on ice and agitated gently (30min). Centrifugation was carried out to pellet the cells (3000rpm, 15min, 4°C). The supernatant was discarded and the cells were resuspended in cold TB (0.4ml). The competent cells were left on ice for 2h prior to use (149).

2.10 Transformation of *E. coli* Competent Cells with Recombinant DNA

The competent cells were gently resuspended and 100µl of the suspension transferred to a sterile Eppendorf tube. This was then left on ice (15min) and DNA was added (up to 40ng).

The tube was tapped gently and left on ice (30min). The cells were then heat shocked (37°C, 5min) and warm LB (37°C, 1ml) was added. The tube was then incubated (37°C, 1h), centrifuged (15000rpm, 15min, RT) to pellet the cells, the supernatant discarded and the pellet resuspended in LB (50µl). The suspension was spread to dryness on selective agar plates and incubated (37°C, 16h) (149). Ready-made competent cells were transformed according to the manufacturers instructions.

2.11 Preparation of Plasmid DNA

Plasmid DNA was prepared using the Promega Wizard™ *Plus* Minipreps DNA purification system (Promega).

2 12 Digestion of DNA with Restriction Endonucleases

Typically the required amount of DNA (0.5-1µg) was treated with the appropriate amount of enzyme and buffer and the sample was then placed at the appropriate temperature for the required amount of time (buffer and temperature conditions for each enzyme were as advised by the manufacturers). Blue/orange loading dye (Promega), typically 2µl/10µl of incubation mixture was added and the samples were subjected to electrophoresis on agarose. The gels were then viewed and photographed under ultraviolet light (149).

2 13 Electrophoresis of DNA

The required amount of agarose was added to TAE buffer and heated at 100°C until it dissolved. The solution was allowed to cool to 55°C and ethidium bromide was added to a final concentration of 0.5µg/ml. The gel was then poured into the casting mould and allowed to set at room temperature (149).

2.14 Purification of DNA

DNA was purified from either agarose or from solution using the Prep A Gene® kit from Biorad.

2.15 Amplification and Mutagenesis of DNA

PCR and sequencing reactions were done using a Perkin Elmer 480 thermal cycler. The following were placed in a PCR tube (0.5ml) - 2 Ready to Go PCR™ beads (Pharmacia), DNA template (1μl), primer 1 (forward) (5μl), primer 2 (reverse) (5μl) and distilled water (39μl). These were then overlayed with PCR oil and cycled 30 times at 95°C for 1 min, 54°C for 1 min and 72°C for 2 min. Heating at 72°C for 5 min terminated the reaction. The PCR product was then subjected to agarose gel electrophoresis and the required band was excised and the DNA purified as described in section 2.14. In mutagenic PCR reactions the resulting PCR product (megaprimer) was used as primer 2 in the second reaction (150).

2.16 PCR Screen

A single colony was picked from a plate and gently touched on a fresh agar plate before being resuspended in water (50μl). The cell suspension was boiled (5 min) and then the debris centrifuged (13000rpm, 5 min). A sample was removed (5 μl) and used in a PCR reaction to amplify the gene using the appropriate primers. The PCR conditions are described in section 2.15.

2.17 Automated DNA Sequencing

Automated DNA sequencing was carried out on an ABI prism 377 DNA sequencer using the Sanger dideoxy chain termination method. The following were placed in a PCR tube (0.5ml) DNA template (~5 pmol) (10μl), primer (1μl), distilled water (1μl) and DNA sequencing pre-mix (Amersham) (8μl). The reaction mixture was overlayed with oil and cycled 30 times at 96°C for 30sec, 45°C for 15 sec and 60°C for 4 min. Sequencing data was analysed using the ABI Prism editview software.

2.18 Precipitation of DNA

To the DNA sample ammonium acetate (7.5M, 1/3 vol) and ethanol (100%, 4 vol) were added. The solution was left on ice (2h) and then centrifuged (15 min, 13000rpm). The supernatant was discarded, the pellet washed with ethanol (70%, 250μl), centrifuged (15min, 13000rpm), the supernatant discarded and the pellet dried under vacuum.

2.19 Cloning into Plasmid Vectors

The DNA fragment (or PCR product) cut with suitable restriction enzymes (13 µl), the host vector cut with suitable restriction enzymes (3 µl), 10X T4 DNA ligase buffer (2 µl) and T4 DNA ligase (2 µl) were placed in an Eppendorf. A control with water (13 µl) instead of the gene or PCR product was also set up. The reaction was left at room temperature for 24-48h and then transformed into a suitable cell line (as section 2.10).

2.20 SDS Polyacrylamide Gel Electrophoresis (SDS PAGE)

SDS PAGE was used to analyse proteins on the basis of their molecular weight. The technique used was the discontinuous buffer system of Laemmeli (151).

2.21 Protein Concentration Assays

The protein concentration was determined according to Bradford using bovine serum albumin as a reference (152). Alternatively, protein concentration was measured using the following extinction coefficients. Biotin synthase ($\varepsilon_{274nm} = 3.3 \times 10^4 M^{-1} cm^{-1}$, $\varepsilon_{330nm} = 1.4 \times 10^4 M^{-1} cm^{-1}$, $\varepsilon_{420nm} = 6.0 \times 10^3 M^{-1} cm^{-1}$, $\varepsilon_{453nm} = 7.1 \times 10^3 M^{-1} cm^{-1}$, $\varepsilon_{540nm} = 3.5 \times 10^3 M^{-1} cm^{-1}$)(66). FLDR ($\varepsilon_{456nm} = 7100 M^{-1} cm^{-1}$) (111). FLD ($\varepsilon_{466nm} = 8250 M^{-1} cm^{-1}$ FLD has a ratio of $A_{274nm} / A_{466nm} = 5.8$) (104).

2 22 Mini Induction of Proteins

A single colony from a freshly transformed plate was placed in LB or 2YT (2ml - 10ml) containing ampicillin. The cells were grown to an $OD_{600nm} = 1.0$ and divided equally into two aliquots. One sample was induced with IPTG (1mM) while the other served as a control. Both samples were then allowed to grow for a further three hours prior to being centrifuged (13000rpm, 30s). The supernatants were discarded and the pellets were resuspended in SDS sample buffer (100µl), boiled (5min) and loaded (15µl) onto a SDS gel (15%).

2.23 Preparation of a *bio*⁻ Cell Free Extract

LB (10ml) containing tetracycline (10μg/ml) was inoculated with PCOi from either frozen stock or a fresh agar plate. The culture was grown overnight (37°C, shaking 250rpm) before being subcultured into fresh LB containing tetracycline (2.5 ml into 250ml x 4). The cells were grown as before for 6h. Centrifugation (5000g, 10min, 4°C) was carried out to harvest the cells and the cell pellet was washed and resuspended in buffer A (1 ml of buffer per 0.25 g of cells). The cell suspension was sonicated for 15 min (30s on with 30s rest, 4°C) and the sonicated sample was then centrifuged (10000rpm, 20min, 4°C) to get rid of cellular debris. The supernatant cell free extract was aliquoted into Eppendorf tubes and stored frozen (-80°C) in glycerol (15 %).

2.24 Large Scale Preparation of *E.coli* Flavodoxin

Transformant JM101/pDH1 was grown in 2 - 10 litres of LB containing ampicillin (100μg/ml) to OD_{600nm} = 1.0 and production of FLD was induced by the addition of IPTG (100μM). Riboflavin (5mg/l) was also added to the culture at the time of induction. The cells were harvested 6 hours after induction and then the cells (*ca* 1.5g/l wet weight) were washed by resuspension in ice-cold buffer B, broken by intermittent sonication (30s on, 30s off for 15 min) and the cell lysate collected after centrifugation. Protamine sulfate was added to a final concentration of 0.1% (w/v) to the extract and the mixture centrifuged (15000g for 30minutes, 4°C). The filtered (0.45μM) supernatant was loaded directly on a Q-Sepharose 26/10 Hi-Load anion exchange column (2.6cm x 10cm) which had been pre-washed in buffer C and FLD was eluted from the column in a gradient of NaCl (0 - 1M, 10CV) in buffer C, between 375 and 425mM NaCl. The pH of the bright orange FLD-containing fractions was increased to pH 7.5 immediately following elution by dialysis against buffer B. This single-step procedure resulted in a fraction in which >90% of the protein was FLD. Further purification was achieved by a second anion exchange chromatography step using a Resource Q column (0.64cm x 3cm). Protein was loaded in buffer B and eluted using a linear gradient of NaCl (0 - 1M, 10CV) in buffer B. Pure FLD was eluted between 350 and 400mM NaCl. The final FLD fraction was dialysed against buffer B, concentrated by ultrafiltration (Amicon, 10000Da cut-off) to *ca* 5mg/ml and stored frozen at -20°C.

2.25 Large Scale Preparation of *E. coli* Flavodoxin (ferredoxin) $NADP^+$ oxidoreductase

Transformant HMS174 (DE3)/pCL21 was grown in 2 - 10 litres of LB media containing ampicillin (100μg/ml) to an OD_{600nm} = 1.0 and production of FLDR was induced by the addition of IPTG (100μM). Thereafter, growth was continued for 3 hours and the cells (*ca* 2.5g/l wet weight) were harvested by centrifugation (7500rpm for 10 minutes, 4°C), washed by resuspension in ice cold buffer B and lysed by intermittent sonication (30s on, 30s off) for 15 minutes. Cellular debris was removed by centrifugation (10000 rpm for 30 minutes, 4°C) and the filtered (0.45μM) supernatant was loaded directly on a Q-Sepharose 26/10 Hi-Load anion exchange column (2.6cm x 10cm) which had been pre-washed in buffer B. Protein was eluted with a gradient of NaCl (0-1M, 10CV) in buffer B. Yellow FLDR-containing fractions were collected from 130 to 150mM NaCl. These were combined and loaded on a 2', 5'-ADP Sepharose column (1cm x 20cm), pre-equilibrated with buffer B containing 150mM NaCl. Pure FLDR was eluted using buffer B containing 500mM NaCl. The purified enzyme was dialysed against buffer B, concentrated by ultrafiltration (Amicon, 10000Da cut-off) to *ca* 5mg/ml and stored frozen at -20°C.

2.26 Preparation of Biotin Synthase Cell Free Extracts

Wild-type biotin synthase (from HMS174 (DE3)/pET16b/bioB or B834 (DE3)/pET16b/bioB), His_6-tagged biotin synthase (from HMS174 (DE3)/pET6H/bioB) and mutant forms (from HMS174 (DE3)/pC53S, pC57S, pC60S, pC188S and pC288T) were prepared from cultures grown in 2 - 10 l of 2YT media containing ampicillin (100μg/ml). Transformed cells were grown at 37°C (shaking 250rpm) until the OD_{600nm} = 1.0. and transcription induced by addition of IPTG to a final concentration of 1mM. Cells (*ca.* 2.5g/l wet weight) were harvested (5000g for 10 minutes, 4°C) after a further 4 hours of growth. The His_6-tagged protein pellets and mutant pellets were washed by resuspension in ice cold buffer D. The cell pellets from the wild-type biotin synthase clone were washed in buffer B. The cell pellets were lysed by intermittent sonication (30s on, 30s off) for 15 minutes, cellular debris was removed by centrifugation (15000g for 30 minutes, 4°C) and the supernatants were stored frozen (-20°C) in glycerol (15%).

2.27 Purification of Wild-type Biotin Synthase

Protamine sulphate (1%, 0.5ml per 10ml) was added to the cell free extract to remove nucleic acids. Ammonium sulphate (45%) was then added to the supernatnant and centrifuged. The protein pellets were resuspended in buffer B and filtered (0.45μm) prior to being loaded onto a Q-Sepharose 26/10 high load anion exchange column (2.6cm x 10cm) which had been equilibrated with buffer B. The proteins were eluted with an increasing gradient of potassium chloride (0 - 1M, 10CV) in buffer B. The fractions containing biotin synthase eluted at *ca* 300mM salt and were red in colour. They were combined and ammonium sulphate (10%) was added. This was then loaded onto a Phenyl Sepharose hydrophobic interaction column (1cm x 30cm) which had been equilibrated with buffer B containing ammonium sulphate (10%). Biotin synthase was eluted with a decreasing gradient of buffer B containing ammonium sulphate (10 - 0%, 10CV). Biotin synthase eluted at the end of the gradient. The fractions containing biotin synthase were combined and filtration concentrated (Amicon, 10000Da cut-off). The concentrated protein was loaded onto a Sephacryl S-200 HR gel filtration column (2.6cm x 60cm) and eluted with buffer B. Protein samples were stored frozen (-80°C) in glycerol (15%).

2.28 Purification of His_6-tagged Biotin Synthase and Mutants

Transformant HMS174 (DE3) pHisB was grown in 2YT containing ampicillin (100μg/ml) and incubated overnight (37°C, shaking 250rpm). The overnight culture was then subcultured into fresh 2YT amp and incubated as above until the OD_{600nm} = 1.0. The cells were then induced with IPTG (1mM) and grown for a further 3 - 6h. The cells were harvested by centrifugation (7500rpm, 10min, 4°C) and then washed with buffer D. The wet weight of the cells was determined and they were resuspended in buffer D (0.25g cells/1ml buffer). The cells were sonicated on ice (30s on, 30s off, 15min) and centrifuged (10000rpm, 20min, 4°C). The supernatant was filtered (0.45μM filter) and loaded on to a Hitrap® chelating affinity column (5ml, Pharmacia, 4°C) which had been charged with Ni^{2+} ($NiSO_4$, 100mM). The column was then washed with buffer D and the protein eluted with buffer E. The pure protein was immediately dialysed against buffer B and then stored at -20°C in glycerol (15%). Four of the biotin synthase mutants (C53S, C57S, C60S and C288T) were also purified using this protocol.

2.29 Preparation of Apo- and Holo- Wild-type Biotin Synthase and Mutant Proteins

These experiments were carried out using the methods of both Sanyal (66) and Marquet (153).

2.30 Purification of *Azotobacter vinelandii* NifS

The purification and assays were carried out as described by Zheng (92).

2.31 Chemical Cross-linking of Flavodoxin (ferredoxin) $NADP^+$ oxidoreductase and Flavodoxin

Purified FLD (40μM) and FLDR (8μM) were covalently cross-linked using 1-ethyl-3-(dimethylamino-propyl) carbodiimide (10mM) in Hepes buffer (10mM, 2 ml, pH 7.0) at room temperature. Aliquots were withdrawn from the reaction at 15 minute intervals to assess the progress of the reaction by SDS-PAGE. After 1 hour, the reaction was stopped by the addition of ammonium acetate (100mM) and the protein mixture concentrated to approximately 0.5ml by ultrafiltration (using a 10kDa cut-off Centricon concentrator [Amicon]). The cross-linked complex was separated from the FLDR and FLD proteins by gel filtration on FPLC (Superdex 75 column, 1.6 x 60cm) in buffer A containing 50mM KCl (154). The protein (2mg/ml) was stored at -20°C.

2.32 *In vitro* Biotin Production

The assays were carried out aerobically and anaerobically in buffer B. A typical assay mixture contained biotin synthase or mutant protein (5μM), potassium chloride (10mM), dethiobiotin (50μM), SAM (150μM), ferrous ammonium sulphate (5mM), NADPH (1mM), fructose 1,6-bisphosphate (5mM), L-cysteine (500μM), DTT (10mM), PCOi cell free extract (100μl), FLD (12.5μM) and FLDR (2μM). The final reaction volume was typically 1ml. The reaction was incubated at 37°C for 2 hours and then stopped by adding 100μl of 10% TCA. The resulting precipitate was centrifuged and 5μl of the supernatant was used in the bioassay (section 2.34).

2.33 *In vivo* Biotin Production

Transformants of HMS174 (DE3) with pET16b, pET6H, pET16b/bioB, pET6H/bioB, pC53S, pC57S, pC60S, pC188S and pC288T were grown in M9CA media containing dethiobiotin (5μg/ml), glucose (0.4%), thiamine (0.8μg/ml), magnesium sulphate (2mM), calcium chloride (0.1mM) and ampicillin (100μg/ml). At OD_{600nm} = 1.0 the cells were equally divided and one sample was kept as a control while the other was induced with IPTG (1mM). HMS174 (DE3) was used as a control and was grown in the same media minus the ampicillin. Aliquots of the medium (1ml) were removed from both control and induced samples at various time intervals and held at 4°C. The cells were then pelleted by centrifugation and 5μl of the supernatants were used in the bioassay (section 2.34).

2.34 *Lactobacillus* Bioassay

In vitro and *in vivo* biotin production was determined using the *Lactobacillus assay* (155).

2.35 Steady-state Kinetics

UV/Vis spectroscopy and steady-state kinetics were carried out using a Unicam UV4 and Shimazdzu 1201 spectrophotmeters. Steady-state kinetic parameters for FLDR and FLD were measured at 30°C in buffer B. Reduction of cytochrome *c* (horse heart, type 1) was monitored by absorbance increase of the Sorret band (ε_{550nm} = 22640$M^{-1}cm^{-1}$). Reduction of potassium ferricyanide was measured by absorbance decrease at 420nm (ε = 1010$M^{-1}cm^{-1}$).

Measurements of P-450BM3 haem domain-catalysed arachidonic acid oxidation supported by FLDR and FLD were performed as described previously for the catalysis of pregnenolone oxidation by P-450c17 (113). To determine the mechanistic nature of the FLDR/FLD/P-450BM3 interactions, a series of oxidation rate measurements were performed in the presence of saturating NADPH (1mM), FLD (25μM), FLDR (0.25-10μM) and the P-450BM3 haem domain at 0.76μM, 2.54μM or 3.81μM. Reaction rates were determined at 30°C in buffer B and the reciprocals of the data plotted against the reciprocals of the concentration of FLDR for each concentration.

2.36 Pre-steady State Kinetics

Stopped flow kinetic analyses were carried out using an Applied Photophysics SF.17 MV spectrophotometer. Reactions were performed anaerobically at 30°C in buffer B. Absorbance

changes associated with flavin reduction of FLDR (40μM) by NADPH (4μM - 2mM) were monitored at 456nm. The electron transfer from FLDR to FLD was monitored at 583nm (formation of FLD blue semiquinone, $\varepsilon = 4933 M^{-1}cm^{-1}$) after mixing reduced FLDR (40μM, pre-reduced with 2mM NADPH or sodium dithionite) with FLD (20μM).

When sodium dithionite was used, FLDR was reduced completely in an anaerobic environment with excess reductant, then separated from the dithionite by gel filtration under anaerobic conditions. Reoxidation of FLDR was measured by mixing the reduced protein (80μM) with a sub-stoichiometric quantity of NADPH (40μM) and monitoring the absorbance increase at 456nm. Reoxidation of the FLD semiquinone (absorbance decrease at 583nm) was measured after anaerobic reduction of the enzyme with excess sodium dithionite, isolation of the reduced enzyme by gel filtration and dilution of reduced FLDR into aerobic buffer. Reduction of cytochrome *c* was measured at 550nm after reaction of reduced FLDR (10- 50μM enzyme + 2mM NADPH) with cytochrome *c* (horse heart, type 1;4μM). Analysis of stopped-flow data were performed using the SF.17 MV software and Origin (Microcal), both of which use non-linear least-squares regression analysis.

2.37 Elemental Analyses

Inductively coupled plasma atomic emission spectroscopy [ICP-AES] was used for metal analyses. All data were interpreted using thermospec/CID software. The R.F. Power was 1150 watts, the nebulizer flow was 30 psi, the pump rate was 100rpm and the purge time was 90s. $Fe(NO_3)_3$ (0.01-100ppm; 180nM-1.8mM) and $Ni(NO_3)_2$ (0.0001-1.0ppm; 1.7nM - 17mM) solutions were used as standards. All biotin synthase samples (27μM) and standard solutions were made up in buffer B (156).

Chemical analysis for iron was carried out using the Ferrozine assay as described by Stookey using the standard described above (157). Labile sulfide analysis was determined as previously reported (66).

2.38 Mass Spectrometry

Electrospray mass spectrometry was performed on a Micromass Platform II quadrupole mass spectrometer equipped with an electrospray ion source. The mass spectrometer cone voltage was set to 70V and the source temperature to 65°C. Protein samples were separated on a Gilson HPLC system using a Aquapure reverse phase C-4 column at a constant TFA

concentration of 0.1% using a linear gradient of 10-100% acetonitrile in water over 40 min at a flow rate of 1ml/min. The total ion count of all the ions in the m/z range 500 to 2000 and the UV chromatogram at 280nm were recorded for the revered-phase HPLC separation. The mass spectrometer was scanned at intervals of 0.1s, the scans accumulated, the spectra combined and the average molecular mass determined using the MaxEnt and Transform algorithms of MassLynx software.

2.39 Electroblotting of Proteins

Protein samples were run on a SDS gel (15%, 40min, 200V), and then the gel was soaked in electroblot buffer (5 min). At the same time the problot membrane (same size as gel) was soaked in methanol for a few seconds. The electroblot was set up with the membrane closest to the anode and the gel closest to the cathode. Transfer was carried out at 50V for 2h at RT. The membrane was rinsed with distilled water, stained with Ponceau S (2% in 1% acetic acid, 1min) and then rinsed with distilled water. The bands of interest were then excised using a scalpel.

2.40 Tryptic Digest of Proteins

Protein samples were separated on SDS gels (15%) and stained with Coomassie G-250. The protein bands of interest were excised along with a control band of gel that contained no detectable protein. The gel strips were allowed to dry before being resuspended in AB buffer (20µl), chopped into 2-3mm pieces and put into Eppendorf tubes. AB buffer (100µl) and modified trypsin (1µl of 20µg/50µl) were then added. Samples were incubated overnight (37 °C, shaking 250rpm), centrifuged (13000rpm, 10min) and the supernatants transferred to fresh tubes. AB buffer (100µl) was added to the pellet which was then left at 37 °C for 1h. Samples were centrifuged as before and the supernatants combined. The supernatants were stored at -20°C until needed.

Aqueous acetonitrile (40%) was sometimes used as an alternative to AB in the above digest.

2.41 Protein Sequencing

N-terminal sequencing was done using an ABI 477A protein sequencer using the automated Edmann degradation method (158). Tryptic digests were separated using an ABI 130A

microbore HPLC using solvent A (0.1% TFA in water) and solvent B (0.08% TFA in 70% acetonitrile). The proteins were eluted with a linear gradient from 0 to 70% solvent B over 1h. The flow rate was 100µl/min at 220nm. The collected protein peaks were then sequenced.

2.42 Potentiometric Titrations

All redox titrations were conducted within a Belle Technology glove box under a nitrogen atmosphere (O_2 < 5p.p.m). Degassed, concentrated protein samples were passed through an anaerobic Sephadex G25 column (1 x 20cm) immediately on admission to the glove box. The column was equilibrated and proteins were eluted with buffer B. Protein solutions were titrated electrochemically according to the method of Dutton using sodium dithionite as reductant and potassium ferricyanide as oxidant (159). Mediators were introduced prior to titration; typically 2-hydroxy-1,4-napthaquinone (5µM), benzyl viologen (1µM) and methyl viologen (1µM) within sample volumes of 5-10ml. After 10-15 minutes equilibration following each reductive/oxidative addition, spectra were recorded between 350 and 800nm. The electrochemical potential of the sample solutions were monitored using a CD740meter (WPA) coupled to either Pt/calomel or Pt/Ag.AgCl combination electrodes (Russell pH Ltd.) at 25 ± 2°C. The electrodes were calibrated using the Fe^{III}/Fe^{II} EDTA couple as a standard (+108mV). The calomel and Ag.AgCl electrodes were corrected by +244 ± 2mV and +198 ± 3mV respectively, both relative to the normal hydrogen electrode. For experiments involving FLDR, UV/Vis spectra were affected by the slow formation of a protein precipitate, which resulted in a small increase in baseline absorbance with time. This was corrected for by transforming each spectrum with a $1/\lambda$ subtraction calculated to return the absorbance at 800nm back to zero (at this wavelength chromophore absorbance is minimal). All data manipulations and non-linear least squares curve fitting of electrochemistry data were conducted using Origin (Microcal).

2.43 Fluorimetry

All experiments were carried out using a Shimadzu RF530IPC spectrofluorimeter. Excitation and emission fluorescence was carried out on free FMN (4µM). For excitation spectra the emission wavelength was 525nm (slit width 1.5nm) and the excitation wavelength was from 450nm to 700nm (slit width 3nm). For emission spectra the excitation wavelength was 450nm (slit width 1.5nm) and the emission wavelength from 450nm - 700nm (slit width 3nm). Flavin fluorescence was carried out on free FMN (0.7µM) and FLD (9.8µM) with an excitation

wavelength of 450nm (slit width 3nm) and an emission wavelength from 450nm to 700nm (slit width 5nm). It was also carried out on both FLD (73μM) and FLDR (50μM) in the presence of GdnHCl (between 0 and 6.7M). The excitation was at 450nm (slit width 5nm) and the emission was between 500 and 600nm (slit width 10nm). A time course was carried out on FLD (240μM) in GdnHCl (6.7M) where samples were removed at time intervals between with the final sample being boiled (5min). Tryptophan fluorescence was carried out on both FLD (480nM) and FLDR (310nM) in the presence of GdnHCl (between 0 and 6.7M). The excitation was at 290nm (slit width 5nm) and the emission was between 300nm and 400nm (slit width 5nm). All experiments were carried out in buffer B in a 1cm fluorimetry cell.

2.44 Circular Dichroism

All CD experiments were carried out on a Jasco Spectroplarimeter. Far UV (190nm-260nm) CD of FLD (30μM), FLDR (20μM) and a one to one mixture of FLD (15μM) and FLDR (10μM) was measured in buffer B at 10nm/min in a 0.02cm cell. Near UV CD (260nm-320nm) of FLD (75μM), FLDR (50μM) and a one to one mixture of FLD (37.5μM) and FLDR (50μM) were measured at 10nm/min in a 0.5cm cell. Visible CD of FLD (75μM), FLDR (50μM) and a one to one mixture of FLD (37.5μM) and FLDR (50μM) were measured at 20nm/min in a 0.5cm cell. Far UV, near UV and visible CD of FLD and FLDR were also measured in the presence of varying concentrations of GdnHCl using the same concentrations and conditions mentioned above.

2.45 Analytical Ultracentrifugation

In order to determine the operational molecular masses of FLDR and FLD (15μM) sedimentation equilibrium (SE) and velocity (SV) studies were performed on a Beckman Optima XL-A AUC. The AUC was equipped with 6-channel, 1.2 cm pathlength centrepieces and scanning optics to measure the equilibrium solute distribution.

2.46 Crystallisation Trials

Structure screen I (Molecular Dimensions Ltd) was used and an aliquot of each solution (300μl) was placed in a well of a Linbro® multi-well plate. Concentrated protein samples

(5mg/ml, 2µl) and well solution (2µl) were placed on a siliconised cover slip which was then placed upside down over a parrafin wax coated well lip in a hanging drop fashion.

2.47 Sequence Alignments

Swissprot (http://www.expasy.ch/sprot/) and the Genomes Representation Organisation (http://www.ncbi.nlm.nih.gov/Entrez/Genome/org.htm) databases were used to search for amino acid sequences which were then aligned using Expasy (http://www.expasy.ch/), Clustal W (http://www2.ebi.ac.uk/clustalw/) and Alscript (160).

2.48 Vector NTI 5

This programme was used for drawing plasmids, manipulation of both nucleic acid and protein sequences and primer design.

Chapter 3: Characterisation of FLDR and FLD

3.1 Introduction

FLDR is a monomeric (247 amino acids, M_r 27620) enzyme which contains FAD. FLD is a small (177 amino acids, M_r 19606) acidic flavoprotein which contains FMN as its prosthetic group. FLD is used in electron transport where it transfers electrons from NADPH *via* FLDR to a variety of systems. Characterisation of these proteins is essential to understand their roles in numerous biological pathways.

The aim of this work was to obtain milligram quantities of homogeneous *E. coli* FLDR and FLD for characterisation by a number of biophysical techniques, including SDS PAGE, electrospray mass spectrometry, potentiometric titrations, AUC, fluorimetry and circular dichroism.

The plasmid, pDH1, was a gift from Rowena Matthews and David Hoover. The plasmid, pEE1010, was a gift from Elizabeth Haggard Lindquist. Claire Leadbeater and Dominic Campopiano did the subcloning and construction of pCL21 and I would like to thank them for allowing me to use their data.

3.2 Cloning of the *fldr* and *fldA* genes

The *fldr* gene was amplified from the plasmid pEE1010 using the primers RED FOR (5'-CAG GAG AAT T**CC ATG G**CT GAT TGG GTA ACA GGC-3') which incorporated a *Nco*I site (5'-C/CATGG-3' in bold) and RED REV (5'-ATA A**GG ATC C**GC TTA CCA GTA ATG CTC CGC TGT CAT-3') which incorporated a *Bam*HI site (5'-G/GATCC-3' in bold). The PCR product and pET16b were both digested with *Nco*I and *Bam*HI. They were ligated together and the resulting plasmid was named pCL21 (Figure 3-1a).

FLD was produced from pDH1 transformed into *E. coli* JM101. pDH1 is a p*Trc*99A-derivative with the *fldA* gene cloned downstream of a powerful P_{trc} promoter system that is IPTG inducible (Figure 3-1b). P_{trc} is a hybrid of the *trp* and *lac* -10 and -35 promoters.

Figure 3-1a

The plasmid pCL21 (6389bp), which contains the *fldr* gene inserted using *Nco*I / *Bam*HI sites, was used for the overexpression of FLDR. The gene is under control of the T7 promoter-driven system.

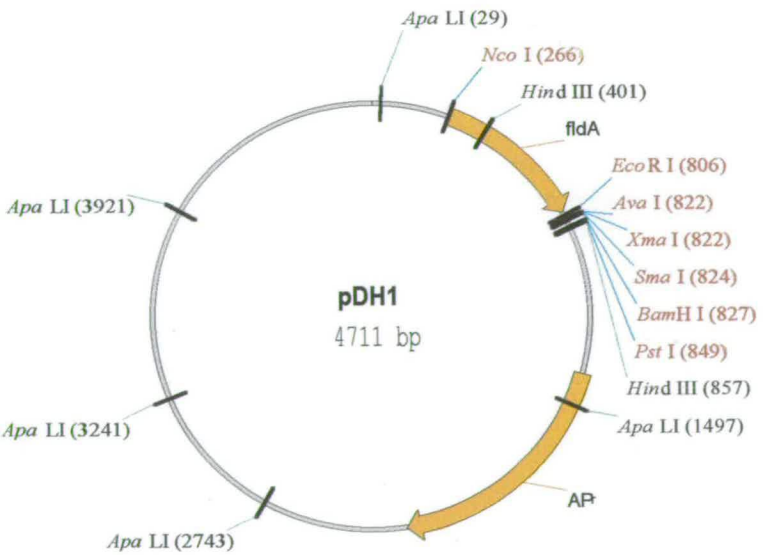

Figure 3-1b

Plasmid pDH1 (4711bp), that contains the *fld*A gene, cloned downstream of the P_{trc} promoter and upstream of a strong *rrn*B transcription termination signal.

3.3 Overexpression and purification of FLDR

E. coli HMS174 (DE3)/pCL21 was used to overexpress FLDR and the protein was purified by sequential chromatography steps on Q-Sepharose and 2', 5'-ADP Sepharose. Samples were analysed at all steps by SDS-PAGE (Figure 3-2) and UV/visible spectroscopy. Routinely, approximately 23mg of pure FLDR/litre of cells were produced. The re-cloning of the *fldr* gene into vector pET 16b (to generate pCL21) along with an improved purification scheme (2 steps rather than 4) allowed significantly higher levels of recovery of FLDR compared to the original clone in pEE1010, which gave *ca* 3.5mg/l. Transformants of pCL21 in strain BL21 (DE3) resulted in even higher expression of *fldr* (*ca* 35mg/l); but the specific activity of the purified FLDR was considerably lower than that purified from the HMS174 (DE3) strain, probably due to low flavin content.

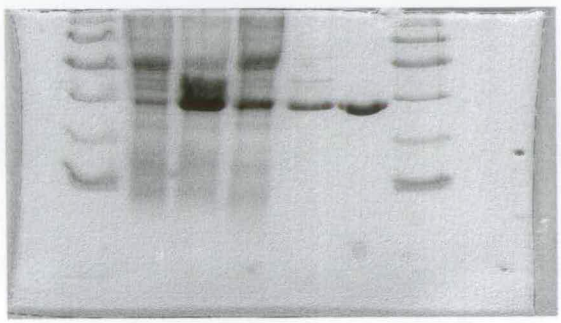

Figure 3-2

SDS PAGE of *E. coli* Flavodoxin $NADP^+$ oxidoreductase purification steps. Lane 1: Molecular weight standards (94000, 67000, 43000, 30000, 20100, 14400 Da), Lane 2: Uninduced intact cells, Lane 3: Induced intact cells, Lane 4: Cell lysate, Lane 5: Q-Sepharose, Lane 6: 2', 5'-ADP Sepharose, Lane 7: Low molecular weight standards (as Lane 1).

The molecular weight of the expressed FLDR apoprotein was determined as 27648 Da by electrospray mass spectroscopy. This is 28 Da higher than the predicted molecular mass of 27620 Da calculated from the amino acid sequence derived from the database gene sequence (less the N-terminal methionine). However, the recent solution of the atomic structure of the *E. coli* FLDR indicates that an arginine is present at position 126, as opposed to a glutamine predicted from the gene sequence. The difference in molecular mass of these two residues is exactly 28 Da, corresponding to the apparent discrepancy which is in the DNA sequence and not the atomic structure (110). The isoelectric point of FLDR was measured as 4.8 by

isoelectric focusing; rather more acidic than the theoretical value of 6.19 (SwissProt). FLDR is bright yellow in its oxidised form and it is converted to a neutral blue semiquinone by the addition of one reducing equivalent. FLDR has an extinction coefficient of 7100 $M^{-1}cm^{-1}$ at 456nm (113).

Based on the 7.41-fold purification value calculated using flavin absorbance at this wavelength, the overexpressed FLDR comprises 13.5% of the total soluble protein in the *E. coli* extract (Table 3-1).

Table 3-1

Purification table for *E. coli* $NADP^+$ flavodoxin oxidoreductase. Total protein was estimated by absorbance at 280nm. FLDR was estimated by measurement of absorbance at the peak of the longer wavelength flavin band (ε_{456nm} = 7100 $M^{-1}cm^{-1}$).

Purification step	Total volume (V) (ml)	Total protein ($VxAbs_{280}$)	Total FLDR ($VxAbs_{456}$)	Abs_{456}/Abs_{280}	Purification fold
Lysate	55	833.9	18.26	0.0207	1
Q-Sepharose	80	119.1	9.28	0.0779	3.77
2',5'-ADP Sepharose	35	37.5	5.74	0.1531	7.41

3.4 Overexpression and purification of FLD

The purification of FLD was followed by a combination of SDS-PAGE (Figure 3-4) and spectroscopic characterisation (Table 3-3) on FLD-containing fractions. SDS-PAGE analysis of the purified protein showed a single species which migrated at m = 20 kDa. A molecular weight of 19606 Da was recorded by electrospray mass spectrometry. The isoelectric point of FLD was measured as 3.5 which was slightly more acidic than the theoretical value of 4.21 (SwissProt). Typically, between 20 and 30mg of pure FLD per litre was produced from JM101/pDH1.

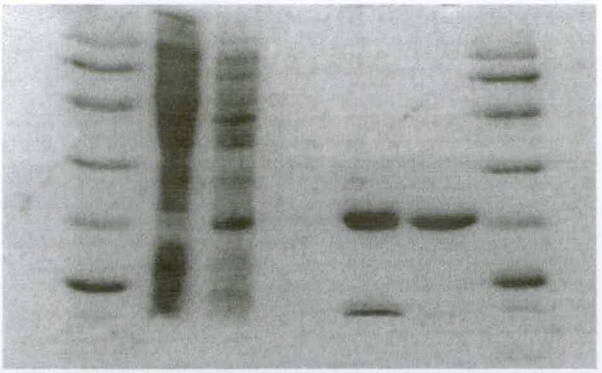

Figure 3-3

SDS PAGE of *E. coli* flavodoxin purification steps. Lane 1: Low molecular weight standards (94000, 67000, 43000, 30000, 20100, 14400 Da). Lane 2: Uninduced cell lysate. Lane 3: Induced cell lysate. Lane 4: Empty. Lane 5: Q-Sepharose. Lane 6: Resource-Q. Lane 7: Low molecular weight standards (as Lane 1).

Fractions containing the protein had a distinct bright orange colour that is expected for flavodoxin in its oxidised state. Pure FLD has an extinction coefficient of 8250 $M^{-1}cm^{-1}$ at 466nm and a ratio of OD_{274}/OD_{466} of 5.8 (104). Total protein recovery was estimated at 37% based on the purity of FLD at the end of the short purification scheme and the assumption that the absorbance at 466nm is specific for the overexpressed protein. Clearly, other *E. coli* flavin-containing proteins (as well as those containing *e.g.* haem or iron-sulfur centres) will have absorbance in this region; so this figure is likely to be an underestimate. Based on an 8.8-fold purification value, the overexpressed flavodoxin comprised 11.4% of the total soluble protein in the *E. coli* extract.

Table 3-2

Purification table for *E. coli* flavodoxin. Total protein was estimated by absorbance at 274nm. FLD was estimated by measurement of absorbance at the peak of the longer wavelength flavin band (ε_{446nm} = 8250$M^{-1}cm^{-1}$).

Purification Step	**Total Volume (V) (ml)**	**Total Protein ($VxAbs_{274}$)**	**Total Flavodoxin ($VxAbs_{466}$)**	**Abs_{466}/Abs_{280}**	**Purification fold**
Cell Lysate	23	1166.1	21.62	0.0185	1
Q-Sepharose	120	62.52	7.68	0.123	6.65
Resource-Q	4.8	46.5	7.54	0.162	8.76

3.5 Spectroscopic Characterisation of FLDR and FLD

FLDR and FLD were examined using UV/visible spectroscopy, fluorescence and CD spectroscopy.

3.5.1 UV/visible spectroscopy of FLDR and FLD

A visible scan was carried out on FLDR (40μM), free FMN (34μM) and on pure oxidised FLD (60μM). The oxidised FLDR had flavin absorbance maxima at 456nm and 400nm, with a shoulder on the longer wavelength band at 483nm (Figure 3-4a).

In the visible region free FMN has absorbance maxima at 373nm (ε_{373nm} = 10400 M^{-1} cm^{-1}) and at 445nm (ε_{445nm} = 12500 M^{-1} cm^{-1}). Oxidised pure FLD had flavin absorbance maxima at 372nm and 466nm, with a distinct shoulder on the longer wavelength band at *ca* 495nm and a less obvious shoulder at *ca* 438nm (Figure 3-4b). As can be seen from Figure 3-4b the environment of FMN is significantly perturbed when it is bound to FLD. The peak in the 373nm region is reduced and shifted slightly to a shorter wavelength and the peak at 445nm is shifted to the longer 466nm wavelength.

3.5.2 Fluorimetry

Fluorimetry is a very useful technique and it can be used to examine many aspects of the nature, integrity and kinetic properties of flavoproteins.

FAD has two absorbance maxima 375nm (9300$M^{-1}cm^{-1}$) and 450nm (11300$M^{-1}cm^{-1}$) and an emission maximum at 525nm when excited at 450nm. The excitation and emission spectra of free FMN (4μM) show that it has absorbance maxima in the visible region at 373nm (ε_{373nm} = 10400 M^{-1} cm^{-1}) and 445nm (ε_{445nm} = 12500 M^{-1} cm^{-1}) and a fluorescence maxima at 525nm (Figure 3-5a).

To examine the fluorescence of FMN when it is bound to FLD, emission spectra of both free FMN (0.7μM) and FLD (9.8μM) were carried out. It is immediately obvious that the fluorescence of the free FMN is greatly reduced when it is bound to FLD (Figure 3-5b).

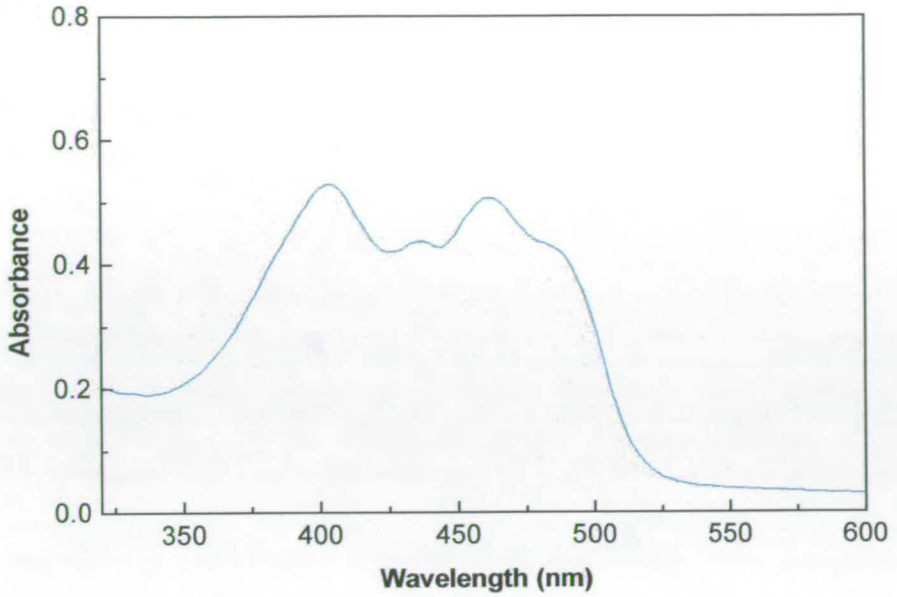

Figure 3-4a

UV/vis spectra of FLDR (40μM) in 100mM sodium phosphate pH7.5.

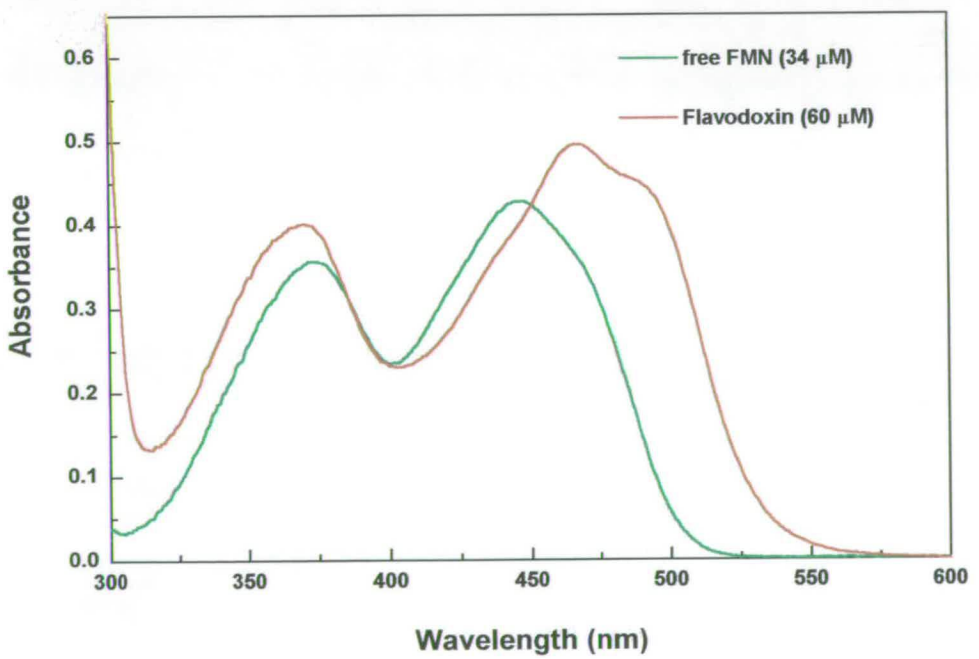

Figure 3-4b

The visible absorption spectra of free FMN (34μM, green) and FLD (60μM, red). The environment of FMN in FLD significantly perturbs the spectrum. The samples were prepared in 100mM sodium phosphate pH7.5.

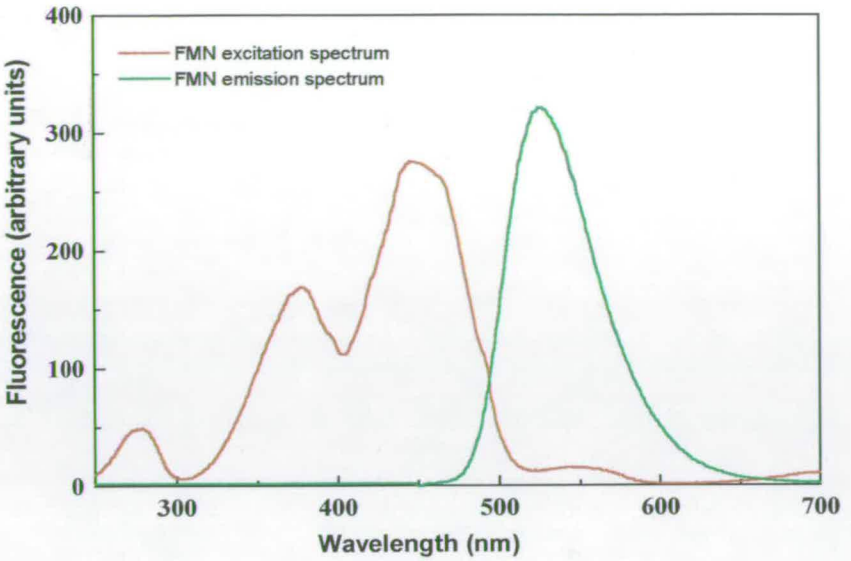

Figure 3-5a

Fluorescence excitation (red line) and emission (green line) spectra of free FMN (4μM, in 100mM sodium phosphate pH7.5). For excitation spectra emission was measured at 525nm with spectral bands widths at 3nm (excitation) and 1.5nm (emission). For emission spectra excitation was at 450nm with spectral band widths at 1.5nm (excitation) and 3nm (emission).

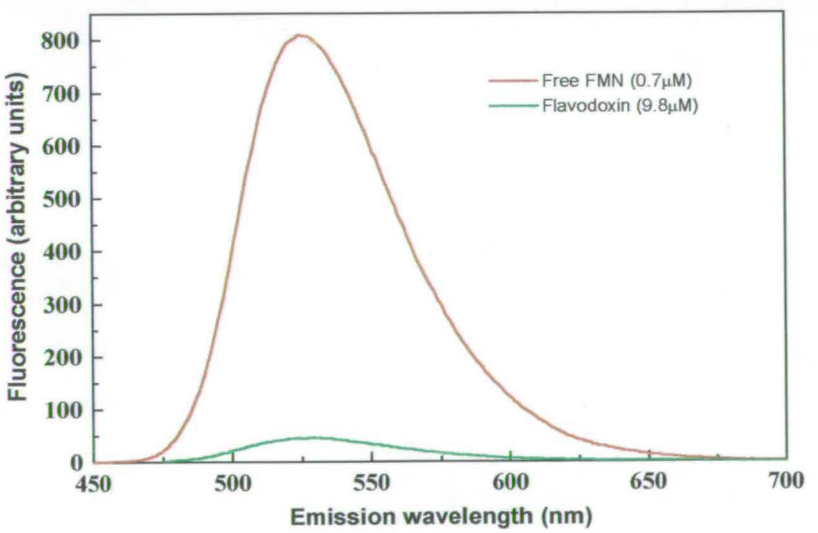

Figure 3-5b

Fluorescence emission spectra of both free FMN (red, 0.7μM) and *E.coli* FMN-containing FLD (green, 9.8μM). FMN fluorescence is very strongly quenched in FLD and the emission intensity is much reduced. Samples were in 100mM sodium phosphate pH7.5 and excitation was at 450nm with spectral band widths at 3nm (excitation) and 5nm (emission).

Chemical denaturation of FLDR and FLD was carried out using GdnHCl and the loss of the protein's tertiary structure was measured. This was achieved by measuring the fluorescence of the aromatic amino acid, tryptophan as its indole ring absorbs UV light at 280nm (ε=5050$M^{-1}cm^{-1}$) and it has an emission maxima between 320-360nm depending on the protein environment. FLDR (310nM) and FLD (480nM) were incubated with varying concentrations of GdnHCl (0 to 6.7M). As can be seen in FLDR the FAD adenine ring causes some quenching of the fluorescence from the isoalloxazine system(Figure 3-6a). As the protein unfolds, the emission maxima shifts from 320nm to 360nm, and the emission intensity increases.

In a similar study with FLD, fluorescence intensity decreases and the emission maximum shifts from 330nm to 350nm as the protein unfolds (Figure 3-6b).

The flavin environments of FLDR and FLD were also examined under denaturing conditions. FLDR (50μM) and FLD (73μM) were incubated in varying concentrations of GdnHCl (0-6.7M). Examination of the results of FLDR fluorescence show that GdnHCl induces unfolding of the enzyme and releases quenching of the FAD fluorophore by the enzyme (Figure 3-7a). The fluorescence is enhanced so much at 6M GdnHCl that the enzyme had to be diluted four-fold to keep the spectrum on scale.

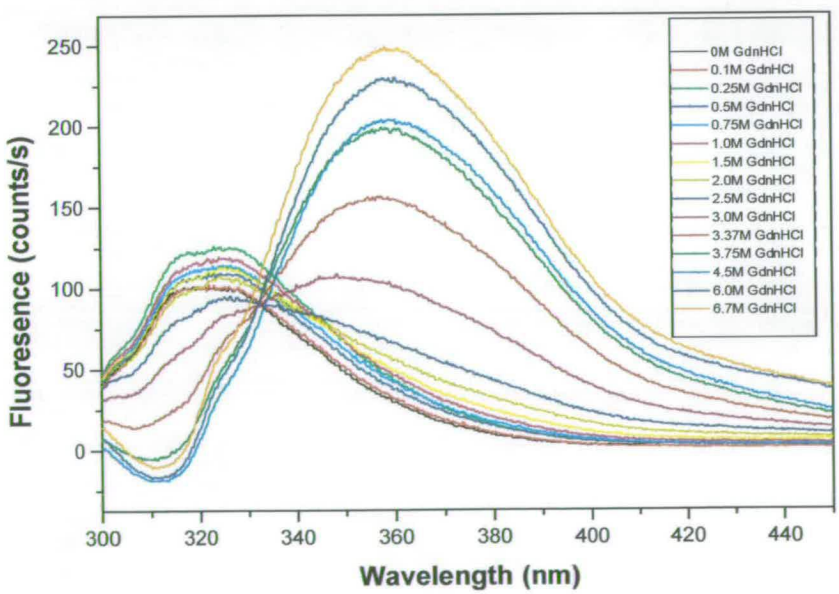

Figure 3-6a

GdnHCl-induced tryptophan fluorescence of FLDR (310nM). Excitation was carried out at 290nm and emission was measured between 300nm to 400nm (spectral band width was 5nm). All samples were in 100mM sodium phosphate pH7.5. Inset shows molar concentrations of GdnHCl.

FLD flavin fluorescence is also greatly enhanced as the concentration of GdnHCl increases (Figure 3-7b). In both cases, increasing flavin fluorescence may be explained by increased solvent exposure of the bound cofactor, disruption of interactions between flavin and aromatic amino acids (which lead to quenching of fluorescence) or complete dissociation of the flavin. To further examine the FMN environment another experiment was carried out where FLD (240μM) was incubated in GdnHCl (6.7M) and samples were taken over time. The final sample was boiled for 5 minutes to completely denature the protein. From the results it can be seen that the fluorescence increases over time indicating that the protein is very stable and binds its flavin very tightly (Figure 3-7c).

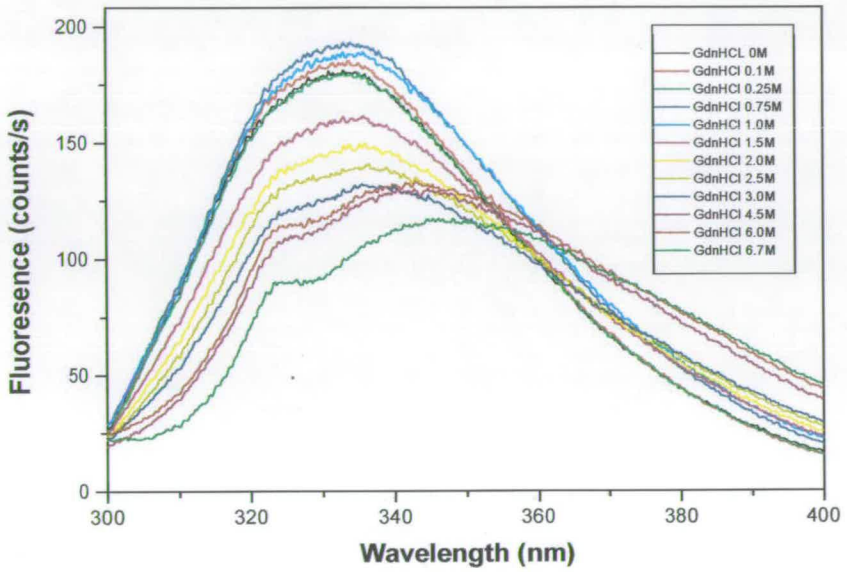

Figure 3-6b

GdnHCl-induced tryptophan fluorescence of FLD (480nM). Excitation was carried out at 290nm and emission was measured between 300nm to 400nm (spectral band width was 5nm). All samples were in 100mM sodium phosphate pH7.5. Inset shows molar concentrations of GdnHCl.

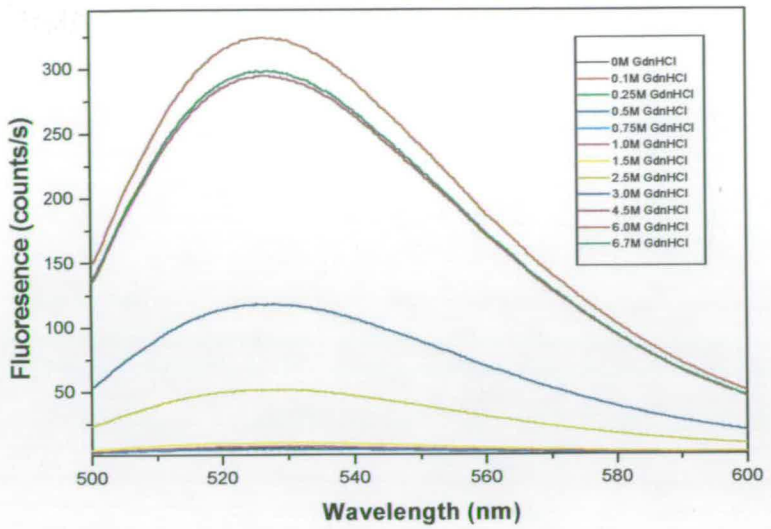

Figure 3-7a

GdnHCl-induced flavin fluorescence of FLDR (50μM, 100mM sodium phosphate pH7.5) was incubated with GdnHCl (0-6.7M). Excitation was at 450nm and fluorescence spectra were recorded between 500nm and 600nm. Spectral band widths were 5nm (excitation) and 10nm (emission). Inset shows molar concentrations of GdnHCl.

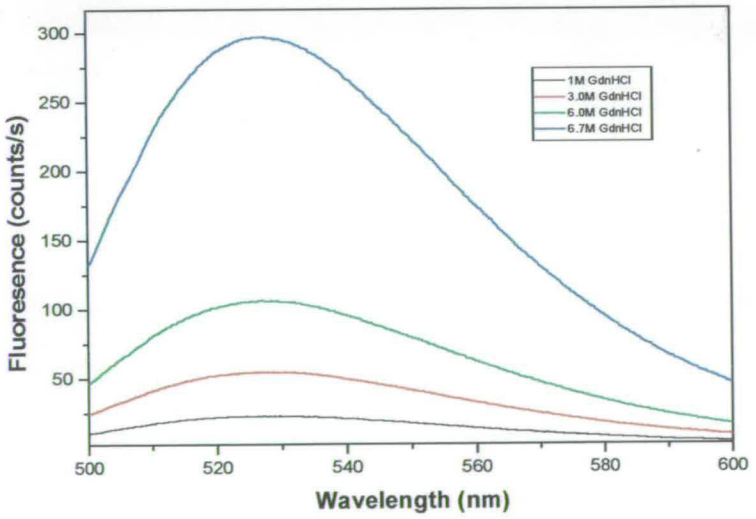

Figure 3-7b

GdnHCl-induced flavin fluorescence of FLD (73μM, 100mM sodium phosphate pH7.5) was incubated with GdnHCl (0-6.7M). Excitation was at 450nm and fluorescence spectra were recorded between 500nm and 600nm. Spectral band widths were 5nm (excitation) and 10nm (emission). Only selected spectra shown. Fluorescence was enhanced as GdnHCl concentration was increased and the FLD unfolded, exposing the FMN cofactor. Inset shows molar concentrations of GdnHCl.

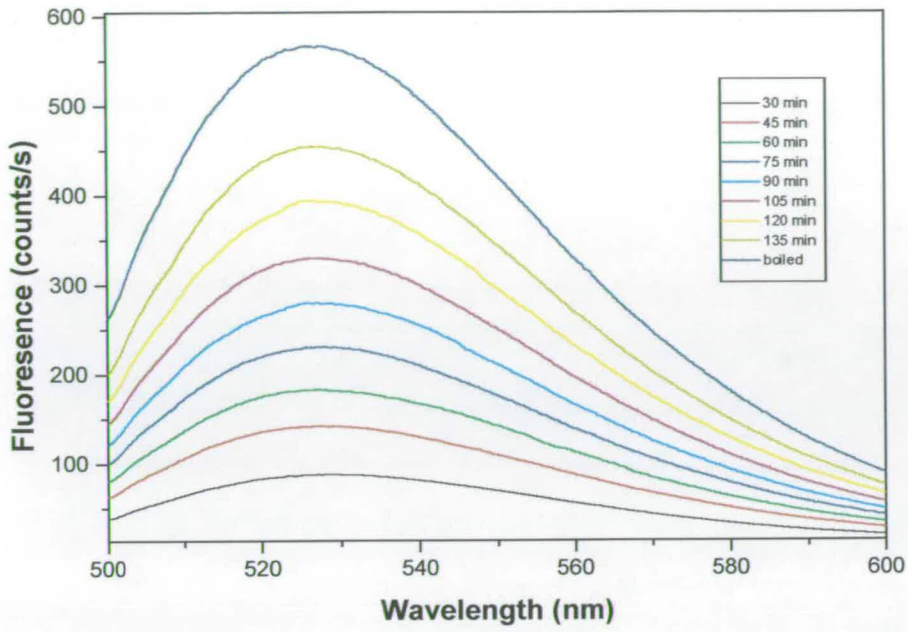

Figure 3-7c

GdnHCl-induced flavin fluorescence in FLD (240μM, 100mM sodium phosphate pH7.5). FLD was incubated with GdnHCl (6.7M) and samples were analysed over time. Excitation was at 450nm and fluorescence spectra were recorded between 500nm and 600nm. Spectral band widths were 5nm (excitation) and 10nm (emission). An increase in fluorescence was observed over time indicating that the protein binds its flavin very tightly and long incubations in the the powerful denaturant are required to dissoicate the cofactor.

3.5.3 Circular Dichroism Spectroscopy

Various CD experiments were carried out on FLDR and FLD both individually and also on a mixture of both proteins. CD in the far-UV range (190-260nm) indicates the presence of a large amount of secondary structure in both proteins (Figure 3-8a). FLDR and FLD show similar CD spectra with negative ellipicity from 202nm to 250nm and positive ellipticity at wavelengths lower than the abcissa at 202nm.

The far-UV CD of the physical mix and the algebraic mix (the combined spectra of the individual proteins) of FLDR and FLD show similar spectra (Figure 3-8b). There is no significant change in intensity of the signal indicating that there are no large changes in secondary structure of either FLDR or FLD when they are physically mixed.

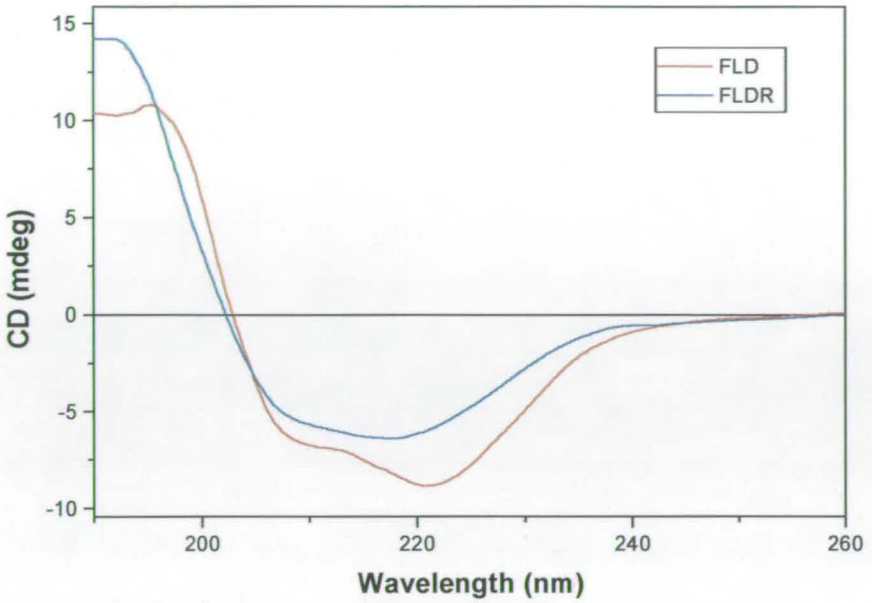

Figure 3-8a

Far-UV CD (190-260nm) of FLDR (20μM) and FLD (30μM) in 50mM Tris-HCl pH7.5, scanned at 10nm/min in a 0.5cm cell. The proteins have distinctive CD spectra, reflecting different secondary structure contents.

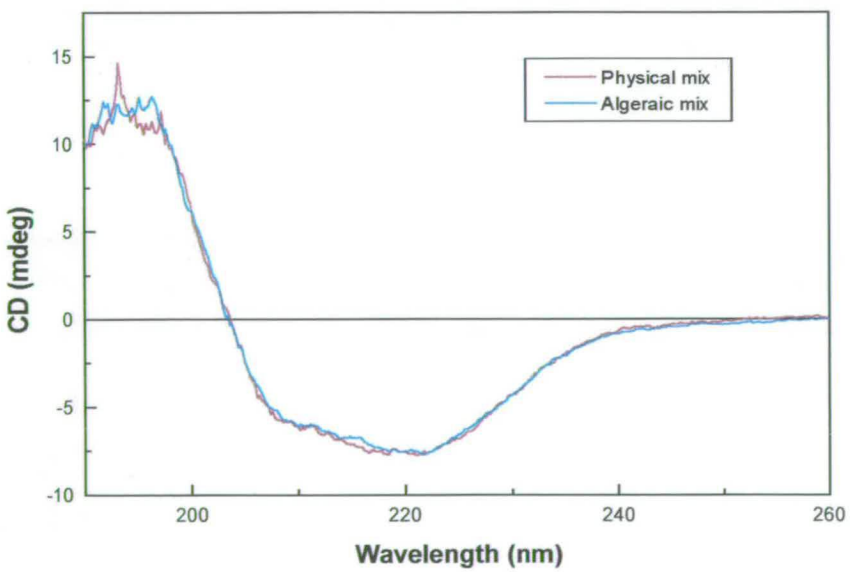

Figure 3-8b

Far-UV CD (190-260nm) of both the physical and algebraic mixes of FLDR (10μM) and FLD (15μM) in 50mM Tris-HCl pH7.5, scanned at 10nm/min in a 0.5cm cell. The algebraic and physical mixtures are essentially identical indicating that FLDR/FLD interactions do not result in major structural alterations.

The near-UV CD (260 - 320nm) signal of FLDR shows positive ellipticity with a large maxima at 274nm. The intensity of the signal may derive from stacking interactions between FAD and one or more aromatic residues of FLDR (Figure 3-9a). The spectra of FLD is more complex and has negative ellipticity from 260nm to 283nm. It then shows positive ellipticity from 283nm to 304nm with peaks at 290nm and 298nm. The spectrum suggests that there are contributions from a number of distinct aromatic amino acids in different environments. Near-UV CD spectra of the algebraic mix of FLDR and FLD shows positive peaks at 270nm, 283nm and 290nm. This spectra of the physical mix is very similar to that of the algebraic mix. However, its intensity is decreased indicating that there is a change in the environment of the aromatic amino acids (Figure 3-9b). The spectra also cross the axes at different points and cross each other at approximately 295nm. this suggests that FLDR/FLD docking does result in alterations in the environments of aromatic amino acids (i.e. tertiary structure perturbations). These strong well defined near UV signals indicate that the aromatic amino acids of the proteins are in well defined chiral environments.

Visible CD (300nm – 500nm) shows clear signals for the flavin cofactors, FAD and FMN (Figure 3-10a). The visible CD spectra of FLDR shows that it has positive ellipicity in the region of the first flavin absorption band (385nm) with a peak at 388nm and a less intense band of negative ellipticity in the region of the second flavin absorption band (456nm), centered at 454nm. FLD shows negative ellipicity from 300nm to 450nm with a maximum CD at 365nm.

The physical and algebraic mixes show small changes in the spectra in the visible CD region with maxima at 350nm and 390nm (Figure 3-10b). The fact that the spectra change slightly and cross each other at approximately 355nm indicates that there is a small change in the environment of one or both of the flavin cofactors on mixing of the two proteins.

Incubation of FLDR with increasing amounts of GdnHCl (0 – 7.04M) causes the loss of secondary structure as can be seen by changes in the far-UV spectra in the 220nm region (Figure 3-11a). The intensity of CD decreases from 210-240nm, consistent with loss of secondary structure. There is a major loss of secondary structure at GdnHCl concentrations higher than 1.5M.

The far-UV CD spectra of FLD in varying concentrations of GdnHCl show that FLD is very stable and shows only very small alterations in secondary structue even at 7M GdnHCl (Figure 3-11b).

Near-UV and visible CD (260 – 600nm) denaturation studies (0 – 5.6M GdnHCl) show that there is a gradual decrease in the overall CD intensity of the FLDR spectra up to concentrations of 4M GdnHCl, indicating loss of the FAD cofactor (Figure 3-12a). There is no change in the FLD spectra (Figure 3-12b) even at GdnHCl concentrations greater than 6M

indicating that the FMN cofactor is still bound. Both proteins are quite stable under strong denaturing conditions, with FLD being particularly robust.

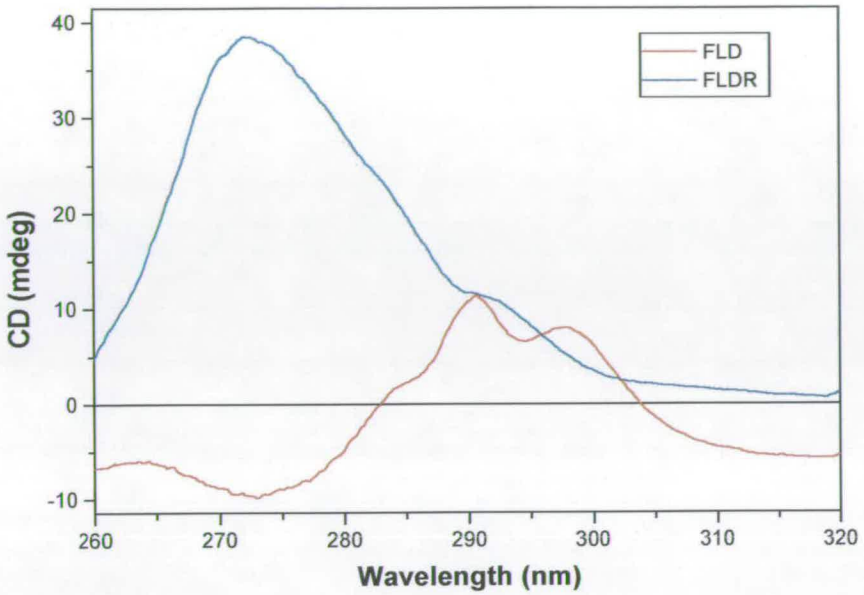

Figure 3-9a

Near-UV CD (260 - 320nm) of FLDR (50μM) and FLD (75μM) in 50mM Tris-HCl pH7.5. The samples were scanned at 10nm/min in a 0.02cm cell.

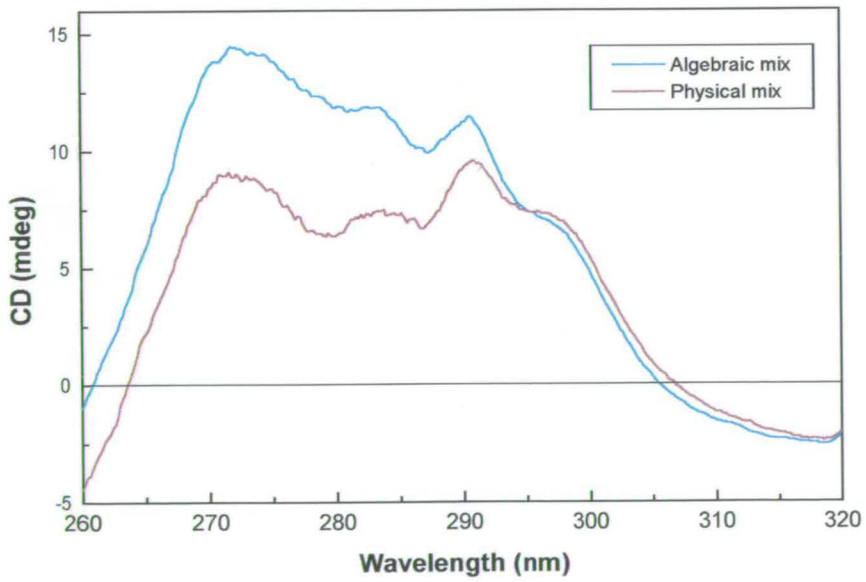

Figure 3-9b

Near-UV CD (260 - 320nm) of both the physical mix of FLDR (25μM) and FLD (37.5μM) and also the algebraic mix. The samples were in 50mM Tris-HCl pH7.5 and were scanned at 10nm/min in a 0.02cm cell.

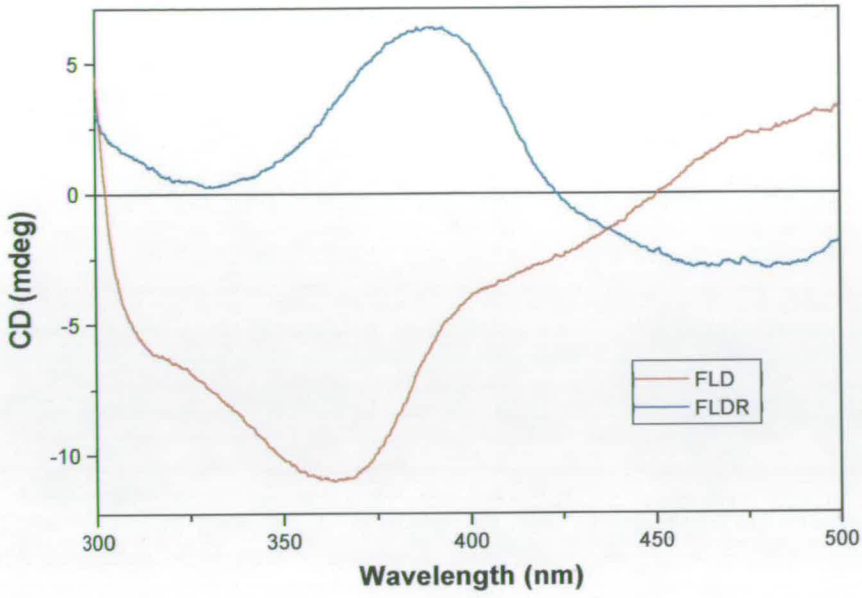

Figure 3-10a

Spectra of the visible CD (300 – 500nm) of FLDR (50μM) and FLD (75μM) in 50mM Tris-HCl pH7.5. The samples were scanned at 20nm/min in a 0.5cm cell.

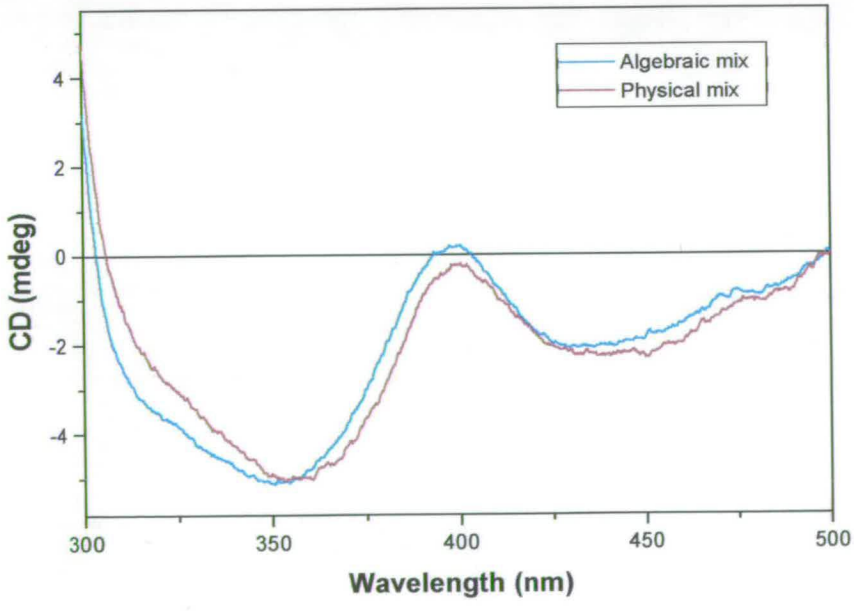

Figure 3-10b

Spectra of the visible CD (300 – 500nm) of both the physical and algebraic mixes of FLDR (25μM) and FLD (37.5μM). The samples were in 50mM Tris-HCl pH7.5 and were scanned at 20nm/min in a 0.5cm cell.

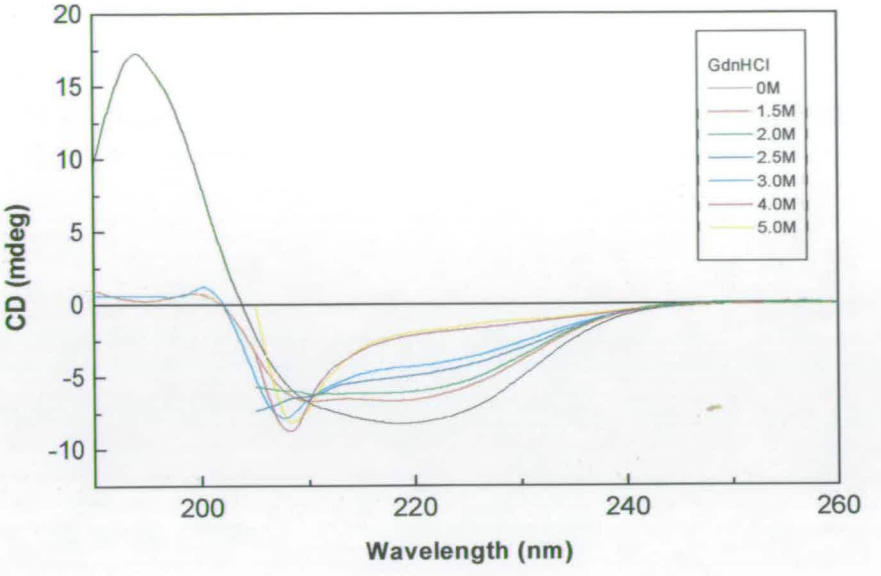

Figure 3-11a

Spectra of the far-UV CD (300 – 500nm) of FLDR (25μM) in the presence of varying concentrations of GdnHCl (0 – 5.0M). The samples were in 50mM Tris-HCl pH7.5 and were scanned at 20nm/min in a 0.5cm cell. Inset shows molar concentrations of GdnHCl.

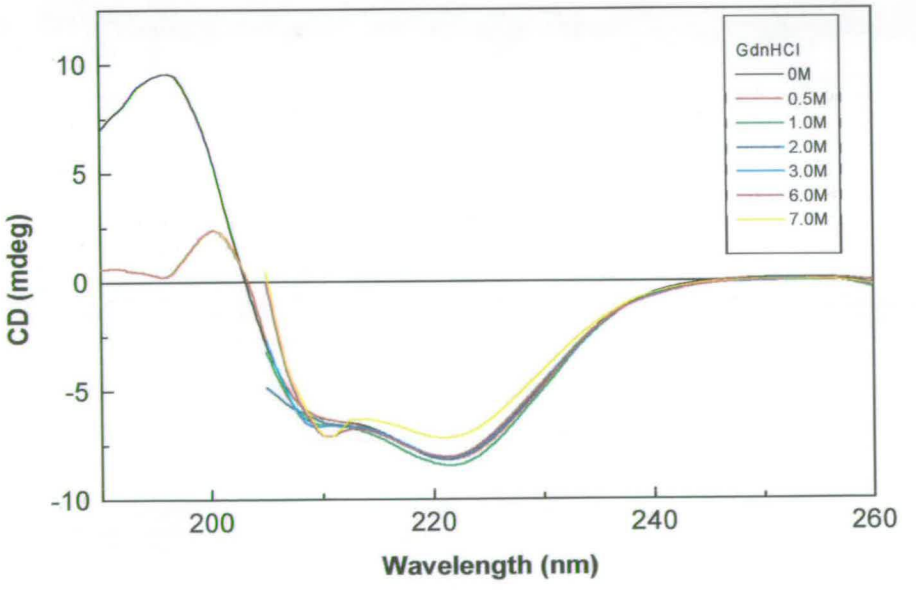

Figure 3-11b

Spectra of the far-UV CD (190 – 260nm) of FLD in varying concentrations of GdnHCl (0 – 7.04M).Samples were in 50mM Tris-HCl pH7.5 and were scanned at 10nm/min in a 0.5cm cell. Inset shows molar concentrations of GdnHCl.

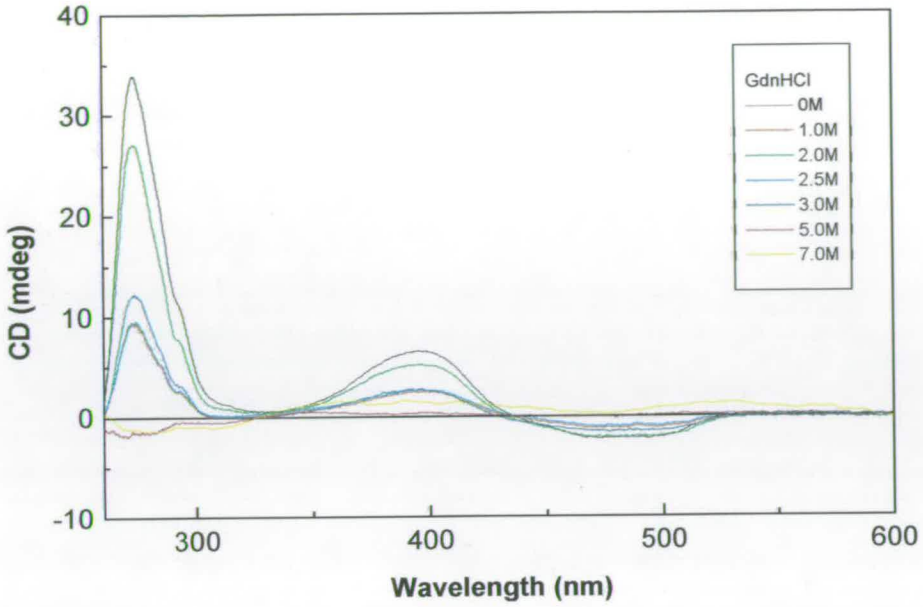

Figure 3-12a

Spectra of the near-UV and visible CD (300 – 500nm) of FLDR in varying concentrations of GdnHCl. The samples were in 50mM Tris-HCl pH7.5 and were scanned at 20nm/min in a 0.5cm cell. Inset shows molar concentrations of GdnHCl.

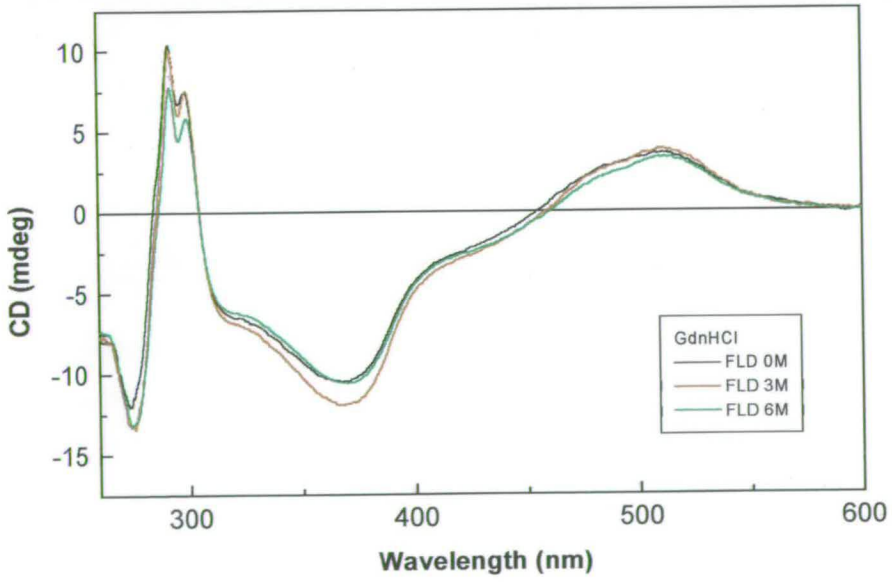

Figure 3-12b

Spectra of near-UV and visible CD (260 – 600nm) of FLD in varying concentrations of GdnHCl (0 – 5.6M). Samples were in 50mM Tris-HCl and were scanned at in a 0.5cm cell. Inset shows molar concentrations of GdnHCl.

3.6 FLDR-FLD cross-linked complex

The FLDR-FLD complex was generated using EDC, a water-soluble carbodiimide, as a cross-linking agent. The time course of the production of the complex is shown in Figure 3-13a. A higher molecular weight band appears which is not present in the initial sample. The complex was purified from unreacted FLDR/FLD using gel filtration on FPLC (Figure 3-13b). It should be noted that during the incubation there was also the appearance of FLD at slightly lower M_r values so it is possible that covalent modifications of FLD carboxyl groups by EDC to N-acylurea derivatives was also taking place (148). It could also be simple degradation.

It appears that only a single species was produced in the reaction with an apparent molecular mass (by SDS-PAGE) of 47kDa. The complex was analysed by electrospray mass spectrometry and a molecular weight of 47430Da was obtained. This is close to the predicted value for a 1:1 EDC-linked complex of FLDR/FLD (47360Da). There was no evidence for self-complexation of FLDR or FLD after EDC treatment - suggesting that the interactions between FLDR/FLD are stronger than those between FLD/FLD or FLDR/FLDR. Visible spectra of the complex showed absorbance maxima at 379.5nm and 462nm, with shoulders at *ca* 487nm and 404nm (Figure 3-14). These absorbance characteristics are different from those of the individual FLDR and FLD, with the absorbance maxima located between the peaks of the isolated flavoproteins. Addition of NADPH was seen to induce a decrease in the intensity of the flavin spectrum, but not to induce the formation of a species absorbing in the 550-600nm region which suggests that there was no formation of the neutral blue semiquinone form expected for the FMN in FLD. This, in turn, suggests that the cross-linked protein may not be oriented suitably for efficient FAD to FMN electron transfer. The spectra is almost identical to that obtained for the *Desulfovibrio vulgaris* FLD and spinach FLDR complex (148).

3.7 Analytical Ultracentrifugation

Preliminary sedimentation equilibrium (SE) studies were carried out on FLDR and FLD. In early experiments sample columns were scanned at 456nm for FLDR and 466nm for FLD but these cofactors were found to be too unstable to act as reliable stoichiometric labels for the proteins themselves. For this reason, in later experiments the protein wavelength of 280nm was used. In solution FLDR appears to be monomeric, giving a whole-cell weight average mass at infinite dilution of 29kDa. FLD, on the other hand, appears to exist in a monomer-dimer equilibrium (at a 0.15μM it has a whole-cell weight average mass of 26kDa) with a K_d in the region of 1μM.

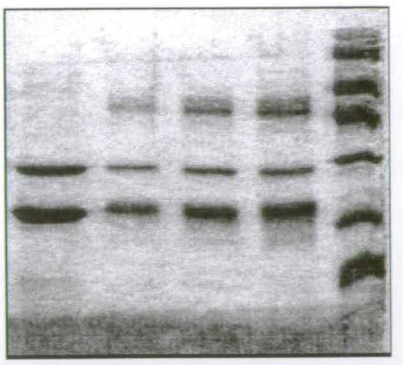

Figure 3-13a

SDS PAGE gel of formation of EDC-linked FLDR/FLD complex. Lane 1: pure FLDR and FLD proteins; no EDC added. Lane 2: 15min after addition of 10mM EDC. Lane 3: 30mins after addition of EDC. Lane 5: 1h after addition of EDC. Lane 5: Molecular weight standards (94000, 67000, 43000, 30000, 20100, 14400 Da).

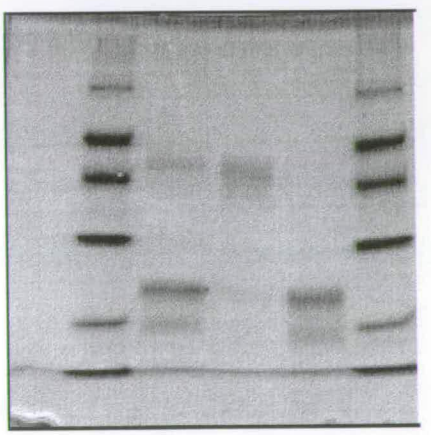

Figure 3-13b

SDS-PAGE gel showing purification of EDC-linked FLDR/FLD complex using FPLC (Superdex 75). Lane 1: Molecular weight standards (94000, 67000, 43000, 30000, 20100, 14400 Da). Lane 2: Complex/FLDR/FLD mixture prior to gel filtration. Lane 3: FPLC fraction containing complex. Lane 4: FPLC fraction containing FLDR/FLD. Lane 5: as Lane 1.

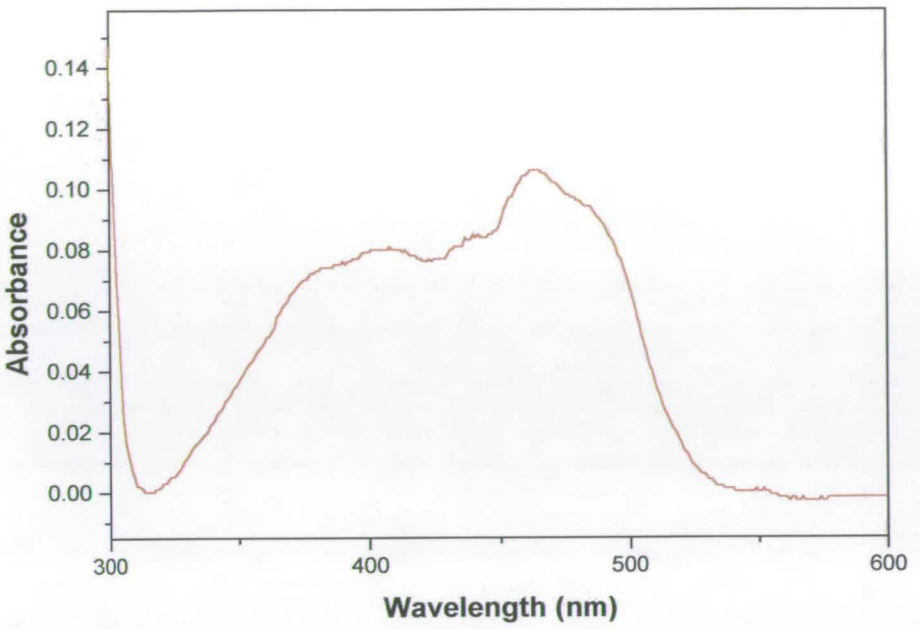

Figure 3-14

The visible absorption spectra of the EDC-linked FLDR/FLD complex. The samples were prepared in 100mM sodium phosphate pH7.5.

3.8 Enzyme activities

Purified FLDR has NADPH-dependent reductase activity towards a variety of electron acceptors. Using cytochrome *c* as the acceptor, a k_{cat} of 141.3 ± 5.3 mol/min/mol and a K_m of 17.6 ± 2.15μM were measured. With saturating cytochrome *c*, the K_m for NADPH was estimated at 3.85 ± 0.5μM. Under similar conditions, potassium ferricyanide was reduced with a K_m of 23.6 ± 3.2μM and a k_{cat} of 1610.3 ± 50.1 mol/min/mol. Purified FLD acts as a single electron shuttle and it is able to stimulate the rate of FLDR-dependent cytochrome *c* reduction approximately 6-fold. With saturating cytochrome *c* (100μM) and FLDR at 16.65nM, a Michaelis curve was obtained for the stimulation of cytochrome *c* reductase activity by FLD indicating an apparent V_{max} of 272 ± 11.5 mol/min/mol and an apparent K_m of the FLD for the FLDR of 6.84 ± 0.68μM (Table 3-3).

Table 3-3

Steady-state kinetic parameters for FLDR. Rates of reduction of artificial electron acceptors were measured at 550nm for cytochrome *c* (22640 $M^{-1}cm^{-1}$) and 420nm for potassium ferricyanide (1010 $M^{-1}cm^{-1}$). Rates were measured at 30°C in 100mM sodium phosphate buffer (pH 7.5) with saturating (200μM) NADPH. The K_m for NADPH was determined under conditions of saturating cytochrome *c* (150μM). The K_m for the FLD was determined under conditions of saturating cytochrome *c* and NADPH, with the FLDR at 16.65nM.

Substrate	k_{cat} (mol/min/mol)	K_m (μM)
Potassium ferricyanide	1610.3 ± 50.1	23.6 ± 3.2
Cytochrome *c*	141.3 ± 5.3	17.6 ± 2.15
NADPH	----	3.85 ± 0.5
FLD	----	6.84 ± 0.68

The purified EDC-linked complex of FLDR/FLD was also catalytically active. With cytochrome *c* as the acceptor, a k_{cat} of 109 ± 4.5 mol/min/mol and a K_m of 87 ± 8.2μM were measured. Using potassium ferricyanide, under similar conditions, a k_{cat} of 782 ± 3.5 mol/min/mol and a K_m of 33 ± 6.4 μM were measured. Both the rate of reduction and the affinity of these substrates for the complex were lower than those for FLDR on its own (Table 3-4).

Table 3-4

Steady-state kinetic parameters for the EDC-linked complex of FLDR/FLD.

Substrate	k_{cat} (mol/min/mol)	K_m (μM)
Potassium ferricyanide	782.0 ± 35	33.2 ± 6.4
Cytochrome *c*	109.2 ± 4.5	87.4 ± 8.2

Rates of FLDR-catalysed cytochrome *c* reduction were measured in buffer B containing various concentrations of GdnHCl, and also in fresh buffer B following dilution from GdnHCl-containing solutions. In both cases 15min pre-incubation with the denaturant at 30°C were performed prior to enzyme assays. FLDR assayed in the presence of GdnHCl shows a decline in activity at concentrations of GdnHCl greater than 1.0M (Figure 15a).However, there is a large increase in activity between 0-1M GdnHCl. The stimulation of activity may be due to minor structural changes in FLDR that enhance binding of cytochrome *c*, or electron transfer to cytochrome *c*. The continuous decrease in ferricyanide reduction activity with increasing GdnHCl shows that the effect is specific for cytochrone *c*. Following dilution of GdnHCl-treated samples to fresh assay buffer, assays of both cytochrome *c* and ferricyanide indicate that activity decreased at concentrations higher than 1.0M GdnHCl and declined to less than 5% of the original value by 5.0M (Figures 15b and 15c).

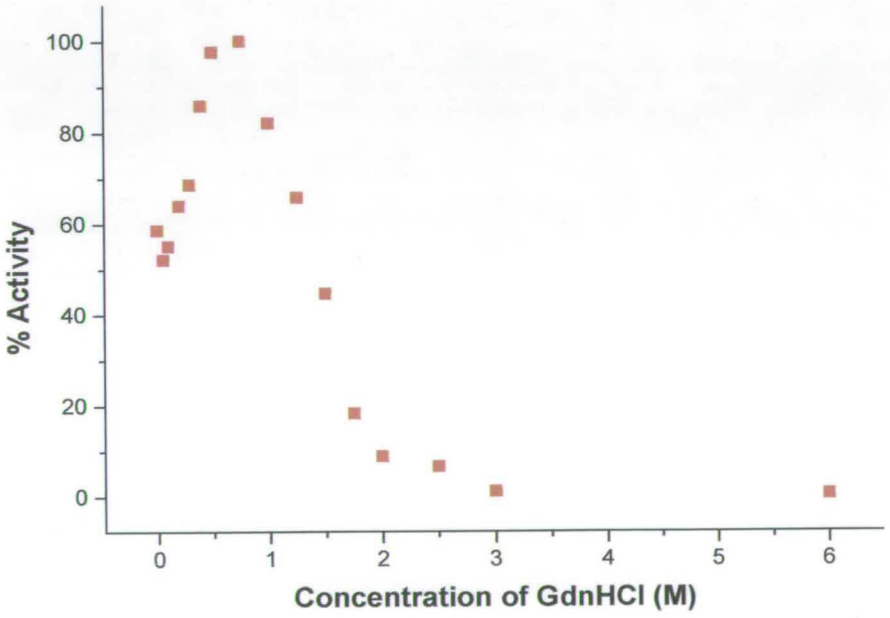

Figure 3-15a

Effect of GdnHCl on the enzymatic activity of cytochrome *c* reduction by FLDR. Prior to measurements being taken the samples were incubated for 15min at 30°C in 100mM sodium phosphate pH7.5 at the indicated concentrations of GdnHCl.

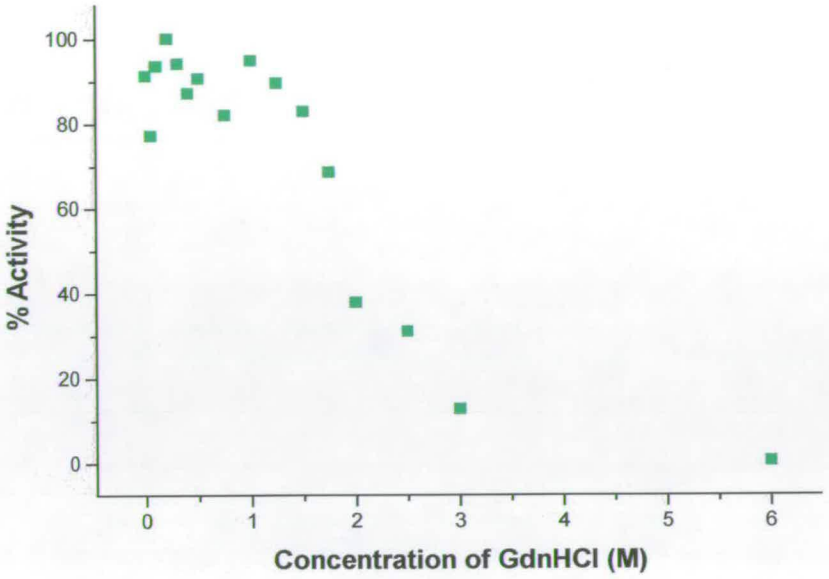

Figure 3-15b

Cytochrome *c* reductase activity was measured following dilution of FLDR in GdnHCl-free assay buffer at 30°C. Prior to measurements being taken, the samples were incubated for 15min at 30°C in 100mM sodium phosphate pH7.5 and the indicated concentrations of GdnHCl.

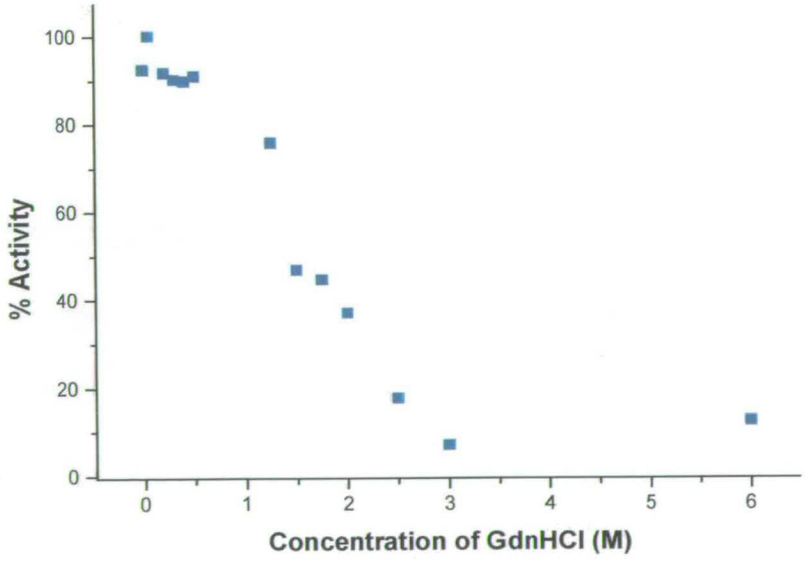

Figure 3-15c

Ferricyanide reductase activity was measured following dilution of FLDR into GdnHCl-free assay buffer. Prior to measurements being taken, the samples were incubated for 15min at 30°C in 100mM sodium phosphate pH7.5 and the indicated concentrations of GdnHCl.

3.9 Stopped-flow characterisation

Investigations of the rates of reduction of FLDR (40μM) with NADPH (4μM - 2mM) were performed with measurement of the rate of decrease in absorbance at 456nm, the oxidised FLDR absorbance maximum. The rate observed was 15 ± 2 s^{-1}, regardless of the concentration of NADPH. A similar value was obtained when the concentration of FLDR was altered. Attempts to measure the rate of electron transfer between NADPH-reduced FLDR and FLD (following the formation of FLD semiquinone at 583nm) proved difficult under aerobic conditions due to the slow rate of this process and the relatively rapid reoxidation of the FLDR. To solve this problem, solutions were degassed and made up anaerobically prior to performing the stopped-flow experiments. The rate of formation of FLD semiquinone was seen to be very slow when reduced FLDR (40μM) was mixed with FLD (20μM), regardless of whether NADPH (500μM - 2mM) or sodium dithionite was used as the reductant. Over the first 60 seconds, a single exponential rate of only (3.4 ± 0.2) x 10^{-2} s^{-1} was recorded in the presence of 2mM NADPH.

To compare the reduction of an artificial electron acceptor on stopped flow/steady state time scales, the reduction of cytochrome *c* by FLDR was investigated. NADPH (2mM)-reduced FLDR (10-50μM) was mixed with cytochrome *c* (4μM) and absorbance monitored at 550nm. A k_{cat} of 29 ± 2 s^{-1} and a K_m of 12.58 ± 1.1μM were calculated by fitting the first order rate data against [cytochrome *c*] to a rectangular hyperbola on Origin software. To measure the rate of reoxidation of the reduced FLDR, the enzyme was reduced aerobically in the stopped-flow apparatus by mixing with a sub-stoichiometric quantity of NADPH, and the subsequent increase in absorbance at 456nm was followed. At 30°C, FLDR (80μM) was observed to reoxidise after rapid mixing with NADPH (60μM) with a rate of (5.44 ± 0.5) x 10^{-2} s^{-1} (3.26min^{-1}). To measure reoxidation of the FLD semiquinone, we initially attempted the same experiment as used for FLDR - employing 80μM FLD and 60μM sodium dithionite as the reductant. However, it was found that reduction of FLD by the dithionite was very slow - with the semiquinone taking several minutes to form completely. Instead, the FLD was reduced with an excess of dithionite under anaerobic conditions - until the semiquinone formation was seen to be complete (maximal absorbance at 583nm). Thereafter, excess dithionite was removed from the FLD by gel filtration (G25) within the anaerobic glove box and the reduced FLD removed from the anaerobic environment. The reduced FLD was then diluted to 30μM in oxygenated buffer, the buffer bubbled with air for 2 minutes and the rate of reoxidation of the semiquinone measured at 583 nm under steady-state conditions. The semiquinone was seen to be air stable, taking several hours to reoxidise completely. The reoxidation trace at 583nm fitted accurately to a single exponential curve, with a rate of 3.85 ± 0.11hr^{-1} (0.642 min^{-1}). All stopped-flow data is tabulated (Table 3-5).

Table 3-5

Stopped-flow parameters for oxidation/reduction reactions involving FLDR and FLD. Reaction rates were determined at 30°C in 100mM sodium phosphate buffer (pH 7.5). Measurement of FLDR reduction was made at 456nm, FLD reduction to its semiquinone at 583nm and cytochrome *c* reduction at 550nm. Reoxidation of FLDR and FLD were monitored at the same λs used to measure their reduction.

Stopped-flow rate	**k (s^{-1})**
FLDR reduction (by NADPH)	15 ± 2 (900 min^{-1})
FLDR oxidation	$(5.44 \pm 0.5) \times 10^{-2}$ (~3.3 min^{-1})
FLD reduction (by FLDR)	$(3.4 \pm 0.2) \times 10^{-2}$ (~2.0 min^{-1})
FLD oxidation	$(1.07 \pm 0.03) \times 10^{-3}$ (3.85 hr^{-1})
cytochrome *c* reduction (by FLDR)	29.0 ± 2.0 (1740 min^{-1})

It is worthy of note that *E. coli* FLDR is capable of reduction of cytochrome *c* in the absence of flavodoxin or alternative protein mediators (*e.g.* ferredoxin). This has not been reported previously. However, the rate is considerably elevated by the presence of *E. coli* FLD. In a recent publication, Jenkins and co-workers reported the kinetics of cytochrome *c* reduction with the *Anabaena variabilis* flavodoxin $NADP^+$ reductase/flavodoxin system (161). In this system, there is negligible flavodoxin-independent cytochrome *c* reduction by the *Anabaena* FLDR. However, the cytochrome *c* turnover number of 1200min^{-1} for the *Anabaena* FLDR/FLD system is much higher than that of its *E. coli* homologue reported here. From stopped-flow studies, the first reduction of cytochrome *c* by reduced FLDR can occur at up to 29s^{-1} (1740 min^{-1}) compared with only 141.3 min^{-1} during steady state. Clearly, the reduction of cytochrome *c* by FLDR is rate-limited by processes other than its binding and the transfer of an electron to the ferric haem.

3.10 Potentiometric Titrations of FLDR and FLD

To gain a clearer understanding of the energetics of FLDR and FLD a potentiometric titration was carried out on the FAD and FMN cofactors in these enzymes. In the following text, E'_1 represents the midpoint potential of the oxidised/semiquinone couple and E'_2 the midpoint potential of the semiquinone/reduced couple of the flavin.

Figure 3-16a shows the redox titration of the *E. coli* FLDR at *ca* 72μM monitored by UV/Vis spectrophotometry between 350 and 800nm. Figure 3-16b plots the proportion of FLDR oxidised based on the sum of the absorbance values between 440nm and 480nm against the potential of the enzyme solution. The 1st electron reduction of FLDR does not result in the accumulation of a stable semiquinone intermediate with long wavelength absorbance. Thus potentiometric data for both 1st and 2nd electron reductions are determined from the continuous decrease in absorbance between 440-480nm. The absorbance *v.* potential data was fitted to the following equation comprising the sum of one 2-electron redox function designed to model the absorbance of a flavin passing through 3 different oxidation states.

$$\text{Flavin absorbance} = \frac{a10^{(E-E'_1)/59} + b + c10^{(E'_2-E)/59}}{1+10^{(E-E'_1)/59} + 10^{(E'_2-E)/59}}$$

Equation 1

a, b, c ≡ absorbance coefficients for oxidised, semiquinone and reduced flavin, respectively. E ≡ electrode potential; E'_1, E'_2 ≡ midpoint potentials for the oxidised/semiquinone couple and the semiquinone/reduced couple, respectively.

In a subsequent experiment, the redox titration of FLDR was repeated in the presence of a saturating concentration (5mM) of 2' adenosine monophosphate (2' AMP), in order to investigate the effects of binding of a nucleotide analogue to the NADPH site on the redox properties of the FAD in FLDR. 2' AMP is non-redox active and thus can be used to in reductive titrations to mimic the effects of binding of $NADP^+$ on the FAD redox properties. In preliminary experiments, the affinity of 2' AMP for FLDR was estimated by measurement of its IC_{50} (~ 1mM) for FLDR-mediated cytochrome *c* reduction. The concentration of 5mM used in the titration was based on this result. An increase in the reduction potentials of both the oxidised/semiquinone (E'_1 elevated by 15mV to -293 ± 6mV) and semiquinone/reduced (E'_2 elevated by 38mV to -230 ± 7mV) couples of FLDR was observed in the presence of 2' AMP.

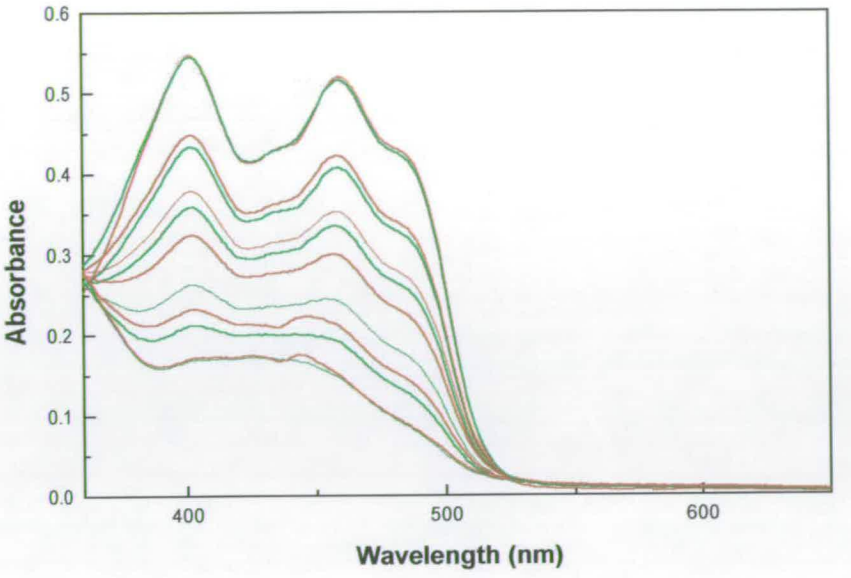

Figure 3-16a

UV-visible spectra of *E. coli* FLDR (72μM) during redox titration. Reductive (sodium dithionite) and oxidative (potassium ferricyanide) titrations were performed anaerobically as described in the previous section. The spectra shown in red are from the reductive titration and the flavin signals become less intense on reduction. The green spectra are from reoxidation of the reduced FLDR and become more intense with successive additions of potassium ferricyanide until the original spectrum of oxidised FLDR returns.

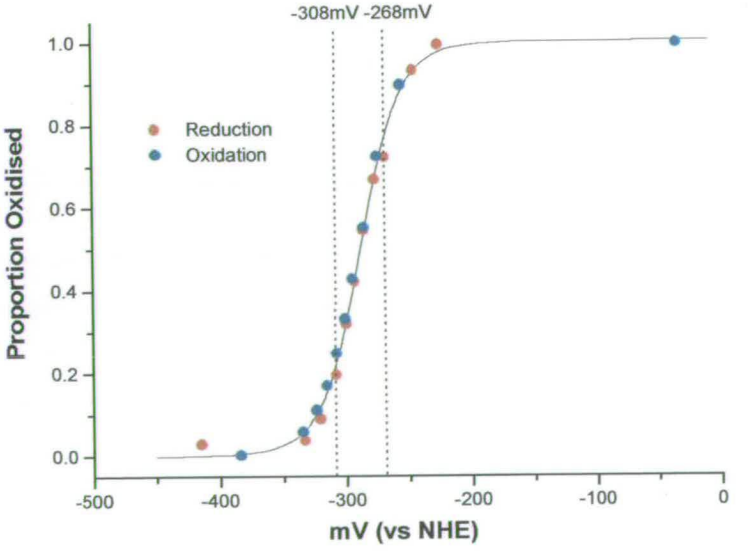

Figure 3-16b

Plot of proportion FLDR oxidised *vs* reduction potential (E', mV) during reductive and oxidative titrations, using absorbance between 440-480nm fitted to Equation 1. From these data E'_1 (ox/sq) = -308 ± 4 mV and E'_2 (sq/red) = -268 ± 4 mV.

The chemical reduction of *E. coli* FLD (*ca* 80μM) was carried out using dithionite and the titration was monitored by visible spectrophotometry between 400nm and 800nm (Figure 3-17a). In the spectrum of the initial fully oxidised sample (shown in magenta) the absorbance maxima at 466nm is obvious. The green spectra show the conversion of the oxidised flavin to its semiquinone form; (shown in blue). It can be seen that the absorbance in the 466nm region decreases as there is an increase in absorbance in the 600nm region (semiquinone region). The protein changed in colour from bright orange to blue showing that *E.coli* FLD has a stable neutral blue semiquinone form. The red spectra show the change from the semiquinone form to the fully reduced form or hydroquinone form (shown in cyan). Oxidative titrations with potassium ferricyanide gave essentially identical results to the reductive titrations, indicating reversibility of the redox protein.

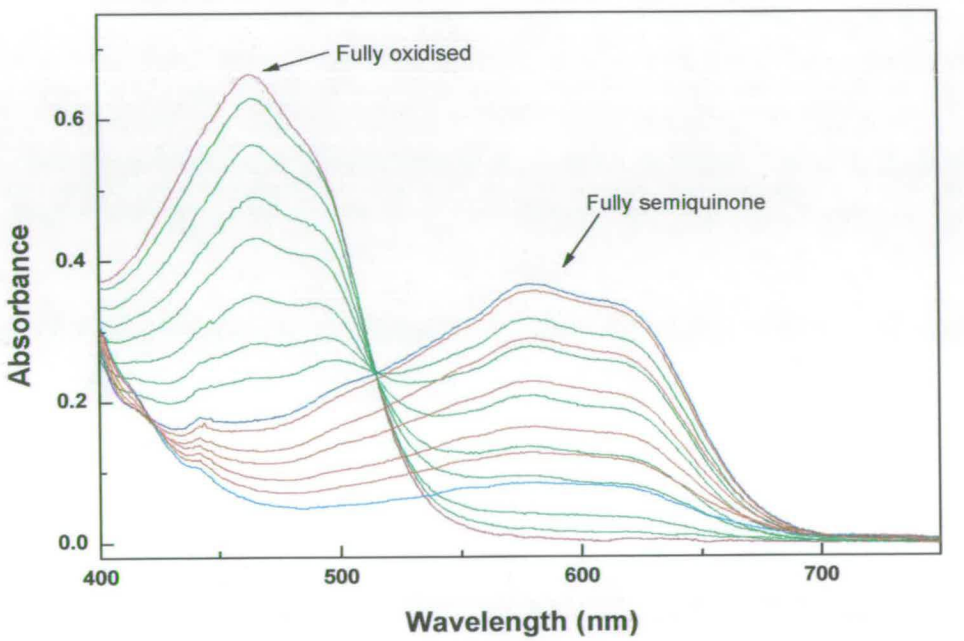

Figure 3-17a

UV-visible spectra of *E. coli* Flavodoxin (80μM) during redox titration. Sodium dithionite reductive titrations were performed anaerobically. The fully oxidised spectrum is shown in magenta and the spectra shown by green lines are those representing the conversion from the oxidised to the semiquinone form; with decreasing absorbance in the 450nm region and increasing absorbance in the 600nm region (semiquinone region). The blue line shows the spectrum of the maximal semiquinone species (absorbance maximum at 583nm). Spectra shown by the red lines are those representing the conversion from the semiquinone to the hydroquinone (fully reduced) form; with decreasing absorbance in the 600nm region. The fully reduced spectrum is shown in cyan. Oxidative titrations with potassium ferricyanide gave essentially identical results to the reductive titrations.

The sum of absorbance values between 550-650nm was plotted against the potential of the enzyme solution (Figure 3-17b). The increase and decrease in absorbance in this 550 - 650nm region reflects the build up (0-1 electron reduced) and loss (1-2 electron reduced), respectively, of the flavodoxin neutral blue semiquinone. The FLD data was also fitted to equation 1. The experiment was done using a calomel electrode, so all data has been amended by the addition of 244mV to correct for the standard hydrogen electrode.

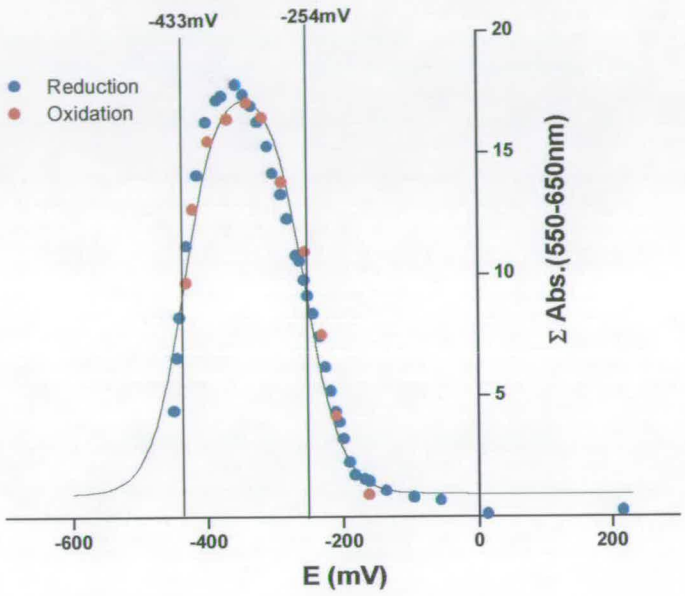

Figure 3-17b

Plot of the sum of absorbance between 550nm and 650nm against electrode potential (E, mV) during reductive and oxidative titrations, fitted to Eqn. 1. From these data, E'_1 (oxidised/semiquinone) = -254 ± 5 mV and E'_2 (semiquinone/reduced) = -433 ± 6 mV.

Values for the reduction potentials are collated in Table 3-6. Although the potentials for the two 1-electron couples of the FLD are very well separated (179mV), this is clearly not so for the FLDR. For the FLDR, the 1st couple (oxidised/semiquinone - E'_1) is calculated to be more negative than the 2nd (semiquinone/reduced - E'_2) by 40mV. In FLDR, the two 1-electron reduction processes appear to occur simultaneously and the data can be represented reasonably accurately by a 2 electron function. The midpoint reduction values in Table 3-6 are compared with those from the homologous domains of flavocytochrome P-450 BM3 and eukaryotic P-450 reductase, and with the potentials of free FAD and FMN.

Analysis of the later data sets for the FLDR was complicated by the tendency of this enzyme to form a precipitate (very slowly) over the course of the experiment. For this reason the quality of these data is not as high as those obtained for FLD. However, correction of these data by subtraction of $1/\lambda$ from each spectrum (to compensate for the small increases in

turbidity) results in values that fit well to the 2 electron Nernst function used to derive the flavin reduction potentials for FLDR.

Based on the wide separation of E'_1 and E'_2 we calculated that a maximum of 94% blue semiquinone was formed during the reductive titration of FLD. As shown in Figure 3-17a the strongly absorbing semiquinone has a peak at approximately 583nm. The maximum absorbance reached by the semiquinone is 56.2% of that of the oxidised flavin band at 466nm. Based on this proportion and the known coefficient of 8250 M^{-1} cm^{-1} for the 466nm band (100), we calculated a coefficient of 4933 M^{-1} cm^{-1} for 100% of the semiquinone.

Table 3-6

Midpoint reduction potentials (E' in mV) for the flavin cofactors in purified *E. coli* FLDR and FLD, calculated from electrode potential *v.* absorbance data. E'_{12} refers to the midpoint potential for the 2-electron reduction of the flavins in each protein, while E'_1 and E'_2 refer to the midpoint reduction potentials for the ox/sq and sq/hq couples, respectively, for FLD and FLDR. The values are compared with those of the FAD and FMN cofactors in the reductase domain of flavocytochrome P-450 BM3 from *B. megaterium* (BM3) (162) and mammalian P-450 reductase (CPR) (163), and with the values for free FAD/FMN (164, 165).

	E'_{12}	E'_1	E'_2
FLDR FAD	-288 ± 4	-308 ± 4	-268 ± 4
FLDR FAD (+2′ AMP)	-261 ± 6	-293 ± 6-	230 ± 7
FLD FMN	-343 ± 6	-254 ± 5	-433 ± 6
BM3 FAD	-332 ± 4	-292 ± 4	-372 ± 4
BM3 FMN	-203 ± 6	-213 ± 5	-193 ± 6
CPR FAD	-327	-290	-365
CPR FMN	-190	-110	-270
FREE FAD	-207	-----	-----
FREE FMN	-205	-172	-238

3.11 Cytochrome P-450 reduction

To analyse the nature and kinetics of the reduction of cytochrome P-450 by the FLDR/FLD system, we examined the ability of these flavoproteins to support the oxidation of arachidonic acid by the haem domain of flavocytochrome P-450 BM3 (166). The FLDR/FLD system was able to transfer electrons to the P-450. At concentrations of 0.762μM P-450, 0.25μM FLDR and 25μM FLD, a rate of 5.48 ± 0.95 mol arachidonic acid oxidised/min was measured. Data were collected from three sets of fatty acid oxidation assays in which the P-450 was maintained at one of three different concentrations (0.76μM, 2.54μM or 3.81μM), FLD was kept constant at 25μM (4-fold in excess of its apparent K_m for FLDR) and FLDR was varied between 0.25μM and 10μM. The plots of the reciprocal rates of these data *v.* the reciprocals of the [FLDR] were used to generate the graph shown in Figure 3-16. The fact that the lines plotted are parallel (not convergent) indicates that the P-450 reduction mechanism is ping-pong in nature, rather than involving a ternary complex between the P-450, FLDR and FLD.

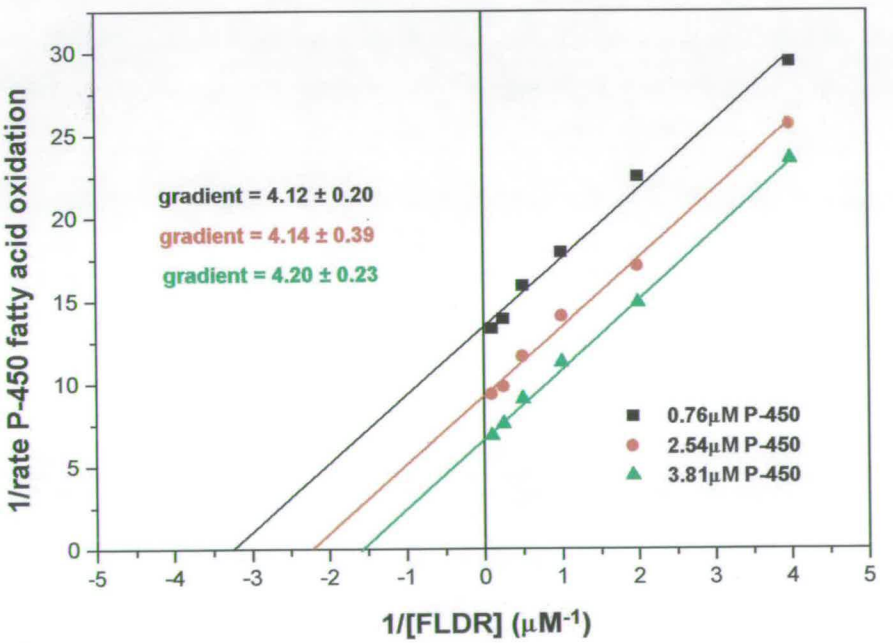

Figure 3-18

Reciprocal plot of P-450 BM3 haem-domain catalysed arachidonic acid oxidation versus concentration of FLDR. The three experimental data sets shown were performed as described in the Materials and Methods section, with P-450 BM3 haem-domain maintained constant at 0.76μM, 2.54μM 0r 3.81μM; FLD maintained at 25μM throughout and FLDR varied between 0.25μM and 10μM. The parallel data plots indicate that a ping-pong mechanism for FLDR/FLD-supported P-450 reduction is likely.

3.12 Discussion

FLDR and FLD are two flavoproteins which transfer electrons to *E.coli* biotin synthase, and which can support heterologously expressed cytochrome *P*-450 in *E.coli* (113). The characterisation of these proteins is central to our understanding of their role in electron transfer to these enzymes, and also to the multiple other redox enzymes with which FLDR/FLD communicates. These include as cobalamin-dependent methionine synthase, biotin synthase, ARR, and PFL.

The quantities of pure FLDR and FLD are considerably higher than those previously reported (107, 113), and this is due to the high levels of expression achievable with the bacteriophage T7 promoter driven system, where expression is induced by providing a source of T7 RNA polymerase in the host cell, and with the efficient purification regimes (including a 2', 5'-ADP Sepharose affinity step for FLDR). Protein purification data indicate that the FLDR and FLD proteins can be overexpressed to at least 10% of total cell protein without notable detrimental effects on cell growth. However, it was noted that transformants of the *fldr* gene in the faster growing BL21 (DE3) strain yielded protein with considerably lower specific activity than that from HMS174 (DE3). This is possibly due to failure of the cells to match FAD synthesis and/or incorporation to the production of FLDR apoenzyme with strong induction under the faster growth conditions.

Both proteins had their masses determined by electrospray mass spectrometry and FLDR shows a discrepancy 28Da from that of the nucleotide sequence (109). The determined atomic structure of FLDR indicates the presence of an arginine as opposed to a glutamine residue at position 126 (110). This difference in mass between these two residues is precisely 28Da; thus these data indicate that the discrepancy is in the DNA sequence and not the atomic structure, and that residue 126 is an arginine. The mass of FLD is exactly that predicted from the amino acid sequence translated from the sequenced DNA (104). The masses determined for FLDR and FLD indicate that significant proportions of the purified proteins retain their initiator methionine residue, and that there are no covalent modifications of either flavoprotein in the homologous host.

Spectroscopic characterisation was carried out on both flavoproteins. UV/visible spectroscopy showed that the two visible flavin absorption bands are shifted slightly to longer wavelengths when a protein matrix surrounds the flavin cofactors. It is obvious from the spectral data that when FMN is surrounded by a protein environment its spectra is significantly different to that of free FMN. This is due to the interaction of the FMN with various amino acid residues of the protein.

Flourimetry was used to examine protein unfolding and the stability of the flavin cofactors on increasing exposure to GdnHCl. When FMN is bound to *E.coli* FLD its fluorescence is

severely quenched and this is due to the preferential energy transfer to the surrounding protein matrix. Denaturation studies were carried out to examine the stability of the FAD and FMN cofactors. Results from both tryptophan and flavin fluorescence experiments show that FLDR and FLD are very stable over a wide range of denaturation conditions and although their cofactors are non - covalently bound they bind very tightly to the protein. FLD in particular is extremely stable.

Circular dichroism (CD) is the differential absorption of the left and right circularly polarised components of plane polarised radiation. It can be used to examine the structure, folding and stability of proteins. Three kinds of information are easily available from CD spectroscopy. Far-UV CD looks mainly at secondary structure, where the principal absorbing groups are the peptide bonds. This information can be quantitative, and estimates of secondary structure can be obtained. FLD and FLDR have distinctive CD spectra in this region and there are no major changes in secondary structure when the two proteins are mixed. Near-UV CD examines the environment of aromatic residues and disulfide bonds. Alterations in protein tertiary structure can be measured with near-UV CD. When FLDR and FLD are mixed there are measurable changes in the spectra when compared to that of the algebraic mix. This indicates that there are alterations of environments of the aromatic residues when a FLDR/FLD complex is formed. In the visible CD range bound chromophores, such as hemes, flavins and PLP, can be examined. When FLDR and FLD are mixed there are small reorientations of one or both flavins when a complex forms, and the alteration of spectra is due to changes in the chiral properties of the flavins. In the denaturation experiments it can be seen that there is a loss of FLDR's secondary structure (at concentrations of GdnHCl >1.5M) and that the chiral environment of FAD is lost (at concentrations of GdnHCl greater than 4M). FLD is extremely stable and shows no loss of FMN, even under extremely harsh denaturing conditions.

Carbodiimides have often been used to covalently stabilise protein partners whose interaction is mainly electrostatic in nature. As there is currently no structural data on a complex of FLDR and FLD the two proteins were chemically crosslinked to examine electron transfer between the flavin cofactors. The fusion was catalytically active, although flavin-flavin interaction was sub-optimal.

Analytical ultracentrifugation SE studies show that FLDR appears to be monomeric in solution, giving a whole-cell weight average mass at infinitive dilution of 29kDa. FLD, on the other hand, appears to undergo a monomer-dimer equilibrium (at 0.15μM it has an apparent whole-cell weight average mass of 26kDa) with a K_d in the region of 1μM. The crystal unit cell of FLD contains two polypeptide chains which appear to interact through an interface rich in polar residues. Thus dimerisation of the 19.7kDa species by a similar interaction in solution is not inconceivable. Preliminary SE studies of the FLDR/FLD mixture have been

performed, but at low protein concentrations interactions (if any) between FLDR and FLD are not detected.

The electron transfer from FLDR to its physiological acceptor FLD was examined by both steady-state and stopped-flow kinetics. Steady-state studies show that FLDR is capable of reduction of cytochrome *c* in the absence of FLD or alternative protein mediators (e.g. ferredoxin). However, the rate is considerably elevated (6-fold) by the addition of FLD indicating that FLD must transfer electrons to cytochrome *c* at a greater rate than FLDR. Recently Jenkins and coworkers reported the kinetics of cytochrome *c* reduction with the *Anabaena variabilis* FLDR/FLD system. In this system there is negligible FLD-independent cytochrome *c* reduction by the *Anabaena* FLDR. The turnover number ($1200min^{-1}$) for the *Anabaena* FLDR/FLD system is much higher than that of its *E. coli* homologue. From stopped-flow studies it is impossible to determine a K_d of FLDR/FLD due to the slow rate of electron transfer which is 100,000 times slower than similar systems (167). The first reduction of cytochrome *c* by reduced FLDR can occur at up to $29s^{-1}$ ($1740min^{-1}$) compared with only $141.3min^{-1}$ during steady-state. Clearly, the reduction of cytochrome *c* is rate-limited by processes other than its binding and the transfer of an electron to the ferric haem. The crosslinked complex was active in reducing cytochrome *c* and ferricyanide. The rate of reduction and affinity were lower for the complex when compared to FLDR on its own. This indicates that crosslinking of the proteins is probably holding them in a rigid conformation where they lack the ability to move free and to dock naturally.

Redox reactions are essential to life and proteins allow electrons to travel great distances. The potentiometric data of FLD demonstrates clearly that it stabilises a neutral blue semiquinone form of FMN and that the FLD hydroquinone cannot be postulated as a realistic electron transferase to biological systems; since the midpoint reduction potential for the sq/hq couple is some 100mV more negative than that of the $NADPH/NADP^+$ couple (and 165mV and 125mV more negative than those of the FLDR ox/sq and sq/hq couples, respectively). The midpoint reduction potential values for the FLD (-254mV [ox/sq] and -433mV [sq/red]) are similar to those obtained from non-recombinant *E. coli* FLD and flavodoxins from other species (168). The reduction potential of free FMN (E'_1 = -172mV and E'_2 = -238mV) is very different from that of FMN bound in flavoproteins (169). When FMN is bound in *E.coli* FLD its redox values are more negative than those of the FMN which is due to the cofactors interactions with the protein matrix.

The reduction potential values of FLDR show that it does not stabilise a semiquinone, with the potential of the first electron reduction being more positive than that of the second. Repeats of the FLDR redox titration in the presence of a saturating concentration of 2' AMP indicated that the midpoint potentials of both the ox/sq and sq/red couples are elevated by binding this nucleotide analogue and that E'_{12} is increased by 27mV from -288 ± 4 mV to -

261 ± 6 mV, respectively. The effect of bound nucleotide analogue is similar to that observed previously for the homologous FAD-containing enzymes adrenodoxin reductase (170) and cytochrome b_5 reductase (171) and indicates that the binding of $NADP^+$ to FLDR may exert an important controlling influence on the catalytic properties of the enzyme. The pyridine nucleotide binding may influence the potentials of FLDR (increase them) bringing them closer to that of the ox/sq couple of FLD and this will decrease further the driving force for electron transfer to the FLD. This may at least partially explain the very slow rates of electron transfer measured between FLDR and FLD using stopped-flow spectrophotometry.

The potentiometric data have important implications relative to the mechanism of the reduction of cytochromes P-450 (and other enzyme systems). They indicate that (unless there is a very large increase in the FLD sq/hq couple caused by binding of FLD to P-450) the 2 electrons required for P-450 catalysis must be delivered through 2 consecutive single electron-transfers from FLD sq; as opposed to the 1st FMN-to-haem electron transfer being mediated by FMN hq and the 2nd by FMN sq. This raised the question as to whether these transfers occur in a ternary complex of FLDR/FLD/P-450 or through a ping-pong mechanism in which the FLD may interact firstly with the FLDR and secondly with the P-450. The fact that the flavins in both proteins are relatively exposed suggests that electron transfer between them is likely to be through close approach of the isoalloxazine rings, as opposed to involving a protein pathway (107, 109). The atomic structure of a eukaryotic P-450 reductase also indicates that the edges of the FAD and FMN ring systems in this protein are only 4Å apart and that inter-flavin electron transfer must occur without mediation by any amino acid side chains (172). Thus, it appeared most likely that reduced FLDR and FLD would dock, an electron would be transferred to form the FLD sq and the FLD would then dissociate from the FLDR and associate with a P-450 to reduce this enzyme, again *via* the exposed FMN. The ping-pong kinetic properties of the FLDR/FLD/P-450 BM3 haem domain system are consistent with this model, suggesting that the FLD acts as a shuttle between FLDR and the P-450, as opposed to the three proteins forming a ternary complex for electron transfer. Double displacement/ping pong kinetics are a common mechanism for enzymes with prosthetic groups.

The data presented here clearly define the electron-transfer route through this system as NADPH → FLDR (FAD) → FLD (FMN) and then onto other enzyme partners. This is a similar flavin electron-transfer path as that described previously for the *E. coli* sulfite reductase and for the diflavin reductases of cytochromes P-450 (P-450 reductase or CPR) and nitric oxide synthase (173). In fact, the FLDR and FLD proteins show structural homology to the FAD and FMN domains of CPR (174), and these domains have been expressed independently for both a eukaryotic P-450 reductase and the reductase of flavocytochrome P-450 BM3 - a natural CPR/P-450 fatty acid hydroxylase fusion protein (175, 176). However, it

is of particular interest to note here that the FAD and FMN domains of P-450 BM3 show very different redox characteristics to FLDR and FLD; with the blue semiquinone being found on the FAD domain of P-450 BM3 (156). In P-450 BM3, the FAD hydroquinone is thermodynamically unfavourable, while it is the FMN of FLD in the *E. coli* system which stabilises a semiquinone. In all three systems the high and low potential flavins are the FMN and FAD, respectively. However, both the E'_1 and E'_2 values for FLDR are considerably less negative than those for the related reductases. Also, the ox/sq and sq/red couples for FLD are both more negative than those for the P-450 BM3 and CPR (163) systems. Indeed, the sq/red couple of FLD has a very negative potential (-433mV) which makes electron-transfer *via* an NADPH-driven system virtually impossible. The results indicate that the overall driving force (*i.e.* the difference in reduction potential) for single electron-transfer from NADPH-reduced FLDR to oxidised FLD is considerably less than those are for CPR and BM3. In addition, the binding of nucleotide ($NADP^+$) to FLDR may result in further increase in the flavin reduction potentials (as we have shown with 2′ AMP) and decrease further the driving force for electron transfer to FLD. Our stopped-flow data are consistent with these findings. The rate of reduction of FLDR ($15s^{-1}$) is markedly slower than that seen in the P-450 BM3 system (> $700s^{-1}$) and the reduction of FLD by reduced FLDR is also very slow (0.034 s^{-1}). Modelling studies in our lab have indicated that reduction of FLDR is slow because residue W248 has to move out of the way to let NADPH dock. This finding highlights an obvious target residue for future mechanistic studies of FLDR mutants.The systems that FLDR and FLD supply with electrons usually do not need fast turnover rates, so there may be no real evolutionary pressure to create a redox system with high electron transfer rates.

Other work that was carried out to examine whether FLDR and FLD interact strongly did not lead to any conclusive results. Protein interaction studies were carried out by attaching FLD to Sephadex and passing FLDR over it. No binding occurred. The reverse was then attempted, in which the *fldr* gene was expressed with a N-terminal histidine tag, so that the protein could then be bound to a nickel column. Unfortunately the His_6 FLDR was not active and did not appear to fold properly. FLD did not bind to the His_6 FLDR. Preliminary Biacore experiments gave results which were inconclusive as it was unknown if the immobilised FLD was in a homogeneous layer on the Biacore chip surface.

These results are published and a copy of the publication is to be found as Appendix I (112).

Chapter 4: Characterisation of Wild-type and Mutant Biotin Synthases

4.1 Introduction

The aim of this work was to clone the *bioB* gene into a suitable vector to achieve a high level of protein expression and to develop a simple, efficient purification system to allow preparation of large amounts of homogeneous protein for characterisation. The characterisation of biotin synthase is essential to gain a clearer understanding into the mechanism of biotin production. In order to gain an insight into which protein residues are involved in the co-ordination of the Fe-S clusters of biotin synthase site-directed mutagenesis was carried out on five cysteine residues. The mutant proteins were then characterised using a variety of biophysical and chemical techniques.

4.2 Cloning of the *bioB* Gene

The vector pUC18/RBS (a modified version of pUC18 which contains a ribosome binding site and a *Nco*I site) was used for the initial cloning of *bioB* genes. A 1041bp *Nco*I / *Bam*HI fragment from pB030 (a gift from Lonza AG) containing the *bio*B gene was cloned into the same sites of pUC18/RBS and the resultant plasmid named pUC18/RBS/bioB (Figure 4-1a).

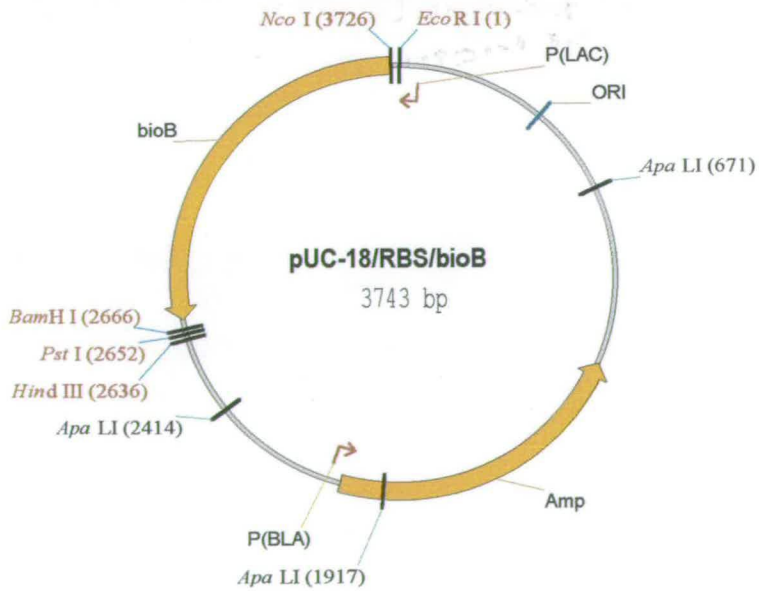

Figure 4-1a

A diagram illustrating the plasmid pUC18/RBS/bioB (3743bp) which contains the *bioB* gene (1041bp) and the pBR322A-derived ampicillin resistance gene and origin of replication.

We overproduced the protein using the pET system that is based on a T7 promoter driven system. The cloned gene is under control of strong bacteriophage T7 transcription and translation signals. IPTG induces protein expression. The bioB gene was cloned into the vector pET16b (Novagen) using the *Nco*I and *Bam*HI restriction sites. The resultant plasmid was called pET16b/bioB (Figure 4-1b).

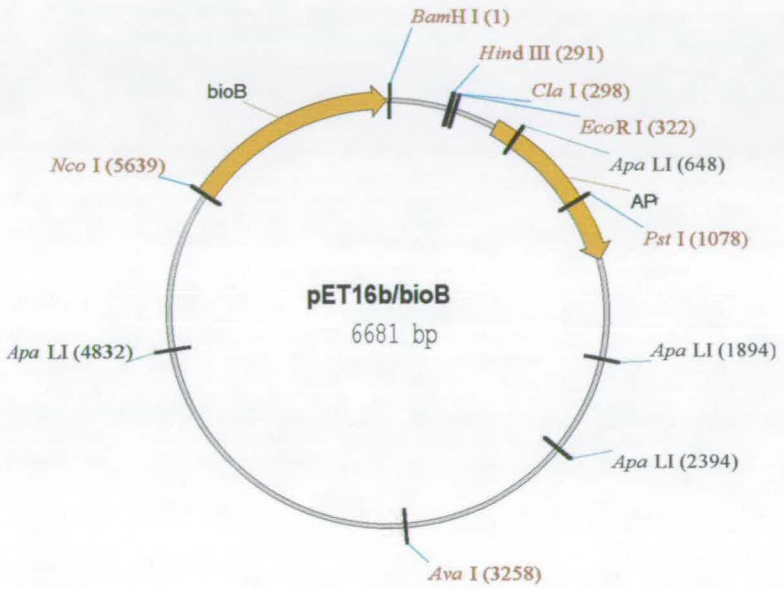

Figure 4-1b

The plasmid pET16b/bioB (6681bp) which contains the *bioB* gene under control of the T7 promoter driven system.

4.3 Overexpression and Purification of Wild-Type Biotin Synthase

Wild-type biotin synthase was overexpressed in both B834 (DE3) and HMS174 (DE3) cell lines. Expression levels were virtually identical but HMS174 (DE3) gave a better control of expression and so was the cell line most frequently used. Optimal yields of protein was obtained by aerobic cell growth in 2YT at 37°C. The expressed protein was then purified using the method described by Sanyal *et al* (66). In our hands we found this purification procedure both technically difficult and time consuming although the procedure provided *ca* 80% pure biotin synthase. The protein contained some high molecular weight contaminants. We found it impossible to reproduce the purification of biotin synthase using a cobalt column,

as described by Marquet and coworkers (177). To overcome these problems we decided to express the protein with an N-terminal polyhistidine tag to allow it to be purified using immobilised metal affinity chromatography (IMAC). The *bio*B gene was cloned into the *Nco*I and *Bam*HI sites of the vector pET6H (a derivative of pET11d). This fused the 5'-terminus of the gene to a sequence encoding a MHHHHHHA tag (Figure 4-2).

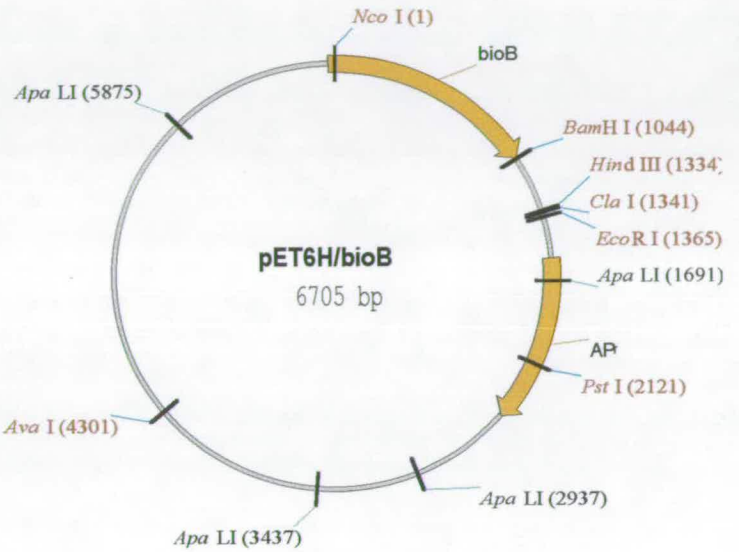

Figure 4-2
The plasmid pET6H/bioB (6705bp) which contains the *bioB* gene

4.4 Overexpression and Purification of His_6-Tagged Biotin Synthase

Overexpression of His_6-tagged biotin synthase was carried out in HMS174 (DE3) and gave comparable expression levels compared to wild-type biotin synthase. Purification was carried out in a single step on a nickel column. We were routinely able to prepare 20mg of >95% pure His_6-tagged biotin synthase per litre of transformed cell culture (Figure 4-3).

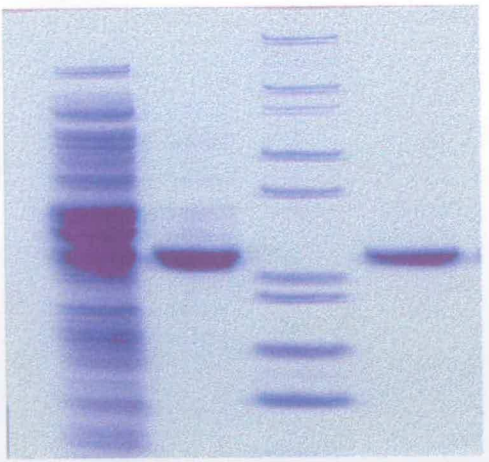

Figure 4-3

SDS-polyacrylamide gel electrophoresis analysis of His_6-tagged biotin synthase. Protein samples were applied to polyacrylamide gel electrophoresis (15%) in the presence of SDS (0.1%) as follows: lane 1, Cell free extract, lane 2, wild-type biotin synthase, lane 3, molecular weight markers (Mark 12, Novex) from the top 200kDa, 116.3kDa, 97.4kDa, 66.3kDa, 55.4kDa, 36.5kDa, 31kDa, 21.5kDa and 14.4kDa and lane 4, His_6-tagged biotin synthase

4.5 N-Terminal Protein Sequencing

Both wild type and His_6-tagged biotin synthase were electroblotted and N-terminal protein sequencing was used to confirm their amino acid sequence. Occasionally the His_6-tagged biotin synthase was seen as a double band on SDS gels. These two bands were electroblotted and digested with trypsin before being sequenced. The higher band was His_6-tagged biotin synthase while the lower band was biotin synthase minus the first 63 amino acids (approximately 6000Da short of the complete protein). As there was no small molecular weight bands present on the gel it appears that this 6000Da peptide was being cleaved into fragments. It appears that this degradation is a consequence of oxidation during SDS PAGE as stronger reducing conditions (i.e. increased DTT concentrations) alleviates this double band effect. Electrospray mass spectrometry revealed that the protein was in fact homogeneous and does not appear to contain any small peptide fragments.

On occasion, preparations of His_6-tagged biotin synthase exhibited two faint bands, which copurified on the nickel column. The impurities had molecular weights of approximately 14kDa and 20kDa according to SDS PAGE. These were electroblotted and sequenced. The 14kDa band was found to be superoxide dismutase (178) which is a metal binding protein and the 20kDa band to be the histidine rich protein SlyD (179). Both of these two impurities could be easily removed using gel exclusion chromatography.

4.6 Mass Spectrometry

The molecular weights of wild type and His_6-tagged biotin synthase were confirmed by electrospray mass spectrometry. The results were within 0.1% of the expected values for the polypeptide chains indicating that the Fe-S cluster is lost under the mass spectrometry conditions (Table 4-1).

Table 4-1

Molecular mass of both wild-type biotin synthase and His_6-tagged biotin synthases measured by electrospray mass spectrometry*.

Protein	Expected (Da)	Actual (Da)
Wild-type biotin synthase	38648	38646
His_6-tagged biotin synthase	39673	39666

* A 5μl sample of biotin synthase (20μM) in TFA/acetonitrile/water (0.1%/50%/50%) solution was used in the measurement. The instrument was calibrated with a myoglobin standard. The estimated error of the molecular mass for each protein is within 0.1%.

4.7 *In Vivo* Assay for Biotin Production

HMS174 (DE3) cells did not produce detectable levels of biotin either on their own or when transformed with pET16b or pET6H and so were used as a control. To examine whether or not the His_6-tag affected biotin synthase activity an *in vivo* assay was carried out using HMS173 (DE3) cells transformed with either pET16b/bioB or pET6H/bioB. All the cells grew in a similar fashion and both were active in that they produced biotin (Table 4-2). There was no difference in the cells transformed with pET16b/bioB when compared to those that were producing His_6-tagged protein indicating that the tag does not seem to affect the activity of wild-type biotin synthase.

Table 4-2

In vivo production of biotin*.

Protein	Biotin produced
Wild-type biotin synthase	+
His_6-tagged biotin synthase	+

*Biotin production was measured using the *Lactobacillus* assay as described in the Materials and Methods section (+ = biotin produced and - = no biotin production).

4.8 Elemental Analyses

Analyses for iron, sulfur and nickel was carried out on both proteins using ICP-AES (150) and the ferrozine method (151) The protein concentrations were adjusted to *ca* 26μM (based on a monomeric weight of 38648Da for wild-type biotin synthase and 39673Da for His_6-tagged biotin synthase). The amount of sulfur (as S^{2-}) in His_6-tagged biotin synthase was virtually identical to that in the untagged protein and similar to the value previously reported by Sanyal *et al* (66). Analysis for nickel content proved that there was negligible nickel binding. ICP-AES iron analysis on the purified proteins revealed a 1:1 ratio between protein and iron in both wild type and His_6-tagged biotin synthase (Table 4-3) in agreement with previously reported values (153) although it should be noted that Sanyal has reported a 1:2 ratio (66). The ferrozine iron assay gave a slightly lower protein:Fe ratio than that obtained by ICP-AES (Table 4-4).

Table 4-3

ICP-AES iron analysis on wild-type biotin synthase and His_6-tagged biotin synthase proteins*.

Protein	Protein:Fe ratio
Wild-type biotin synthase	1 : 0.96
His_6-tagged biotin synthase	1 : 0.94

* Protein samples (26μM) and standards ($Fe(NO_3)_3$) were in 100mM sodium phosphate pH7.5

Table 4-4

Results of the Ferrozine iron assay*.

Protein	Protein : Fe ratio
Wild-type biotin synthase	1 : 0.68
His_6-tagged biotin synthase	1 : 0.72

* Protein samples (26μM) and standards ($Fe(NO_3)_3$) were in 100mM sodium phosphate pH7.5

4.9 Preparation of Wild-type and His_6-tagged Apoenzymes and the Reconstitution of [2Fe-2S] Cluster containing Holoenzymes

In order to try to increase the iron content of wild-type biotin synthase and His_6-tagged biotin synthase the apoenzymes were prepared anaerobically using sodium dithionite and EDTA. The samples were then desalted using a G10 gel filtration column. ICP-AES analysis and UV-visible spectroscopy confirmed the absence of iron in both proteins. The Fe-S clusters were then reconstituted by incubation of the apoenzyme with $FeCl_3$ and Na_2S. The reconstituted holoenzyme has an increased protein : Fe ratios which were comparable to those previously reported (Table 4-5) (153).

Table 4-5

ICP-AES iron analysis on wild-type biotin synthase and His_6-tagged biotin synthase apoenzymes and reconstitiuted holoenzymes*

Protein	Apoenzyme : Fe ratio	Holoenzyme : Fe ratio
Wild-type biotin synthase	1 : 0.11	1 : 1.37
His_6-tagged biotin synthase	1 : 0.11	1 : 1.37

* Protein samples (26μM) and standards ($Fe(NO_3)_3$) were in 100mM sodium phosphate pH7.5

4.10 Spectral Characteristics

Solutions of wild type and His_6-tagged biotin synthase were both reddish brown in colour and they showed virtually identical UV-visible spectra with a maximum at 274nm, a shoulder at 330nm and a distinctive peak at 420nm (Figure 4-4a). These spectra are similar to that of other [2Fe-2S] proteins. The apoenzymes lose their absorbance in the 420nm region. The reconstituted holoenzymes have spectra similar to the purified samples.

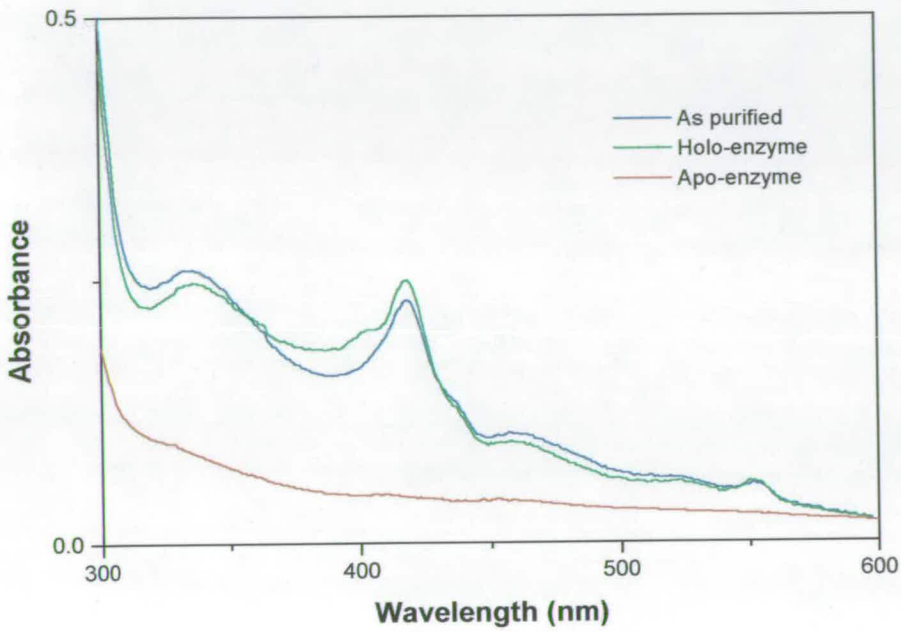

Figure 4-4a

UV-visible spectra of wild type, His_6-tagged biotin synthases – as purified, apoenzmes and reconstituted holoenzymes. The spectra are from samples of all proteins (1mg/ml) in 100mM sodium phosphate pH7.5.

Biotin synthase exhibits absorption spectra with extinction coefficients indicative of a single [2Fe-2S] cluster in each subunit. Anaerobic reduction with excess sodium dithionite results in a decrease in the visible absorbance at all wavelengths >350nm (Figure 4-4b). The resulting spectrum is characteristic of proteins containing [4Fe-4S] clusters (83). To examine the reversibility of this reductive cluster conversion the [4Fe-4S] sample was exposed to air. Gradual bleaching of the visible absorption occurred which indicates that there was cluster degradation of the sample. However, comparison of spectra taken during the oxidation indicates that some reformation of the [2Fe-2S] cluster occurs indicating that the presence of [2Fe-2S] clusters in biotin synthase is a result of aerobic purification.

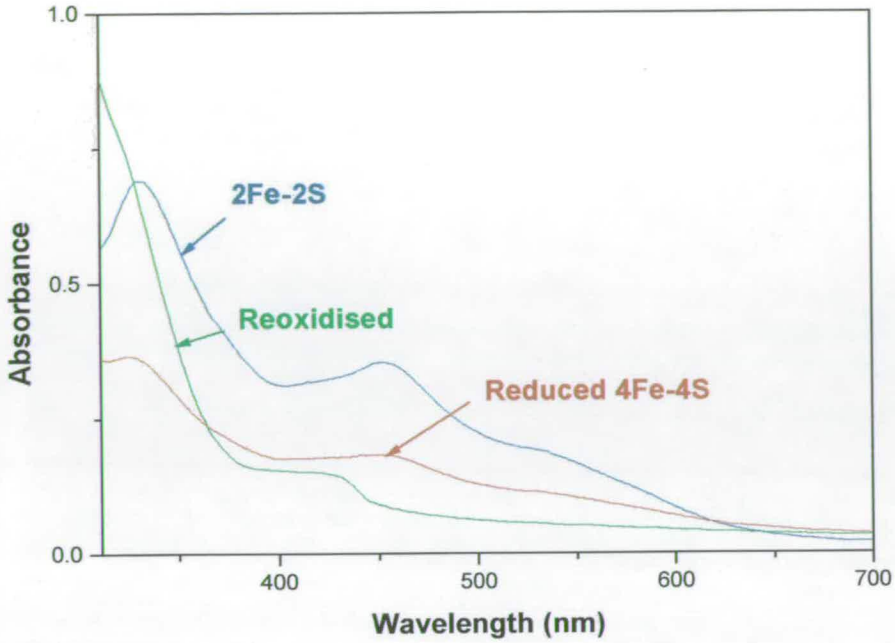

Figure 4-4b

Reduction and reoxidation of biotin synthase. The [4Fe-4S] form of biotin synthase (red) was prepared by anaerobic incubation of [2Fe-2S] biotin synthase (blue) was in the presence of excess sodium dithionite. The sample was then exposed to air for 5h at room temperature (green spectra). The spectra are from samples of all proteins (1mg/ml) in 100mM sodium phosphate pH7.5.

4.11 *In Vitro* Assay for Biotin Production

The *in vitro* activities of both proteins were determined using the *Lactobacillus* assay. Biotin was produced by all three forms of both the wild type and the His_6-tagged proteins (Table 4-6). The addition of pure *A. vinelandii* NifS (20μM) to the assay mixture had no apparent effect on the amount of biotin produced. There was no difference in the levels of biotin produced when the samples were incubated aerobically or anaerobically.

Table 4-6

In vitro biotin production*.

Protein	As purified	Apoenzyme	Reconstituted holoenzyme
Wild-type biotin synthase	+	+	+
His_6-tagged biotin synthase	+	+	+

*Biotin production was measured using the *Lactobacillus* assay in the presence of biotin synthase (5μM), potassium chloride (10mM), dethiobiotin (50μM), AdoMet (150μM), $Fe(NH_4)_2(SO_4)_2$ (5mM), NADPH (1mM), fructose 1,6-bisphosphate (5mM), L-cysteine (500μM), DTT (10mM), PCOi cell free extract (100μl), FLD (12.5μM) and FLDR (2μM). The reaction mixture was incubated for 2h at 37 C (+ = biotin produced and - = no biotin production).

4.12 Crystallisation Studies

Both PEG and ammonium sulphate crystallisation screens were set up using wild type and His_6-taggged biotin synthase. Unfortunately no crystal forms were found in either screen.

4.13 Amino Acid Sequence Analysis

A sequence alignment search was carried out using the amino acid sequence of *E. coli* biotin synthase. Twenty-six sequences were found in the databases that were homologous to *E. coli* biotin synthase. A number of these sequences contained some very highly conserved residues and there were also two extended conserved motifs. Alignment of these twenty-four sequences can be seen in figure 4.5.

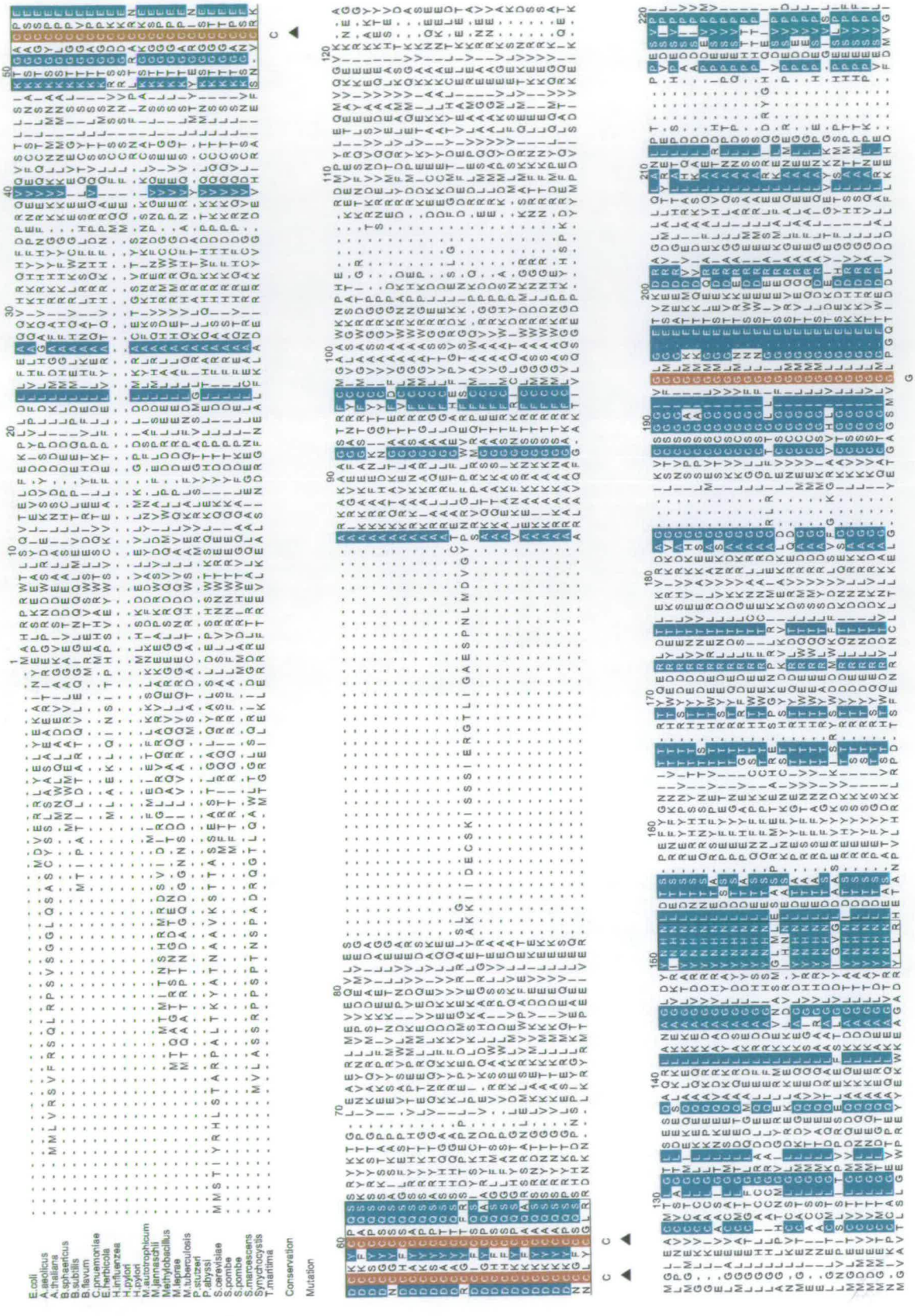
E.coli
A.aeolicus
A.thaliana
B.sphaericus
B.subtilis
B.flavum
C.pneumoniae
E.herbicola
H.influenzae
H.pylori
M.auroraphicum
M.jannaschii
Methylobacillus
M.leprae
M.tuberculosis
P.stuzeri
P.abyssi
S.cerevisiae
S.pombe
S.marcescans
Synychocystis
T.maritima
Conservation
Mutation

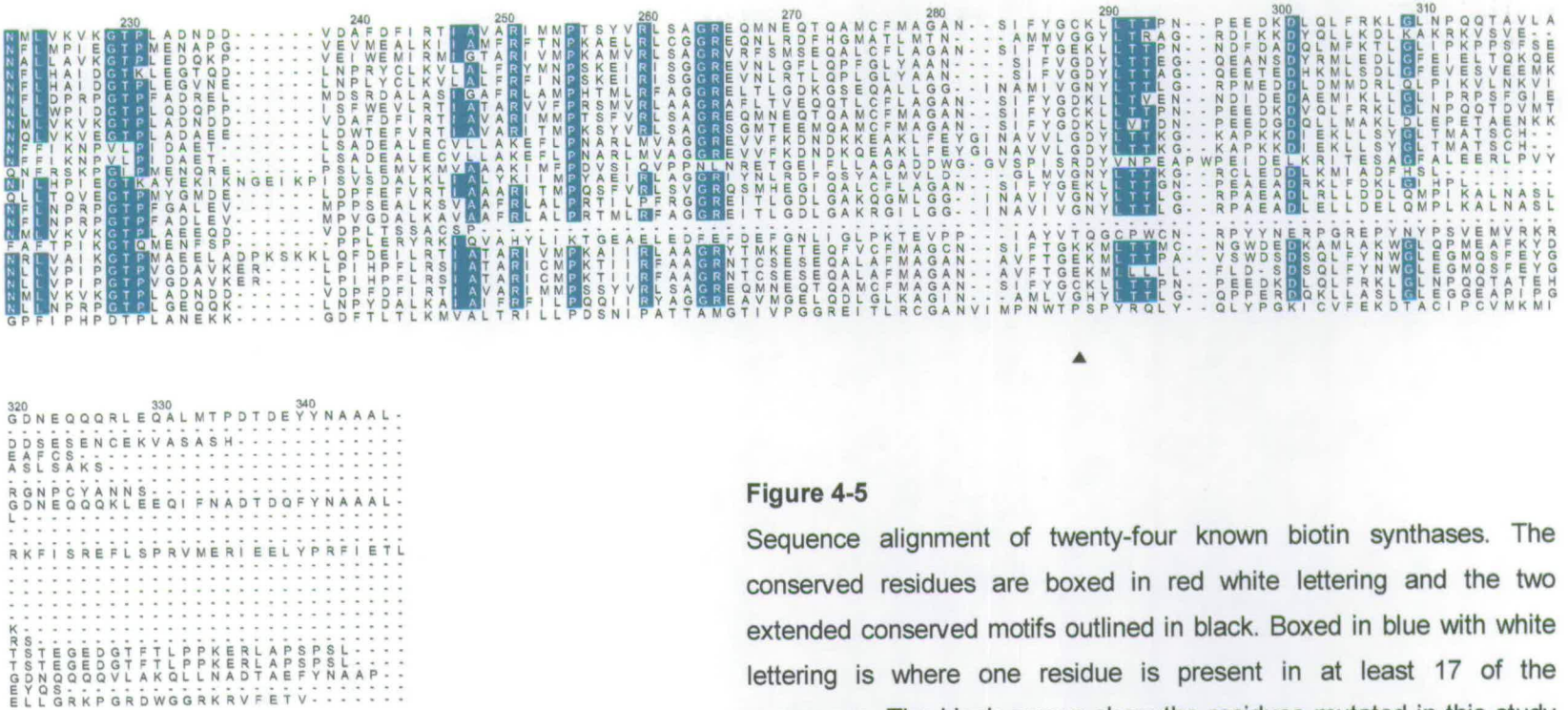

Figure 4-5

Sequence alignment of twenty-four known biotin synthases. The conserved residues are boxed in red white lettering and the two extended conserved motifs outlined in black. Boxed in blue with white lettering is where one residue is present in at least 17 of the sequences. The black arrows show the residues mutated in this study and the residue numbering is that of the *E.coli* sequence. (The Swissprot or Entrez accession numbers from the top are P12996, O67104, P54967, P19206, P53557, P46396, Q9Z6L5, Q47862, P44987, O25956, Q9ZJK8, O27266, Q58692, P94966, P46715, O06601, CAB56476, CAB49138, P32451, O60050, O59778, P36569, P73538 AND AE001782_5). The sequence alignment was carried out using Expasy and Clustal W and the data formatted using Alscript.

4.14 Essential Cysteine Residues of Biotin Synthase

Spectroscopic studies on biotin synthase, PFL activase and LIPA (73, 78, 135) suggest that three cysteine residues from each monomer are required to co-ordinate the Fe in the [2Fe-2S] clusters of the oxidised dimer and that two of these are required ligands in the reduced catalytically active form. Five cysteine residues (C53, C57, C60, C188 and C288) were replaced separately with serine or threonine residues by site-directed mutagenesis (threonine was chosen as a replacement for C288 since it enabled us to engineer a *Kpn*I restriction site into the *bioB* gene to facilitate mutant selection). Each of the mutant proteins was overproduced in *E.coli* HMS174 (DE3) and its catalytic activity determined. Since the His_6-tagged biotin synthase showed identical *in vitro* spectroscopic parameters and catalytic activity to wild-type protein the mutant *bioB* genes were also expressed as histidine-fusion proteins. Each of the mutant proteins was purified using IMAC under identical conditions to the histidine-tagged wild-type biotin synthase except for mutant C188S that despite numerous attempts (low temperature induction, IPTG concentrations <0.1mM) remained intractably insoluble. Protein purity was estimated by SDS PAGE (Figure 4-6).

Figure 4-6

SDS-polyacrylamide gel electrophoresis analysis of His_6-tagged biotin synthase and mutants C53S, C57S, C60S and C288T. Protein samples were applied to polyacrylamide gel electrophoresis (15%) in the presence of SDS (0.1%) as follows: lane 1, His-tagged, lane 2, C53S; lane 3, C57S; lane 4, C60S; lane 5, C288T and lane 6, low molecular weight markers in kDa – 140, 96, 64, 43, 30, 20 and 14.4 (Amersham Pharmacia). Coommassie Blue was used for staining.

4.15 Mass Spectrometry of the Cysteine Mutants

All the mass spectrometry results were within 0.1% of the expected values for the mutant proteins (Table 4-7).

Table 4-7

Molecular mass of the *E.coli* biotin synthase cysteine mutants measured by electrospray mass spectrometry*.

Protein	Expected	Actual
C53S	39657	39656
C57S	39657	39658
C60S	39657	39652
C288T	39671	39670

*5μl samples of protein (20μM) in TFA/acetonitrile/water (0.1%/50%/50%) solution was used in the measurement. The instrument was calibrated with a myoglobin standard. The estimated error of the molecular mass for each protein is within 0.1%.

4.16 *In Vivo* Assay for Biotin Production

In vivo biotin production was carried out with the five mutant plasmids. All the clones grew as vigorously to those of the wild type and His_6-tagged biotin synthase but only the non-conserved C288T mutant produced significant amounts of biotin. Cells expressing the C53S, C57S, C60S or C188S mutants did not produce any detectable quantities of biotin (Table 4-8).

Table 4-8

In vivo production of biotin*

Protein	Biotin produced
C53S	-
C57S	-
C60S	-
C188S	-
C288T	+

*Biotin production was measured using the *Lactobacillus* assay (+ = biotin produced and - = no biotin production).

4.17 Elemental Analyses

Analyses for iron and sulfur was carried out on all the mutant proteins using ICP-AES, the Beinert method and the ferrozine method. The protein concentrations were adjusted to *ca* 26μM (based on a monomeric weight 39657Da). The amount of iron and sulfur in C53S, C57S and C60S was negligible but in C288T it was the same as that for wild type and His_6-tagged biotin synthase (Table 4-9).

Table 4-9

ICP-AES iron analysis on the cysteine mutants*.

Protein	Protein : Fe ratio
C53S	1 : 0.13
C57S	1 : 0.21
C60S	1 : 0.21
C288T	1 : 0.77

* Protein samples (26μM) and standards ($Fe(NO_3)_3$) were in 100mM sodium phosphate pH7.5

The protein : Fe ratio determined by the Ferrozine assay gave slightly lower results than that of the ICP-AES (Table 4-10).

Table 4-10

Results of the Ferrozine iron assay*.

Protein	Protein : Fe ratio
C53S	1 : 0.09
C57S	1 : 0.07
C60S	1 : 0.11
C288T	1 : 0.44

* Protein samples (26μM) and standards ($Fe(NO_3)_3$) were in 100mM sodium phosphate pH7.5

4.18 Preparation of Mutant Apoenzymes and the Reconstitution of [2Fe-2S] Cluster containing Holoenzymes

The mutant proteins were incubated with sodium dithionite and EDTA to remove their Fe-S clusters and to produce their apoenzymes. To try to increase their iron and sulfur content their holoenzymes were reconstituted by incubation with Fe^{3+} and S^{2-}. Only C288T showed any increase in iron and sulfur. There was no change for the three conserved cysteine mutants (Table 4-11).

Table 4-11

ICP-AES iron analysis on the mutant proteins*.

Protein	Protein : Fe ratio	Protein : Fe ratio
C53S	1 : 0.07	1 : 0.47
C57S	1 : 0.06	1 : 0.27
C60S	1 : 0.06	1 : 0.44
C288T	1 :0.04	1 : 1.59

* Protein samples (26μM) and standards ($Fe(NO_3)_3$) were in 100mM sodium phosphate pH7.5

4.19 Spectral Characterisation

The mutants (C53S, C57S and C60S) were colourless and their spectra showed no peaks indicative of the presence of an Fe-S cluster. Moreover, their spectra did not show any significant changes even after prolonged incubation with $FeCl_3$ and Na_2S. The spectra of the three forms of C288T were virtually identical to that of both the wild-type and the His_6-tagged biotin synthases (Figure 4-7).

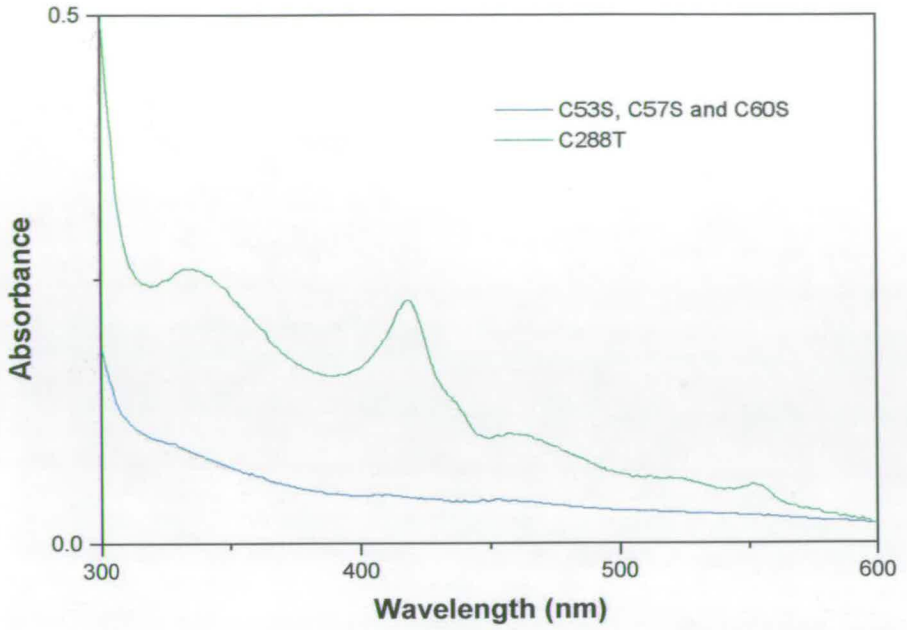

Figure 4-7

UV-visible spectra of cysteine mutants. The spectra are from samples of all proteins (1mg/ml) in 100mM sodium phosphate pH7.5. Wild-type, His_6-taggged and C288T biotin synthases have almost identical adsorption spectra (green spectra). The three mutants (C53S, C57S and C60S) are very similar to each other (blue spectra).

4.20 *In Vitro* Assay for Biotin Production

The *in vitro* activities of the cysteine mutants were determined using the *Lactobacillus* assay. Biotin was produced by the C288T mutant but not by the three other cysteine mutants (Table 4-12). There was no difference in biotin production between aerobic and anaerobic incubations.

Table 4-12

In vitro biotin production*.

Protein	As purified	Apoenzyme	Reconstituted holoenzyme
C53S	-	-	-
C57S	-	-	-
C60S	-	-	-
C288T	+	+	+

*Biotin production was measured using the *Lactobacillus* assay in the presence of biotin synthase or mutant protein (5μM), potassium chloride (10mM), dethiobiotin (50μM), AdoMet (150μM), $Fe(NH_4)_2(SO_4)_2$ (5mM), NADPH (1mM), fructose 1,6-bisphosphate (5mM), L-cysteine (500μM), DTT (10mM), PCOi cell free extract (100μl), FLD (12.5μM) and FLDR (2μM). The reaction mixture was incubated for 2h at 37 C (+ = biotin produced and - = no biotin production).

4.21 Discussion

Biotin synthase has two dimeric forms that contain different types of Fe-S clusters. In its oxidised form the protein contains a single [2Fe-2S] cluster in each monomer unit but on reduction this converts to a single [4Fe-4S] cluster in the dimer. EPR and Raman spectroscopy studies have provided evidence that in the oxidised [2Fe-2S] form biotin synthase has one iron which is co-ordinated to two cysteines and one iron which is co-ordinated to a cysteine and an oxygenic ligand (83, 180). In contrast, after dithionite reduction a [4Fe-4S] cluster is formed in which each iron is co-ordinated to a single cysteine sulfur. A possible mechanism for this interconversion has been proposed by Johnson (180). It has been speculated that the cysteine residues of the highly conserved "cysteine box" GXCXXXCXXCXQ motif of these proteins are involved in Fe-S cluster binding. This is supported by the fact that an identical motif is found in other Fe-S cluster proteins such as LIPA (Swissprot accession number: P25845) (73), ARR-AE (P39329) (71), LAM (74), the nitrogen fixation B gene product (P11067) (75), pyrrolo-quinoline-quinone synthase (Q01060) (77), PFL-AE (P09374) (78), NARA protein (P39757) (81), FNR (P03019) (76), benzylsuccinate synthase activating enzyme (CAA05050) (72), spore photoproduct lyase (P37956) (79), molybdenum cofactor synthase (O27593) (80) and the thiamine synthase H

gene product (P30140) (79). Mutational studies on PFL-AE have shown that the three cysteine residues of the "cysteine box" are vital for its activity (141).

Our attempts to purify wild-type biotin synthase from overexpressing clones using previously reported methods afforded protein that was *ca.* 80% pure contaminated with several high molecular weight contaminants. To circumvent this problem we elected to clone the *bio*B gene with an N-terminal His_6-tag and to purify the fusion protein using Ni-bound affinity chromatography. This appeared to be a safe approach since *E. coli* biotin synthase has a relatively long N-terminal sequence, which is either not present or unconserved in the ORF's of genes from other species, and the tag was unlikely to affect enzymatic activity.

A further significant result was that the *in vivo* activity of the N-terminus His_6-tagged biotin synthase proved indistinguishable from that of the wild-type protein. The His_6 tag allowed purification of much larger quantities of homogeneous *E. coli* biotin synthase than previously available. Typically, protein of >95% homogeneity could be isolated in a single chromatographic operation.

N-terminal sequencing was used to check the amino acid sequence and mass spectrometry was used to verify the molecular weights and the homogeneity of the proteins. One small problem with the nickel affinity column was the copurification of superoxide dismutase and SlyD but this was easily resolved by the addition of a gel exclusion step. *In vitro* biotin production was very small (0.2mol biotin/mol protein/h) but was similar to reported values (66, 90, 122). Preliminary crystal trials were unsuccessful perhaps due to the pure enzyme being present in a number of different forms.

Metal analyses on both the wild-type and the His_6-tagged protein revealed that they contained the same amount of Fe as that reported by Marquet and her coworkers (153) but less than that reported by Sanyal (66). This is possibly a result of the high protein expression levels. Shortage of free intracellular Fe^{2+} and/or the fact that the enzyme involved in cluster formation in the cell is expressed at wild-type levels and would lead to a proportion of the biotin synthase population being formed with incomplete clusters. In order to increase the iron content of biotin synthase, the apoenzyme was prepared anaerobically by treatment of the proteins with sodium dithionite and EDTA and the [2Fe-2S] cluster was reconstituted by incubation with $FeCl_3$ and Na_2S. Although the concentration of biotin synthase with intact [2Fe-2S] clusters was significantly increased by this procedure both the apoenzyme and the reconstitute holoenzyme produced equal amounts of biotin which was virtually the same as wild type and His_6-tagged biotin synthases. This suggests that there is sufficient iron and sulfur in the assay mixture to reconstitute the cluster *in situ.* Clearly, biotin synthase is not acting as a true catalyst and one reasonable explanation for this is that an unknown cofactor(s) (possibly the sulfur donor) is missing from the reaction mixture. Addition of pure *A. vinelandii* NifS did not seem to visibly affect the reaction. Although NifS has been shown to

regenerate Fe-S clusters in other enzymes it may be that a NifS-like enzyme is not used by biotin synthase or that the *A. vinelandii* enzyme does not function with *E. coli* biotin synthase. Sequence similarity searches reveal that there at least twenty known species of bacteria, yeast and plants which contain a *bio*B gene sequence similar to that from *E.coli*. To date, biotin synthase from *B. sphaericus* (65), *A. thaliana* (43), *S. cerevisiae* (44), and *E. coli* (66) have been cloned, overexpressed and purified. Sufficient complementation analysis has been carried out on *Methylobacillus, B. flavum (67), B. subtilis* (68), *E. herbicola* (69) and *S. marcescens* (70) to confirm that they also express active biotin synthases. Sequence alignment reveals a number of conserved regions. There are 25 completely conserved residues, four of which are cysteine. Three of these (C53, C57, C60) lie in the fifteen residue 'cysteine box' motif [K(S/T)GXCXE(D/N)CX(Y/F)CXQS] and the fourth (C188 in the *E. coli* sequence) is remote.

To determine which of the cysteine residues are involved in stabilising the [2Fe-2S] and [4Fe-4S] forms of biotin synthase single point mutations were made of five cysteine residues (C53, C57, C60, C188 and C288) to either serine or threonine. The choice of cysteine substitution by hydroxylated residues was made to preserve as much as possible the H-bonding character and the side chain geometry of the original cysteine residues. All the mutant proteins were expressed as His_6-tag fusions and purified using IMAC chromatography. The molecular weights of all the polypeptides were verified by mass spectrometry and the purified proteins were characterised by UV-visible spectrophotometry, Ni, Fe and S analyses and *in vivo* and *in vitro* assays for biotin production.

Wild-type biotin synthase, His_6-tagged biotin synthase and the His_6-tagged non-conserved mutant C288T all had similar UV-visible spectrophotometric characteristics that were indicative of intact [2Fe-2S] cluster formation. All of these proteins, along with their apoproteins and reconstituted holoproteins, were active both *in vivo* and *in vitro*. In contrast, C53S, C57S and C60S were all colourless and their absorption spectra showed no indication of the presence of [2Fe-2S] clusters indicating that these residues are absolutely vital for Fe-S cluster formation which is in turn crucial for activity. C188S proved to be insoluble and could only be characterised *in vivo* where it did not produce biotin. The fact that only three cysteine residues appear to be needed for [2Fe-2S] cluster binding (180) and that the C53S, C57S and C60S mutants are inactive suggest that C188 may be required for correct folding of the protein. Attempts to induce Fe-S cluster formation by incubation of these mutants with excess reagents did not result in any significant increase of iron binding.

The only cysteine mutant of *E. coli* biotin synthase which was catalytically active and could support formation of a [2Fe-2S] cluster was C288T, the mutant of the non-conserved cysteine residue, showing that the presence of C288 is not essential for folding, [2Fe-2S] and [4Fe-4S] cluster formation or for activity. In contrast, all the conserved residues C53, C57 and C60 of

the 'cysteine-box' are proven to be absolutely crucial for both the formation of the [2Fe-2S] cluster and the activity of the enzyme. These results are consistent with recent mutational studies on PFL-AE where it was also found that mutations of cysteine residues in the 'cysteine-box' abolish metal binding (141).

Since the completion of these experiments, Hewitson and coworkers have published work on *E. coli* biotin synthase mutants (181). In their paper they report the mutation of the residues C53, C57 and C60 to alanine. In contrast to our findings their alanine mutants still have the ability to bind the Fe-S cluster but they prove inactive *in vitro* which is in agreement with our results. They speculate that alternative residues could act as substitute ligands to the Fe-S cluster but that the mutant protein is unable to undergo the reductive 2Fe-2S to 4Fe-4S cluster rearrangement.

In the absence of crystallographic evidence, this work is a step towards the definition of the essential protein residues involved in the mechanism of Fe-S cluster formation (180) in biotin synthase and the relevance of these to the catalytic action of the enzyme. The inference of spectroscopic studies on *E. coli* biotin synthase is that a hydroxylated residue is also involved in the initial [2Fe-2S] cluster formation and here the conserved 'cysteine-box' residues T/S50 and S63 are obvious candidates. Another region in the protein that is almost completely conserved is the sequence Y150, N151,H152, N153 and L154 which is also found in lipoic acid synthase (84). Biotin synthase mutants at sites within these sequences are the subject of current studies. We have recently described the overexpression, purification and redox characteristics of the flavoprotein components of the *E. coli* biotin synthase system, FLD and FLDR (112), and the fact that it is now possible to obtain relatively large quantities of these and functional, homogeneous *Bio*B protein should facilitate examination of the protein-protein and protein-cofactor interactions involved the redox chemistry of the biotin synthase complex. Despite the enormous amount of research that has been carried out over the past thirty years a lot of work still has to be done to solve the problem that is the biotin synthase reaction.

These results are published and a copy of the publication forms Appendix II (182).

Chapter 5: References

5.1 References

1. Wildiers, E. (1901) *Lacellute* **18,** 313
2. Williams, R., J, Lyman, C. M., Goodyear, G. M.,Truesdail, H. J. H. and Holaday, D. (1943) *J. Am. Chem. Soc.* **55,** 2912
3. Whitehead, C. C. (1988) *Biotin in animal nutrition*, Hoffmann La-Roche, Basel
4. Kögl, F. and Tonnis, B. (1936) *Z. Physiol Chem.* **242,** 43-73
5. Du Vigneaud, V., Melville, D. B., Moyer, A. W. and Hoffman K. (1942) *J. Biol. Chem.***146,** 475
6. Harris, S. A. (1943) *Science* **97,** 447
7. Goldberg, M. W. and Sternbach, H. (1946), United States Patent
8. McGarrity, J., T. Tenud, L. and Meul, T. (1988), European Patent Office
9. Lynen, F., Knappe, J., Lorch, E., Jutting, G. and Rungelman, E. (1959) *Agnew Chem.* **71,** 481-486
10. Tipton, P. A. and Cleland, W. W. (1988) *Biochem.* **27,** 4317-4325
11. Ogita, T. and Knowles, J. R. (1988) *Biochem.* **27,** 8028-8033
12. Knappe, J. (1970) *Ann. Rev. Biochem.* **39,** 757
13. Eisenberg, M. A. (1973) *Adv. Enzymol. Rel. Areas Mol. Biol.* **38,** 317-372
14. Cerry, M., Julakoba, O. and Pacek, J. (1974) *Coll. Czech Chem.Comm.* **39,** 1391
15. Moss, J. and Lane, M. D. (1971) *Adv. Enzymol.* **35,** 321-442
16. Kasow, D. P. and Lane, M. D. (1962) *Biochem. Biophys. Res. Comm.* **7,** 439-443
17. Hillier, Y., Gershoni, J. M., Bayer, E. A. and Wilchek, M. (1987) *Biochem. J.* **248,** 167-171
18. Wilchek, M. and Bayer, E. A. (1988) *Anal. Biochem.* **171,** 1-32
19. Lindqvist, Y. and Schneider, G. (1996) *Curr. Biol.* **6,** 798-803
20. Swick, H. M. and Klein, C. L. (1985) *Ann New York Acad. Sci.* **447,** 430
21. Baldet, P., Gerbling, H., Axiotis, S. and Douce, R. (1993) *Eur. J. Biochem.* **217,** 479-485
22. del Campillo Campbell, A.,Kayajanian, G.,Campbell, A. and Adhya, S. J. (1967) *J. Bacteriol.* **94,** 2065-2066
23. Rolfe, B. and Eisenberg, M. A. (1968) *J. Bacteriol.* **96,** 515-524
24. Taylor, A. L. (1970) *Bacteriol. Rev.* **34,** 155-175
25. Cleary, P. P. and Campbell, A. (1972) *J. Bacteriol.* **111,** 830-839
26. Rolfe, B. (1970) *Virol.* **42,** 643-661
27. Scharwz, M. (1966) *J. Bacteriol.* **92,** 1083-1089

28. Campopiano, D. J (1999) Personal Communication
29 Eisenberg, M. A. (1975) *Metabolic Pathways* 27, Academic Press, New York
30. Barker, D. F. and Campbell, A. M. (1981) *J. Mol. Biol.* **146,** 469-492
31. Adhya, S.,Cleary, P. P. and Campbell, A. (1968) *Proc. Natl. Acad. Sci. USA* **61,** 956-962
32. Guha, A., Saturen, Y. and Szybalski, W. (1971) *J. Mol. Biol.* **56,** 53-62
33. Otsuka, A. and Abelson, J. (1978) *Nature* **276,** 689-694
34. Heinz, E. B., Phillips, D. A. and Streit, W. R. (1999) *Mol.Plant-Microbe Interact.* **12,** 803-812
35. Pai, C. H. and Lichstein, H. C. (1965) *Biochim. Biophys. Acta* **100,** 28-35
36. Eisenberg, M. A. and Starr, C. (1968) *J. Bacteriol.* **96,** 1291-1297
37. Jacob, F. and Monod, J. (1961) *J. Mol. Biol* .**3,** 318-356
38. Eisenberg, M. A., Prakesh, O. and Hsuing, S. (1982) *J. Biol. Chem.* **257,** 15167-15173
39. Howard, P. K., Shaw, J. and Otsuka, A. (1985) *Gene* **35,** 321-331
40. Wilson, K. P., Shewchuk, L. M., Brennan, R. G. and Otsuka, A. J. (1992) *Proc. Natl. Acad. Sci. USA* **89,** 9257-9261
41. Baldet, P., Gerbling, H., Axiotis, S. and Douce, R. (1993) *Arch. Biochem. Biophys.* **30,** 67-73
42. Weaver, L. M., Yu, F., Wurtele, E. S. and Nicolau, B. J. (1996) *Plant Physiol.* **110,** 1021-1028
43. Baldet, P., Alaban, C. and Douce, R. (1997) *FEBS Letts.* **419,** 206-210
44. Flint, D. H. and Allen, R. M. (1997) *Meth. Enzymol.* **279,** 349-356
45. Parry, R. J. (1983) *Tetrahedron* **39,** 1215-1238
46. Ploux, O., Soulare, P., Marquet, A., Gloecker, R. and Lemoine, Y. (1992) *Biochem. J.* **287,** 685-690
47. Ifuku, O., Miyaoka, H., Koga, N., Jiro, S., Haze, S., Wachi, Y. and Kajiwa, M. (1994) *Eur. J. Biochem.* **220,** 585-591
48. Sanyal, I., Lee, S. and Flint, D. (1994) *J. Am. Chem. Soc.* **116,** 2637-2638
49. Lemoine, Y., Wach, A. and Jeltsch, J. (1996) *Mol. Microbiol.* **19,** 639-647
50. Ploux, O. and Marquet, A. (1992) *Biochem. J.***238,** 327-331
51. Alexeev, D., Alexeeva, M., Baxter, R. L., Campopiano, D. J., Webster, S. P. and Sawyer, L. (1998) *J. Mol. Biol.* **284,** 401-419
52. Pai, C. H. (1971) *J. Bacteriol.* **112,** 1280-1287

53. Kack, H., Sandmark, J., Gibson, K., Schneider, G. and Lindqvist, Y. (1999) *J. Mol. Biol.* **291,** 857-876

54. Alexeev, D. (1999) Personal Communication

55. Krell, K. and Eisenberg, M. A. (1970) *J. Biol. Chem.* **245,** 6558-6566

56. Otsuka, A., Buonocristiani, M. R., Howard, P. K., Flamm, J., Johnson, C., Yamomoto, R., Uchida, K., Cook, C., Ruppert, J. and Matzuki, J. (1988) *J. Biol. Chem.* **263,** 19577-195785

57. Alexeev, D., Bury, S. M., Boys, C. W. G., Sawyer, L., Ramsey, A. J., Baxter, H. C. and Baxter, R. L. (1994) *J. Mol. Biol.***235,** 774-776

58. Sakurai, R. K., Imai, Y., Masuda, M., Komatsobara, S. and Tosa, T. (1994) *J. Biotechnol.* **36,** 63-73

59. Gloecker, R., Oshawa, I., Speck, D., Ledoux, C., Bernard, S., Zinsius, M., Villeval, D., Kisou, T., Kamogawa, K. and Lemoine, Y. (1990) *Gene* **87,** 63-70

60. Alexeev, D., Baxter, R. L. and Sawyer, L. (1994) *Structure* **2,** 1062-1072

61. Huang, W. J., Lindqvist, Y., Schneider, G., Gibson, K. J., Flint, D. H. and Lorimer, G. (1994) *Structure* **2**, 407-414

62. Baxter, R. L. and Baxter, H. C. (1994) *J. Chem. Soc., Chem. Comm.* 759-760

63. Baxter, R. L., Ramsey, A. J., McIver, L. and Baxter, H. C. (1994) *J. Chem. Soc., Chem. Comm.* 559-560

64. Gibson, K. J., Lorimer, G. H., Rendina, A. R., Taylor, W. S., Cohen, G., Gatenby, A. A., Payne, W. G., Roe, C., Lockett, B. A., Nudelman, A., Marcoveiei, D., Nachum, A., Wexler, B. A., Marsilii, E. L., Turner, I. M., Howe, L. D., Kalbach, C. E. and Chi, H. (1995) *Biochem.* **34,** 10976-10984

65. Florentin, D., Bui, B., Marquet, A., Ohshiro, T. and Izumi, Y. (1994) *Comptes Rendus Del'Academie des Sciences* **317,** 485-488

66. Sanyal, I., Cohen, G. and Flint, D. H. (1994) *Biochem.* **33,** 3625-3631

67. Serebriiskii, I. G., Vassin, V. M. and Tsygankov, Y. D. (1996) *Gene* **175,** 15-22

68. Bower, S., Perkins, J. B., Rogers, Y., R, Howitt, C. L., Raiham, P. and Pero, J. (1996) *J. Bact.* **178,** 4122-4130

69. Wu, C. H., Chen, H. Y. and Shiuan, D. (1996) *Gene* **174**(2), 251-258

70. Sakurai, N., Imai, Y., Masuda, M., Komatsubara, S. and Tosa, T. (1993) *Appl. Env. Microbiol.* **59,** 2857-2863

71. Ollangier, S., Meier, C., Mulliez, E., Gaillard, J., Schuenemann, V., Trautwein, A., Mattioloi, T., Lutz, M. and Fontecave, M. (1999) *J.Am.Chem. Soc.* **121,** 6344-6350

72. Leuthner, B., Leutwin, C., Schulz, H., Horth, P., Haehnel, W., Sclitz, E., Schagger, H. and Heider, J. (1998) *Mol. Microbiol.* **28,** 615-628

73. Ollangier-de Choudons, S. and Fontecave, M. (1999) *FEBS Letts.* **453,** 25-28

74. Frey, P. A. and Reed, G. H. (1993) *Adv. Enzymol. Rel. Areas Mol. Biol.* **66,** 1-39

75. Joerger, R. D. and Bishop, P. E. (1998) *J. Bacteriol.* **170,** 1475-1487

76. Shaw, D. J. and Guest, J. R. (1982) *Nucleic Acids Res.* **10,** 6119-6130

77. Liu, S. T., Lee, L., Tai, C. Y., Hung, C. H., Chang, Y. S., Wolfram, J. H., Rogers, R. and Goldstein, A. H. (1992) *J. Bacteriol.* **174,** 5814-5819

78. Broderick, J. B., Duderstadt, R. E., Fernandez, D. C., Wojtuszewski, K., Henshaw, T. F. and Johnson, M. K. (1997) *J. Am. Chem. Soc.***119,** 7396-7397

79. Fajardo-Cavazos, P., Salazar, C. and Nicholson, W. L. (1993) *J. Bacteriol.* **175,** 1735-1744

80. Smith, D. R., Doucette-Stamm, L. A., Deloughery, C., Lee, H. M., Dubois, J., Aldredge, T., Bashirzadeh, R., Blakely, D., Cook, R., Gilbert, K., Harrison, D., Hoang, L., Keagle, P., Lumm, W., Pothier, B., Qui, D., Spadafora, R., Vicare, R., Wang, Y., Weizerbowski, J., Gibson, R., Jiwani, N., Caruso, A., Bush, D., Safer, H., Patwell, D., Prabhakar, S., McDougall, S., Shimer, G., Goyal, A., Pietrovski, S., Church, G. M., Daniels, C. J., Mao, J. I., Rice, P., Nolling, J. and Reeve, J. N. (1997) *J. Bacteriol.* **179** 7135-7155

81. Glaser, P., Danchin, A., Kunst, F., Zuber, P. and Nakano, M. (1995) *J. Bacteriol.* **177,** 1112-1115

82. Flint, D. H. and Allen, R. M. (1996) *Chem. rev.* **96,** 2315-2334

83. Duin, E. C., Lafferty, M. E., Crouse, B. R., Allen, R. M., Sanyal, I., Flint, D. H. and Johnson, M. K. (1997) *Biochemistry* **36,** 11811-11820

84. Marquet, A., Florentin, D., Ploux, O. and Tse Sum Bui, B. (1998) *J. Phys. Org. Chem.* **11,** 529-535

85. Ifuku, O., Kishimoto, J., Haze, S., Yanagi, M. and Fukushima, S. (1992) *Biosci. Biotech. Biochem.* **56,** 1780-1785

86. Ifuku, O., Koga, N., Haze, S., Kishimoto, J. and Wachi, Y. (1994) *Eur. J. Biochem.* **224,** 173-178

87. Birch, O., Brass, J., Fuhrmann, M. and Shaw, N. (1993) European Patent Office

88. Birch, O. M., Fuhrmann, M. and Shaw, N. M. (1995) *J. Biol. Chem.* **270,** 19158-19165

89. Sanyal, I., Gibson, K. J. and Flint, D. H. (1996) *Arch. Biochem. Biophys.* **326,** 48-56

90. Mejean, A., Tse Sum Bui, B., Florentin, D., Ploux, O., Izumi, Y. and Marquet, A. (1995) *Biochem. Biophys. Res. Comm.* **217,** 1231-1237

91. Jacobson, M R., Brigle, K. E., Bennett, L. T., Setterquist, R. A., Wilson, M. S., Cash, V. L., Beynon, J., Newton, W. E., and Dean, D. (1989) *J. Bacteriol.* 171 1017-1027

92. Zheng, L.,White, R. H.,Cash, V. L.,Jack, R. F. and Dean, D. R. (1993) *Proc. Natl. Acad. Sci. USA* **90,** 2754-2758

93. Zheng, L., White, R. H.,Cash, V. and Dean, D. (1994) *Biochem.* **33,** 4714-4720

94. Hildago, E. and Demple, B. (1996) *J. Biol. Chem.* **271,** 7269-7272

95. Flint, D. H. (1996) *J. Biol. Chem.* **271,** 16068-16074

96. Vetter, H. and Knappe, J. (1971) *Hoppe-Seylers Z Phisiol. Chem.* **352,** 433-446

97. Jarrett, J. T., Huang, S. and Matthews, R. G. (1998) *Biochem.* **37,** 5372-5382

98. Peariso, K., Goulding, C. W., Huang, S., Matthews, R. G. and Renner-Hahn, J. E. (1998) *J. Am. Chem. Soc.***120,** 8410-8416

99. Fuji, K. and Huennekens, F. M. (1974) *J. Biol. Chem.* **249,** 6745-6753

100. Fuiji, K., Galivan, J. H. and Huennekens, F. M. (1977) *Arch. Biochem. Biophys.* **178,** 662-670

101. Blaschkowski, H. P., Neuer, G., Ludwig-Festl, M. and Knappe, J. (1982) *Eur.J. Biochem.* **123,** 563-569

102. Nakayama, H., Midwinter, G. G. and Krampitz, L. O. (1971) *Arch. Biochem. Biophys* **143,** 526-534

103. Osbourne, C., Chen, L. and Matthews, R. G. (1991) *J. Bacteriol.* **173,** 1729-1737

104. Bianchi, V., Eliasson, R., Fontecave, M., Mulliez, E., Hoover, D. M., Matthews, R. G. and Reichard, P. (1993) *Biochem. Biophys. Res. Comm.* **197,** 792-797

105. Hoover, D. H., Matthews, R. G. and Ludwig, M. L. (1993) *Flavins and Flavoproteins* 359-362

106. Hoover, D. M., Jarrett, T. J., Matthews, R. G. and Ludwig, M. L. (1995) *FASEB* **9,** A1286

107. Hoover, D. M. and Ludwig, M. L. (1997) *Prot.Sci.* **6,** 2525-2537

108. Bianchi, V., Reichard, P., Eliasson, R., Pontis, E., Krook, M., Jornvall, H. and Haggard-Ljungquist. (1993) *J. Bacteriol.* **175,** 1590-1595

109. Bianchi, V., Haggard-Ljundquist, E., Pontis, E. and Reichard, P. (1995) *J. Bacteriol.* **177,** 4582-4531

110. Ingelman, M., Bianchi, V. and Eklund, H. (1997) *J. Mol. Biol.* **268,** 147-157

111. Leadbeater, C., McIver, L., Campopiano, D., J, Webster, S. P., Baxter, R. L., Kelly, S. M., Price, N. C., Lysek, D. A., Noble, M. A., Chapman, S. K. and Munro, A. W. (1999) *In press*

112. McIver, L., Leadbeater, C., Campopiano, D. J., Baxter, R. L., Daff, S. N., Chapman, S. K. and Munro, A. W. (1998) *Eur. J. Biochem.* **257,** 577-585

113. Jenkins, C. M. and Waterman, M. R. (1994) *J. Biol. Chem.* **269,** 27401-27408

114. Shaw, N. M., Birch, O. M., Tinschert, A., Venetz, V., Dietrich, R. and Savoy, L. (1998) *Biochem. J.* **330,** 1079-1085

115. Gibson, K. J., Pelleier, D. A. and Turner, I. M. (1999) *Biochem. Biophys.Res. Comm.* **254,** 632-635

116. Heng-Chun, L., McCormick, D. B. and Wright, L. D. (1968) *J. Biol. Chem.* **243,** 6442-6445

117. Parry, R. J. and Kunitani, M. G. (1976) *J. Am. Chem. Soc.* **98,** 4024-4026

118. Parry, R. J. (1980) *Tet. Letts.* **21,** 4783 - 4786

119. Marti, F. B. (1983) in *Edigenossischem Technischen Hochschule*, ETH Zurich, Zurich

120. Marquet, A., Frappier, F., Guillieum, G., Azoulay, M., Florentin, D. and Tabet, B. (1993) *J. Am. Chem. Soc.***115,** 2149-2145

121. Baxter, R. L., Camp, D. J., Cotts, A. and Shaw, N. (1992) *J. Chem. Soc. Perkin Trans.* **1,** 255-258

122. Guianvarc'h, D., Florentin, D., Tse Sum Bui, B., Nunzi, F. and Marquet, A. (1997) *Biochem. Biophys. Res. Comm.* **236,** 402-406

123. Barabiak, J., Moss, M. L. and Frey, P. A. (1989) *J. Biol. Chem.* **264,** 1357-1360

124. Escalettes, F., Florentin, D., Tse Sum Bui, B., Lesage, D. and Marquet, A. (1999) *J. Am. Chem. Soc.* **121,** 3571-3578

125. Ollagnier, S., Mulliez, E., Gaillard, J., Eliasson, R., Fontecave, M. and Reichard, P. (1996) *J. Biol. Chem.* **271,** 9410-9416

126. Ollagnier, S., Mulliez, E., Schmidt, P. P., Eliasson, R., Gaillard, J., Deronzier, C., Bergman, T., Graslund, A., Reichard, P. and Fontecave, M. (1997) *J. Biol. Chem.* **272,** 24216-24233

127. Mulliez, E., Fontecave, M., Gaillard, J. and Reichard, P. (1993) *J. Biol. Chem.* **268,** 2296-2299

128. Sun, D. and Setlow, P. (1993) *J. Bacteriol.* **175,** 1423-1432

129. Sun, X., Eliasson, R., Pontis, E., Andersson, J., Buist, G., Sjoberg, B. and Reichard, P. (1995) *J. Biol. Chem.* **270,** 2443-2446

130. Sun, X., Ollagnier, S., Schmidt, P. P., Atta, M., Mulliez, E., Lepape, L., Eliasson, R., Graslund, A., Fontecave, M., Reichard, P. and Sjoberg, B. (1996) *J. Biol. Chem.* **271,** 6827-6831

131. Ollangier-de Choudons, S. and Fontecave, M. (1999) *FEBS Letts.* **453,** 25-28

132. Leider, K. W., Booker, S., Ruzicka, F. J., Beinert, H., Reed, G. H. and Frey, P. A. (1998) *Biochem.***37,** 2578-2585

133. Hayden, M., Huang, I., Bussiere, D. J. and Ashley, G. W. (1992) *J. Biol. Chem.* **267,** 9512-9515

134. Reed, K. E. and Cronan, J. E. (1993) *J. Bacteriol.* **175,** 132-136

135. Busby, R. W., Schelvis, J. P. M., Yu, D. S., Babcock, G. T. and Marletta, M. A. (1999) *J. Am.Chem. Soc.* **121,** 4706-4707

136. Becker, A., Fritzwolf, K., Kabsch, W., Knappe, J., Schultz, S. and Wagner, A. F. (1999) *Nat. Struct. Biol.* **6,** 969-975

137. Leppanen, V. M., Merckel, M. C., Ollis, D. L., Wong, K. K., Kazrich, J. W. and Goldman, A. (1999) *Structure with Folding and Design* **7,** 733-744

138. Conradt, H., Hohmann-Berger, M., Hohmann, H., Blaschowski, H. P. and Knappe, J. (1984) *Arch. Biochem. Biophys.* **28,** 133-142

139. Wong, K. K., Murray, B. W., Lewisch, S. A., Baxter, M. K., Ridky, T. W., Ulissi-DeMario, L. and Kozarich, J. W. (1993) *Biochem.* **32,** 14102-14110

140. Volker Wagner, A. F. ,Frey, M., Neugebauer, F. A. and Schafer, W. (1992) *Proc. Natl. Acad. Sci. USA* **89,** 996-1000

141. Kulzer, R., Pils, T., Kappl, R., Huttermann, J. and Knappe, J. (1998) *J. Biol. Chem.* **273,** 4897-4903

142. Begley, T. P. (1996) *Nat. Prod. Rep.* **13,** 177-183

143. Taylor, S. V., Kelleher, N. L., Kinsland, C., Chiu, H., Costello, C. A., Backstrom, A. D., McLafferty, F. W. and Begley, T. P. (1998) *J. Biol. Chem.* **273,** 16555-16560

144. Soda,

145. Yanisch-Perron, C., Viera, J. and Messing, J. (1985) *Gene* **33,** 103-108

146. Grant, S. G. N. (1990) *Proc. Natl. Acad Sci* **87,** 4645 - 4649

147. Phillips, T. A., Van Bogelen, R. A. and Neidhardt, F. C. (1984) *J.Bacteriol.* **159,** 283-287

148. Woodcock, D. M. (1989) *Nucl. Acids Res.* **17,** 3469 - 3478

149. Maniatis, T., Fritsch, E. F. and Sambrook, J. (1982) *Molecular Cloning: A Laboratory Manual*

150 Sarker, G. and Sommers, S. S. (1990) *BioTechniques* **8,** 404-407

151. Laemmeli, U. K. (1970) *Nature* **227,** 680-685

152. Bradford, M. M. (1976) *Anal. Biochem.* **72**(248-254)

153. Tse Sum Bui, B., Florentin, D., Fournier, F., Ploux, O., Mejean, A. and Marquet, A. (1998) *FEBS Letts.* **440,** 226-230

154. Colombo Pirola, M., Monti Alessandro, F., Aliverti, A. and Zanetti, G. (1994) *Arch. .Biochem. Biophys.* **311,** 480-486

155. DeMoll, E. and Shive, W. (1986) *Anal. Biochem.* **158,** 55-58

156. Harrison, D. C. (1948) *Quantitative Chemical Analysis*, Freeman and Co., New York

157. Stookey, L. L. (1970) *Anal. Chem.* **42,** 779-781

158. Hayes, J. D., Kerr, L. A. and Cronshaw, A. D. (1989) *Biochem. J.* **264,** 437-445

159. Dutton, P. L. (1978) *Meth. Enzymol.***54,** 411-435

160. Barton, G. J. (1993) *Prot. Eng.***6,** 37-40

161. Jenkins, C. M., Genzor, C. G., Filliat, M. F., Waterman, M. R. and Gomez-Moreno, C. (1997) *J. Biol. Chem.* **272,** 22509-22513

162. Daff, S. N., Chapman, S. K., Turner, K. L., Holt, R. A., Govindaraj, S. and Poulos, T. L. (1997) *Biochem.* **36,** 13816-13823

163. Iyanagi, T., Makino, N. and Mason, H. S. (1974) *Biochem.* **13,** 1701-1710

164. Massey, V. (ed) (1991) *A simple method for the determination of redox potentials.* Flavins and Flavoproteins. Edited by Curti, B., Ronchi, S., and Zanetti, G., Walter de Gruyter, New York

165. Draper, R. D. and Ingraham, L. L. (1968) *Arch. Biochem. Biophys.* **125,** 802-808

166. Miles, J. S., Munro, A. W., Rospendowski, B. N., Smith, W. E., McKnight, J. and Thomson, A. J. (1992) *Biochem. J.* **288,** 503-509

167. Hurley, J. K., Fillar, M. F., Gomez-Moreno, C. and Tollin, G. (1996) *J. Am. Chem. Soc.* **118,** 5526-5531

168. Sykes, G. A. and Rogers, L. J. (1984) *Biochemical Journal* **217,** 845-850

169. Stankovich, M. T. in *Chemistry and Biochmeistry of Flavoenzymes* Vol. I, pp. 401-425

170. Lambeth, J. and Kamin, H. (1976) *J. Biol. Chem.* **251,** 4299-4306

171. Iyangai, T. (1977) *Biochem.* **16,** 2725-2730

172. Wang, M.,Roberts, D. L., Paschke, R., Shea, T. M., Masters, B. S. S. and Kim, J.-J. P. (1997) *Proc. Natl. Acad. Sci. USA* **94,** 8411-8416

173. Abu-Soud, H. M., Feldman, P. L., Clark, P. and Steuhr, D. J. (1994) *J. Biol. Chem.* **269,** 32318-32326

174. Porter, J. D. (1991) *Trends Biochem. Sci.* **16,** 154-158

175. Smith, G. C. M., Tew, D. G. and Wolf, C. R. (1994) *Proc. Natl Acad. Sci. USA* **91,** 8710-8714

176. Govindaraj, S. and Poulos, T. L. (1997) *J. Biol. Chem.* **272,** 7915-7921

177. Tse Sum Bui, B. and Marquet, A. (1997) *Meth. Enz.* **279,** 356-362

178. Imlay, K. R. C. and Imaly, J. A. (1996) *J. Bacteriol.* **178,** 2564-2571

179. Hottenrott, S., Schumann, T., Pluckthun, A., Fischer, G. and Rahfeld, J. (1997) *J. Biol. Chem.* **272,** 15697-15701

180 Johnson, M. K.,Staples, C. R., Duin, E. C., Lafferty, M. E. and Duderstadt, R. E. (1998) *Pure Appl. Chem* **70,** 939-946

181 Hewitson, K. S., Baldwin, J. E., Shaw, N. M. and Roach, P. L. (2000) *FEBS Letts.* **466,** 372-376

182 McIver, L., Baxter, R. L. and Campopiano, D. J. (2000) *J. Biol. Chem.* **275,** 13888-13894

Appendix I

Eur. J. Biochem. 257, 577–585 (1998)

Characterisation of flavodoxin NADP$^+$ oxidoreductase and flavodoxin; key components of electron transfer in *Escherichia coli*

Lisa McIVER, Claire LEADBEATER, Dominic J. CAMPOPIANO, Robert L. BAXTER, Simon N. DAFF, Stephen K. CHAPMAN and Andrew W. MUNRO

Department of Chemistry, Joseph Black Building, The University of Edinburgh, The King's Buildings, West Mains Road, Edinburgh, UK

(Received 19 May/19 June 1998) – EJB 98 0680/4

The genes encoding the *Escherichia coli* flavodoxin NADP$^+$ oxidoreductase (FLDR) and flavodoxin (FLD) have been overexpressed in *E. coli* as the major cell proteins (at least 13.5% and 11.4% of total soluble protein, respectively) and the gene products purified to homogeneity. The FLDR reduces potassium ferricyanide with a k_{cat} of 1610.3 min^{-1} and a K_m of 23.6 μM, and cytochrome *c* with a k_{cat} of 141.3 min^{-1} and a K_m of 17.6 μM. The cytochrome *c* reductase rate is increased sixfold by addition of FLD and an apparent K_m of 6.84 μM was measured for the affinity of the two flavoproteins. The molecular masses of FLDR and FLD apoproteins were determined as 27648 Da and 19606 Da and the isolectric points as 4.8 and 3.5, respectively. The mass of the FLDR is precisely that predicted from the atomic structure and indicates that residue 126 is arginine, not glutamine as predicted from the gene sequence. FLDR and FLD were covalently crosslinked using 1-ethyl-3(dimethylamino-propyl) carbodiimide to generate a catalytically active heterodimer. The midpoint reduction potentials of the oxidised/semiquinone and semiquinone/hydroquinone couples of both FLDR (−308 mV and −268 mV, respectively) and FLD (−254 mV and −433 mV, respectively) were measured using redox potentiometry. This confirms the electron-transfer route as NADPH→FLDR→FLD. Binding of 2′ adenosine monophosphate increases the midpoint reduction potentials for both FLDR couples. These data highlight the strong stabilisation of the flavodoxin semiquinone (absorption coefficient calculated as 4933 M^{-1} cm^{-1} at 583 nm) with respect to the hydroquinone state and indicate that FLD must act as a single electron shuttle from the semiquinone form in its support of cellular functions, and to facilitate catalytic activity of microsomal cytochromes *P*-450 heterologously expressed in *E. coli*. Kinetic studies of electron transfer from FLDR/FLD to the fatty acid oxidase *P*-450 BM3 support this conclusion, indicating a ping-pong mechanism. This is the first report of the potentiometric analysis of the full *E. coli* NAD(P)H/FLDR/FLD electron-transfer chain; a complex critical to the function of a large number of *E. coli* redox systems.

Keywords: flavodoxin; flavodoxin NADP$^+$ oxidoreductase; redox potentiometry; enzyme kinetics; cytochrome *P*-450.

The *Escherichia coli* flavodoxin NADP$^+$ oxidoreductase (FLDR or flavodoxin reductase) and flavodoxin (FLD) are the two flavin-containing components of a short electron-transfer chain from NADPH, which provides electrons for the function of the biotin synthase [1] and cobalamin-dependent methionine synthase systems [2]. The enzymes are also required during anaerobic growth of the organism, participating in the pyruvate formate/lyase system of *E. coli* – a crucial mechanism for the anaerobic generation of pyruvate for glycolysis [3] and in the generation of deoxyribonucleotides through the enzyme anaerobic ribonucleotide reductase [4]. Recently, the FLDR/FLD system has also been recognised as the *E. coli* 'reductase', which can support the function of heterologously expressed eukaryotic cytochromes *P*-450 [5], even though no endogenous *P*-450s have yet been identified in the bacterium.

Correspondence to A. W. Munro, Department of Chemistry, Joseph Black Building, The University of Edinburgh, The King's Buildings, West Mains Road, Edinburgh, EH9 3JJ, UK

Fax: +44 131 650 4760.

E-mail: Andrew.Munro@ed.ac.uk

Abbreviations. CPR, cytochrome *P*-450 reductase; FLD, *E. coli* flavodoxin; FLDR, *E. coli* flavodoxin NADP$^+$ oxidoreductase; IPTG, isopropyl-β, D-thiogalactopyranoside; P-450, cytochrome *P*-450 monooxygenase.

We have overexpressed and purified the FLDR and FLD proteins in order to investigate their function in biotin synthesis and cytochrome *P*-450 reduction. Of particular interest was the analysis of the interactions of the FLDR and FLD proteins and the redox characteristics of these enzymes, since it is known that the cytochromes *P*-450 require two successive single-electron transfers to perform their activation of molecular oxygen. While the flavodoxins have been considered to function as single-electron donors by cycling between the hydroquinone and semiquinone states [6], it is by no means certain that the hydroquinone is a physiologically relevant species in electron-transport chains using NAD(P)H, FLDR and FLD, since the midpoint reduction potential of NAD(P)H (−320 mV) is likely to be considerably higher (more positive) than that of the FLD semiquinone/hydroquinone couple. Indeed, there is evidence to support the utilisation of the flavodoxin semiquinone as the electron donor for methionine synthetase [2, 7]. It is known that flavodoxins, in general, stabilise a semiquinone-1-electron-reduced form as opposed to the 2-electron-reduced hydroquinone. In fact, potentiometric studies on non-recombinant *E. coli* FLD, purified from large-scale cultures, indicated that this enzyme stabilises a blue neutral semiquinone form of FMN [8].

In this paper, we report the results of biophysical studies of the *E. coli* FLDR and FLD, analysing the interactions between

action rates were determined at 30°C in 100 mM sodium phosphate, pH 7.5, and the reciprocals of the data plotted against the reciprocals of the [FLDR] for each concentration of *P*-450 used.

Stopped-flow measurements of transient absorbance changes associated with reduction of FLDR and FLD flavins (decrease in absorbance at 456 nm and increase at 583 nm, respectively), reoxidation of the flavins (same wavelengths) and reduction of cytochrome *c* (550 nm) were made using an Applied Photophysics SF.17 MV stopped-flow kinetics spectrophotometer. Reactions were performed at 30°C in 100 mM sodium phosphate, pH 7.5 (unless otherwise stated). Rates of FLDR−FLD electron transfer were measured after enzyme and buffer solutions had been degassed and bubbled for 15 min with O_2-free N_2. Traces of O_2 were subsequently removed from the enzyme solutions by passing the concentrated stock solutions of enzyme down a G25 gel-filtration column (1×20 cm) within the anaerobic environment of a glove box (Belle Technology). The enzyme solutions were then diluted to the required concentrations, transferred to the stopped-flow syringes and sealed within the glove box before transferring to the stopped-flow apparatus.

Analysis of stopped-flow data was performed using the SF.17 MV software and Origin (Microcal), both of which use non-linear least-squares regression analysis. The reduction of FLDR by NADPH was measured by rapid mixing of NADPH (4 μM−2 mM) with FLDR (40 μM) and monitored at 456 nm (total flavin reduction). The electron transfer from FLDR to FLD was monitored at 583 nm (formation of FLD blue semiquinone) after mixing of 40 μM FLDR (reduced with 2 mM NADPH or sodium dithionite) with FLD (20 μM). When sodium dithionite was used, FLDR was reduced completely in an anaerobic environment with excess reductant, then separated from the dithionite by gel filtration under anaerobic conditions. Reoxidation of FLDR was measured after mixing of enzyme (80 μM) with a sub-stoichiometric quantity of reductant (40 μM NADPH) and monitoring the absorbance increase at 456 nm. Reoxidation of the FLD semiquinone (absorbance decrease at 583 nm) was measured after anaerobic reduction of the enzyme with excess sodium dithionite, isolation of the reduced enzyme by gel filtration and dilution of reduced FLDR into aerobic buffer. Reduction of cytochrome *c* was measured at 550 nm after reaction of reduced FLDR (10−50 μM enzyme + 2 mM NADPH) with cytochrome *c* (horse heart, type 1; 4 μM).

Chemical crosslinking of FLDR and FLD. Purified FLD (40 μM) and FLDR (8 μM) were covalently and specifically crosslinked using 1-ethyl-3-(dimethylamino-propyl) carbodiimide (EDC) (10 mM) in 10 mM Hepes buffer (2 ml, pH 7.0) at room temperature [15]. 10-ml aliquots were withdrawn from the reaction at 15-min intervals to assess the progress of the reaction by SDS/PAGE. After 1 h, the reaction was stopped by the addition of ammonium acetate (100 mM) and the protein mixture concentrated to approximately 0.5 ml by ultrafiltration [using a 10000 Da cut-off Centricon concentrator (Amicon)]. The crosslinked complex was separated from the FLDR and FLD proteins by gel filtration on FPLC (Superdex 75 column, 1.6×60 cm) in 50 mM Tris/HCl, pH 7.5, containing 50 mM KCl.

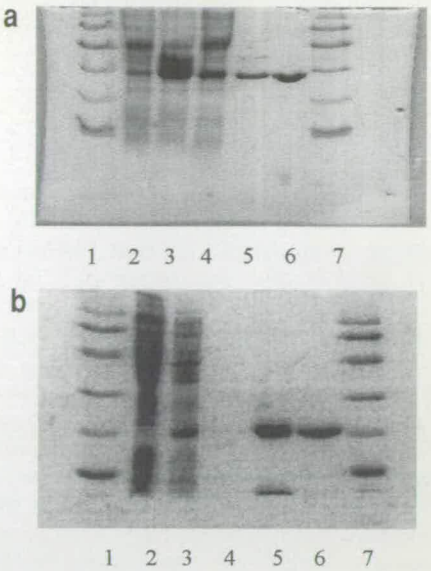

Fig. 1. (a) SDS/PAGE of *E. coli* flavodoxin NADP⁺ oxidoreductase (FLDR) purification steps. Lane 1, low molecular mass standards (94000, 67000, 43000, 30000, 20 100, 14 400 Da); lane 2, uninduced cells; lane 3, induced cells; lane 4, cell lysate; lane 5, Q-Sepharose; lane 6, 2′, 5′-ADP Sepharose; lane 7, low molecular mass standards (as lane 1). (b) SDS/PAGE of *E. coli* flavodoxin (FLD) purification steps. Lane 1, low molecular mass standards (94000, 67000, 43000, 30000, 20 100, 14 400 Da); lane 2, uninduced cell lysate; lane 3, induced cell lysate; lane 4, empty; lane 5, Q-Sepharose; lane 6, Resource-Q; lane 7, low molecular mass standards (as lane 1).

RESULTS

Protein characterisation. *Flavodoxin NADP⁺ oxidoreductase.* FLDR is a monomeric (247 amino acids, M_r 27620 Da) enzyme which contains FAD. *E. coli* HMS174 (DE3)/pCL21 was used to overexpress FLDR. The protein was purified by sequential chromatography steps on Q-Sepharose and 2′,5′-ADP Sepharose (Table 1). Samples were analysed at all steps by SDS/PAGE (Fig. 1a) and ultraviolet-visible spectroscopy. The molecular mass of the expressed FLDR apoprotein was determined as 27648 Da by electrospray mass spectroscopy. This is 28 Da higher than the predicted molecular mass of 27620 Da, calculated from the amino acid sequence derived from the database gene sequence [16] (less the N-terminal methionine). However, the recent solution of the atomic structure of the *E. coli* FLDR indicates that an arginine is present at position 126, as opposed to a glutamine predicted from the gene sequence [17]. The difference in molecular mass of these two residues is exactly 28 Da, corresponding to the apparent discrepancy. The isoelectric point of FLDR was measured as 4.8 by isolelectric focusing; rather more acidic than the theoretical value of 6.19 (SwissProt).

FLDR is bright yellow in its oxidised form and it is converted to a neutral blue semiquinone by the addition of one reducing equivalent. FLDR has an absorption coefficient of

Table 1. Purification table for *E. coli* NADP⁺ flavodoxin oxidoreductase (FLDR). Total protein was estimated by absorbance at 280 nm. FLDR was estimated by measurement of absorbance (Abs) at the peak of the longer wavelength flavin band (456 nm).

Purification step	Total volume (V)	Total protein	Total FLDR	Abs_{456}/Abs_{280}	Purification
	ml	$V \times Abs_{280}$	$V \times Abs_{456}$		-fold
Lysate	55	833.9	18.26	0.0207	1
Q-Sepharose	80	119.1	9.28	0.0779	3.77
2′,5′-ADP Sepharose	35	37.5	5.74	0.1531	7.41

Table 3. Steady-state kinetic parameters for FLDR. Rates of reduction of artificial electron acceptors were measured at 550 nm for cytochrome *c* (22 640 M^{-1} cm^{-1}) and 420 nm for potassium ferricyanide (1010 M^{-1} cm^{-1}). Rates were measured at 30°C in 100 mM sodium phosphate, pH 7.5, with saturating (200 μM) NADPH. The K_m for NADPH was determined under conditions of saturating cytochrome *c* (150 μM). The K_m for the FLD was determined under conditions of saturating cytochrome *c* and NADPH, with the FLDR at 16.65 nM.

Substrate	k_{cat}	K_m
	min^{-1}	μM
Potassium ferricyanide	1610.3 ± 50.1	23.6 ± 3.2
Cytochrome *c*	141.3 ± 5.3	17.6 ± 2.15
NADPH	–	3.85 ± 0.5
FLD	–	6.84 ± 0.68

Table 4. Steady-state kinetic parameters for the EDC-linked complex of FLDR/FLD. Experiments were performed as described above.

Substrate	k_{cat}	K_m
	min^{-1}	μM
Potassium ferricyanide	782.0 ± 35	33.2 ± 6.4
Cytochrome *c*	109.2 ± 4.5	87.4 ± 8.2

Visible spectra of the complex showed absorbance maxima at 379.5 nm and 462 nm, with shoulders at ≈487 nm and 404 nm. These absorbance characteristics are different from those of the individual FLDR and FLD – with absorbance maxima located between the peaks of the isolated flavoproteins. Addition of NADPH was seen to induce a decrease in the intensity of the flavin spectrum, but not to induce the formation of a species absorbing in the 550–600 nm region, suggesting that there was no formation of the neutral blue semiquinone form expected for the FMN in FLD.

Enzyme activities. Purified FLDR has NADPH-dependent reductase activity towards a variety of electron acceptors (Table 3). Using cytochrome *c* (horse heart, Sigma) as the acceptor, a k_{cat} of 141.3 ± 5.3 min^{-1} and a K_m of 17.6 ± 2.15 μM were measured using homogeneous FLDR at 30°C in 100 mM sodium phosphate, pH 7.5. With saturating cytochrome *c*, the K_m for NADPH was estimated at 3.85 ± 0.5 μM. Under similar conditions, potassium ferricyanide was reduced, with a K_m of 23.6 ± 3.2 μM and a k_{cat} of 1610.3 ± 50.1 min^{-1}. Purified FLD acts as a single electron shuttle and is able to stimulate the rate of FLDR-dependent cytochrome *c* reduction approximately six-fold under the above conditions. With saturating cytochrome *c* (100 μM) and FLDR at 16.65 nM, a Michaelis curve was obtained for the stimulation of cytochrome *c* reductase activity by FLD, indicating an apparent V_{max} of 272 ± 11.5 min^{-1} and an apparent K_m of the FLD for the FLDR of 6.84 ± 0.68 μM.

The purified EDC-linked complex of FLDR/FLD was also catalytically active (Table 4). With cytochrome *c* as the acceptor, a k_{cat} of 109 ± 5 min^{-1} and a K_m of 87 ± 8 μM were measured with the complex at 30°C in 100 mM sodium phosphate, pH 7.5. With potassium ferricyanide, a k_{cat} of 782 ± 4 min^{-1} and a K_m of 33 ± 6 μM were measured. Both the rate of reduction and the affinity of these substrates for the complex were lower than those for FLDR on its own (Tables 3 and 4).

Stopped-flow characterisation. Investigations of the rates of reduction of FLDR (40 μM) with NADPH (4 μM–2 mM) were performed with measurement of the rate of decrease in absorbance at 456 nm, the oxidised FLDR absorbance maximum. The rate observed was 15 ± 2 s^{-1}, regardless of the concentration of NADPH. A similar value was obtained when the concentration of FLDR was altered.

Table 5. Stopped-flow parameters for oxidation/reduction reactions involving FLDR and FLD. Reaction rates were determined at 30°C in 100 mM sodium phosphate, pH 7.5, as described in the Experimental Procedures section. Measurement of FLDR reduction was made at 456 nm, FLD reduction to its semiquinone at 583 nm and cytochrome *c* reduction at 550 nm. Reoxidation of FLDR and FLD were monitored at the same wavelengths used to measure their reduction.

Stopped-flow rate	*k*
	s^{-1}
FLDR reduction (by NADPH)	15 ± 2 (900 min^{-1})
FLDR oxidation	(5.44 ± 0.5)×10^{-2} (≈3.3 min^{-1})
FLD reduction (by FLDR)	(3.4 ± 0.2)×10^{-2} (≈2.0 min^{-1})
FLD oxidation	(1.07 ± 0.03)×10^{-3} (3.85 h^{-1})
Cytochrome *c* reduction (by FLDR)	29.0 ± 2.0 (1740 min^{-1})

Attempts to measure the rate of electron transfer between NADPH-reduced FLDR and FLD (following the formation of FLD semiquinone at 583 nm) proved difficult under aerobic conditions due to the slow rate of this process and the relatively rapid reoxidation of the FLDR. To solve this problem, solutions were degassed and made up anaerobically (as described in the Experimental Procedures section) prior to performing the stopped-flow experiments. The rate of formation of FLD semiquinone was seen to be very slow when reduced FLDR (40 μM) was mixed with FLD (20 μM), regardless of whether NADPH (500 μM–2 mM) or sodium dithionite was used as the reductant. Over the first 60 s, a single exponential rate of only (3.4 ± 0.2)×10^{-2} s^{-1} was recorded in the presence of 2 mM NADPH.

To compare the reduction of an artificial electron acceptor on stopped flow/steady-state time scales, the reduction of cytochrome *c* by FLDR was investigated. NADPH (2 mM)–reduced FLDR (10–50 μM) was mixed with cytochrome *c* (4 μM) and absorbance monitored at 550 nm. A k_{cat} of 29 ± 2 s^{-1} and a K_m of 12.58 ± 1.1 μM were calculated by fitting the first-order rate data against [cytochrome *c*] to a rectangular hyperbola on Origin software. All stopped-flow data is tabulated (Table 5).

To measure the rate of reoxidation of the reduced FLDR, the enzyme was reduced aerobically in the stopped-flow apparatus by mixing with a sub-stoichiometric quantity of NADPH and recording the increase in absorbance at 456 nm. At 30°C, FLDR (80 μM) was observed to reoxidise after rapid mixing with NADPH (60 μM) with a rate of (5.44 ± 0.5)×10^{-2} s^{-1} (3.26 min^{-1}). To measure reoxidation of the FLD semiquinone, we initially attempted the same experiment as used for FLDR, employing 80 μM FLD and 60 μM sodium dithionite as the reductant. However, it was found that reduction of FLD by the dithionite was very slow, with the semiquinone taking several minutes to form completely. Instead, the FLD was reduced with an excess of dithionite under anaerobic conditions, until the semiquinone formation was seen to be complete (maximal absorbance at 583 nm). Thereafter, excess dithionite was removed from the FLD by gel filtration (G25) within the anaerobic glove box and the reduced FLD removed from the anaerobic environment. The reduced FLD was then diluted to 30 μM in oxygenated buffer, the buffer bubbled with air for 2 min and the rate of reoxidation of the semiquinone measured at 583 nm under steady-state conditions. The semiquinone was seen to be air sta-

Table 6. Midpoint reduction potentials (E′ in mV) for the flavin cofactors in purified *E. coli* FLDR (NADP⁺ flavodoxin oxidoreductase) and FLD (flavodoxin). Values were calculated from electrode potential versus absorbance data as described in the Results section and in Figs 2 and 3. E'_{12} refers to the midpoint potential for the 2-electron reduction of the flavins in each protein, while E'_1 and E'_2 refer to the midpoint reduction potentials for the oxidised/semiquinone and semiquinone/hydroquinone couples, respectively, for FLD and FLDR. The values are compared with those of the FAD and FMN cofactors in the reductase domain of flavocytochrome *P*-450 BM3 from *Bacillus megaterium* (BM3) [29] and mammalian *P*-450 reductase (CPR) [30], and with the values for free FAD/FMN [31, 32].

	E'_{12}	E'_1	E'_2
FLDR FAD	−288 ± 4	−308 ± 4	−268 ± 4
FLDR FAD (+2′ AMP)	−261 ± 6	−293 ± 6	−230 ± 7
FLD FMN	−343 ± 6	−254 ± 5	−433 ± 6
BM3 FAD	−332 ± 4	−292 ± 4	−372 ± 4
BM3 FMN	−203 ± 6	−213 ± 5	−193 ± 6
CPR FAD	−327	−290	−365
CPR FMN	−190	−110	−270
FREE FAD	−207	–	–
FREE FMN	−205	−172	−238

5 mM used in the titration was based on this result. An increase in the reduction potentials of both the oxidised/semiquinone (E'_1 elevated by 15 mV to −293 ± 6 mV) and semiquinone/reduced (E'_2 elevated by 38 mV to −230 ± 7 mV) couples of FLDR was observed in the presence of 2′ AMP (Table 6).

E. coli flavodoxin. Fig. 5a shows the redox titration of the *E. coli* FLD at ≈80 μM monitored by visible spectrophotometry between 400 nm and 800 nm. Fig. 5b plots the sum of absorbance values between 600 nm and 650 nm against the potential of the enzyme solution. The increase and decrease in absorbance in this region reflects the build up (0−1 electron reduced) and loss (1−2 electron reduced), respectively, of the flavodoxin neutral-blue semiquinone. The FLD data was also fitted to Eqn (1). In this case, E'_1 represents the oxidised/semiquinone couple of FLD and E'_2 the semiquinone/reduced couple.

Values for the reduction potentials of the FLDR and FLD flavins are collated in Table 6. Although the potentials for the two 1-electron couples of the FLD are very well separated (179 mV), this is clearly not so for the FLDR. For the FLDR, the first couple (oxidized/semiquinone − E'_1) is calculated to be more negative than the second (semiquinone/reduced − E'_2) by 40 mV. In FLDR, the two 1-electron-reduction processes appear to occur simultaneously and the data can be represented reasonably accurately by a 2-electron function. The midpoint reduction values in Table 6 are compared with those from the homologous domains of flavocytochrome *P*-450 BM3 and eukaryotic *P*-450 reductase, and with the potentials of free FAD and FMN.

Analysis of the later data sets for the FLDR was complicated by the tendency of this enzyme to form a precipitate (very slowly) over the course of the experiment. For this reason, the quality of these data is not as high as those obtained for FLD. However, correction of these data by subtraction of $1/\lambda$ from each spectrum (to compensate for the small increases in turbidity) results in values that fit well to the 2-electron Nernst function used to derive the flavin reduction potentials for FLDR.

Based on the wide separation of the midpoint reduction potentials of the oxidised/semiquinone and semiquinone/hydroquinone couples of the FLD; we calculate that a maximum of 94% blue semiquinone can be formed during the reductive titration of this protein. As shown in Fig. 5a, the strongly absorbing semiquinone has a peak at approximately 583 nm. The maximum absorbance reached by the semiquinone is 56.2% of that of the oxidised flavin band at 466 nm. Based on this proportion and the known coefficient of 8250 M^{-1} cm^{-1} for the 466-nm band [2], we calculate a coefficient of 4933 M^{-1} cm^{-1} for 100% of the semiquinone.

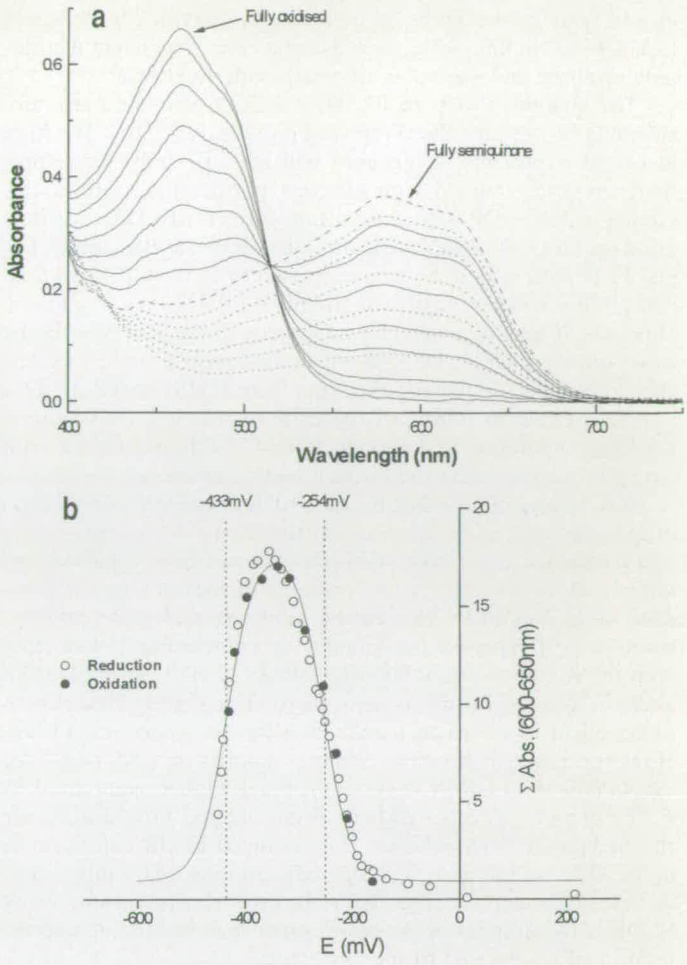

Fig. 5. (a) Ultraviolet-visible spectra of *E. coli* FLD (80 μM) during redox titration. Reductive (sodium dithionite) titrations were performed anaerobically as described in the Experimental Procedures section. The spectra shown by solid lines are those representing the conversion from the oxidised to the semiquinone form; with decreasing absorbance in the 450-nm region and increasing absorbance in the 600-nm region (semiquinone region). The dashed line shows the spectrum of the maximal semiquinone species (absorbance maximum at 583 nm). Spectra shown by dotted lines are those representing the conversion from the semiquinone to the hydroquinone (fully reduced) form; with decreasing absorbance in the 600-nm region. Oxidative titrations with potassium ferricyanide give essentially identical results to the reductive titrations. (b) Plot of the sum of absorbance between 600 nm and 650 nm against electrode potential (E′, mV) during reductive and oxidative titrations, fitted to Eqn. 1, as described in Results. From these data, E'_1 (oxidised/semiquinone) = −254 ± 5 mV and E'_2 (semiquinone/reduced) = −433 ± 6 mV.

DISCUSSION

This is the first report of the determination of all of the reduction potentials for the flavins in the FLDR and FLD system, the flavoprotein electron-transfer chain of the *E. coli* biotin (vitamin H)-synthase system, which also supports the function of heterologously expressed cytochrome *P*-450 in *E. coli* [5]. The knowledge of these values is central to our understanding of the roles of these flavoproteins in electron transfer to these en-

transfer via a NADPH-driven system virtually impossible. The results indicate that the overall driving force, i.e. the difference in reduction potential, for single electron transfer from NADPH-reduced FLDR to oxidised FLD is considerably less than that for CPR and *P*-450 BM3. In addition, the binding of nucleotide ($NADP^+$) to FLDR may result in further increase in the flavin reduction potentials (as we have shown with 2′ AMP) and decrease further the driving force for electron transfer to FLD. Our stopped-flow data are consistent with these findings. The rate of reduction of FLDR ($15\ s^{-1}$) is markedly slower than that seen in the *P*-450 BM3 system ($>700\ s^{-1}$) and the reduction of FLD by reduced FLDR is also very slow ($0.034\ s^{-1}$).

The authors acknowledge support from the University of Edinburgh (LM), the Edinburgh Centre for Protein Technology (CL) and the Biotechnology and Biological Sciences Research Council (DJC and SND). AWM and SKC wish to thank the Royal Society of Edinburgh and Caledonian Research Foundation (Caledonian Research Foundation/Royal Society of Edinburgh Fellowship to AWM and SOEID Fellowship to SKC).

REFERENCES

1. Sanyal, I., Cohen, G. & Flint, D. H. (1994) Biotin synthase − purification, characterization as a [2Fe-2S] cluster protein, and *in vitro* activity of the *Escherichia coli* BioB gene product, *Biochemistry 33*, 3625−3631.
2. Fujii, K. & Huennekens, F. M. (1974) Activation of methionine synthase by a reduced triphosphopyridine nucleotide-dependent flavoprotein system, *J. Biol. Chem. 249*, 6745−6750.
3. Blaschkowski, H. P., Neuer, G., Ludwig-Festl, M. & Knappe, J. (1982) Routes of flavodoxin and ferredoxin reduction in *Escherichia coli* coA acylating pyruvate − flavodoxin and NADPH-flavodoxin oxidoreductases participating in the activation of the pyruvate-formate lyase, *Eur. J. Biochem. 123*, 563−569.
4. Reichard, P. (1993) The anaerobic ribonucleotide reductase from *Escherichia coli*, *J. Biol. Chem. 268*, 8383−8386.
5. Jenkins, C. M. & Waterman, M. R. (1994) Flavodoxin and NADPH-flavodoxin reductase from *Escherichia coli* support bovine cytochrome P450 c17 hydroxylase activities, *J. Biol. Chem. 269*, 27401−27408.
6. Mayhew, S. G. & Tollin, G. (1993) General properties of flavodoxins, in *Chemistry and biochemistry of flavoenzymes* (Müller, F., ed.) pp. 389−426, CRC Press, Boca Raton, Florida.
7. Fujii, K., Galivan, J. H. & Huennekens, F. M. (1977) Activation of methionine synthase: further characterization of the flavoprotein system, *Arch. Biochem. Biophys. 178*, 662−666.
8. Vetter, H. & Knappe, J. (1971) Flavodoxin and ferredoxin of *Escherichia coli*, *Hoppe-Seylers Physiol. Chem. 352*, 433−436.
9. Studier, F. W. & Moffat, B. A. (1986) Use of bacteriophage T7 RNA polymerase to direct selective high-level expression of cloned genes, *J. Mol. Biol. 189*, 113−130.
10. Yanisch-Perron, C., Viera, J. & Messing, J. (1985) Improved M13 phage cloning vectors and host strains: nucleotide sequences of the M13mp18 and pUC19 vectors, *Gene 33*, 103−108.
11. Bianchi, V., Reichard, P., Eliasson, R., Pontis, E., Krook, M., Jornvall, H. & Haggård-Ljungquist, E. (1993) *Escherichia coli* ferredoxin-$NADP^+$ reductase: activation of *Escherichia coli* anaerobic ribonucleotide reduction, cloning of the gene (*FPR*) and overexpression of the protein, *J. Bacteriol. 175*, 1590−1595.
12. Bianchi, V., Eliasson, R., Fontecave, M., Mulliez, E., Hoover, D. M., Matthews, R. & Reichard, P. (1993) Flavodoxin is required for the activation of the anaerobic ribonucleotide reductase, *Biochem. Biophys. Res. Commun. 197*, 792−797.
13. Dutton, P. L. (1978) Redox potentiometry: determination of midpoint potentials of oxidation-reduction components of biological electron transfer systems, *Methods Enzymol. 54*, 411−435.
14. Munro, A. W., Malarkey, K., McKnight, J., Thomson, A. J., Kelly, S. M., Price, N. C., Lindsay, J. G., Coggins, J. R. & Miles, J. S. (1994) The role of tryptophan 97 of cytochrome P-450 BM3 from *Bacillus megaterium* in catalytic function, *Biochem. J. 303*, 423−428.
15. Pirola, M. C., Monti, F., Alverti, A. & Zanetti, G. (1994) A functional heterologous electron-transfer protein complex, *Desulfovibrio vulgaris* flavodoxin covalently linked to spinach ferredoxin-$NADP^+$ reductase, *Arch. Biochem. Biophys. 311*, 480−486.
16. Bianchi, V., Haggård-Ljungquist, E., Pontis, E. & Reichard, P. (1995) Interruption of the ferredoxin (flavodoxin) $NADP^+$ oxidoreductase gene of *Escherichia coli* does not affect anaerobic growth but increases sensitivity to paraquat, *J. Bacteriol. 177*, 4528−4531.
17. Ingelman, M., Bianchi, V. & Eklund, H. (1997) The 3-dimensional structure of flavodoxin reductase at 1.7 Angstrom resolution, *J. Mol. Biol. 268*, 147−157.
18. Miles, J. S., Munro, A. W., Rospendowski, B. N., Smith, W. E., McKnight, J. & Thomson, A. J. (1992) Domains of the catalytically self-sufficient cytochrome P-450 BM3: genetic construction, overexpression, purification and spectroscopic characterization, *Biochem. J. 288*, 503−509.
19. Jenkins, C. M., Genzor, C. G., Fillat, M. F., Waterman, M. R. & Gomez Moreno, C. (1997) Negatively charged *Anabaena* flavodoxin residues [Asp (144) and Glu (145)] are important for reconstitution of cytochrome P450c17 alpha-hydroxylase, *J. Biol. Chem. 272*, 22509−22513.
20. Sykes, G. A. & Rogers, L. J. (1984) Redox potentials of algal and cyanobacterial flavodoxins, *Biochem. J. 217*, 845−850.
21. Lambeth, J. D. & Kamin, H. (1976) Adrenodoxin reductase: properties of the complexes of reduced enzyme with $NADP^+$ and NADPH, *J. Biol. Chem. 251*, 4299−4306.
22. Iyanagi, T. (1977) Redox properties of microsomal reduced nicotinamide adenine dinucleotide-cytochrome b_5 reductase and cytochrome b_5, *Biochemistry 16*, 2725−2730.
23. Hoover, D. M. & Ludwig, M. L. (1997) A flavodoxin that is required for enzyme activation: the structure of oxidized flavodoxin from *E. coli* at 1.8 Å resolution, *Protein Sci. 6*, 2525−2537.
24. Wang, M., Roberts, D. L., Paschke, R., Shea, T. M., Masters, B. S. S. & Kim, J.-J. P. (1997) Three dimensional structure of NADPH-cytochrome P-450 reductase: prototype for FMN- and FAD-containing enzymes, *Proc. Natl Acad. Sci. USA 94*, 8411−8416.
25. Abu-Soud, H. M., Feldman, P. L., Clark, P. & Stuehr, D. J. (1994) Electron transfer in the nitric oxide synthases: characterization of L-arginine analogs that block heme iron reduction, *J. Biol. Chem. 269*, 32318−32326.
26. Porter, T. D. (1991) An unusual, yet strongly conserved flavoprotein reductase in bacteria and mammals, *Trends Biochem. Sci. 16*, 154−158.
27. Smith, G. C. M., Tew, D. G. & Wolf, C. R. (1994) Dissection of NADPH-cytochrome P450 oxidoreductase into distinct functional domains, *Proc. Natl Acad. Sci. USA 91*, 8710−8714.
28. Govindaraj, S. & Poulos, T. L. (1997) The domain architecture of cytochrome P450 BM3, *J. Biol. Chem. 272*, 7915−7921.
29. Daff, S. N., Chapman, S. K., Turner, K. L., Holt, R. A., Govindaraj, S., Poulos, T. L. & Munro, A. W. (1997) Redox control of the catalytic cycle of cytochrome P-450 BM3, *Biochemistry 36*, 13816−13823.
30. Iyanagi, T., Makino, N. & Mason, H. S. (1974) Redox properties of the reduced nicotinamide adenine dinucleotide phosphate-cytochrome P450 and reduced nicotinamide adenine dinucleotide-cytochrome b_5 reductase, *Biochemistry 13*, 1701−1710.
31. Massey, V. (1991) A simple method for the determination of redox potentials, in *Flavins and flavoproteins 1990* (Curti, B., Ronchi, S. & Zanetti, G., eds) pp. 59−66, Walter de Gruyter, New York.
32. Draper, R. D. & Ingraham, L. L. (1968) A potentiometric study of the flavin semiquinone equilibrium, *Arch. Biochem. Biophys. 125*, 802−808.

Appendix II

THE JOURNAL OF BIOLOGICAL CHEMISTRY
Vol. 275, No. 18, Issue of May 5, pp. 13888–13894, 2000
Printed in U.S.A.

Identification of the [Fe-S] Cluster-binding Residues of *Escherichia coli* Biotin Synthase*

Received for publication, November 15, 1999, and in revised form, February 11, 2000

Lisa McIver‡, Robert L. Baxter§, and Dominic J. Campopiano§

From the Edinburgh Centre for Protein Technology, Department of Chemistry, Joseph Black Building, the University of Edinburgh, The King's Buildings, West Mains Road, Edinburgh EH9 3JJ, Scotland, United Kingdom

The gene encoding *Escherichia coli* biotin synthase (*bio*B) has been expressed as a histidine fusion protein, and the protein was purified in a single step using immobilized metal affinity chromatography. The His_6-tagged protein was fully functional in *in vitro* and *in vivo* biotin production assays. Analysis of all the published *bio*B sequences identified a number of conserved residues. Single point mutations, to either serine or threonine, were carried out on the four conserved (Cys-53, Cys-57, Cys-60, and Cys-188) and one non-conserved (Cys-288) cysteine residues, and the purified mutant proteins were tested both for ability to reconstitute the [2Fe-2S] clusters of the native (oxidized) dimer and enzymatic activity. The C188S mutant was insoluble. The wild-type and four of the mutant proteins were characterized by UV-visible spectroscopy, metal and sulfide analysis, and both *in vitro* and *in vivo* biotin production assays. The molecular masses of all proteins were verified using electrospray mass spectrometry. The results indicate that the His_6 tag and the C288T mutation have no effect on the activity of biotin synthase when compared with the wild-type protein. The C53S, C57S, and C60S mutant proteins, both as prepared and reconstituted, were unable to covert dethiobiotin to biotin *in vitro* and *in vivo*. We conclude that three of the conserved cysteine residues (Cys-53, Cys-57, and Cys-60), all of which lie in the highly conserved "cysteine box" motif, are crucial for [Fe-S] cluster binding, whereas Cys-188 plays a hitherto unknown structural role in biotin synthase.

The biotin operon of *Escherichia coli* contains six open reading frames that encode at least four of the proteins essential for the conversion of pimeloyl-CoA to biotin (1). The recent determination of the structure of three of these enzymes, 8-amino-7-oxononanoate synthase (2), 7,8-diaminononanoate synthase (3), and dethiobiotin synthase (4), encoded by the *bio*F, *bio*A, and *bio*D genes respectively, has shed light on the mechanism of the steps involved in the conversion of alanine to dethiobiotin. However, the mechanism of the final step, the conversion of dethiobiotin to biotin catalyzed by biotin synthase (see Scheme 1), remains unresolved.

Numerous studies have shown that a fully functional *in vitro* system for conversion of dethiobiotin to biotin requires not only the product of the *bioB* gene but also several other proteins and low molecular weight molecules. Although the exact components of this system vary between different laboratories, *S*-adenosylmethionine (AdoMet),[1] NADPH, cysteine, DTT, Fe^{2+}, and a reducing system (5) are common to all. The reducing system we and others use consists of flavodoxin (FLD) (6) and flavodoxin (ferredoxin) $NADP^+$ oxidoreductase (FLDR) (7) (which we believe to be the physiological system) which Marquet and co-workers (8) have found can be replaced by a photoreduced deazaflavin. Both systems appear to be equally effective in providing reducing equivalents for the reaction. There is, however, conflicting evidence that other proteins, cofactors, and allosteric activators may also be required for competence of the biotin synthase complex. There is no doubt that addition of extracts derived from *E. coli bioB*$^-$ strains can enhance activity of biotin synthase, but whether this is due to the presence of a thiamine pyrophosphate-stabilized protein (7), high levels of constitutive low molecular weight cellular components such as fructose 1,6-biphosphate and the labile (and as yet uncharacterized) AdoMet-derived product of the 7,8-diaminononanoate synthase reaction (5), or indeed to a combination of several of these factors is still open to question.

Recent results indicate that the sulfur incorporated in the tetrahydrothiophene ring of biotin is ultimately derived from cysteine (7) and that 9-mercaptodethiobiotin (but not 6-mercaptodethiobiotin) can act as an intermediate (9). The intermediacy of 9-mercaptodethiobiotin, racemization at C-9 (10) (but not at C-6 (11)), and the requirement for at least two molecules of AdoMet for each ring formation step provides clues to the mechanism of C–S bond formation (12). Taken together these results suggest that the mechanism involves the following: (*a*) initial AdoMet-dependent radical formation at C-9; (*b*) capture of sulfur by the C-9 radical to form a 9-mercaptodethiobiotin derivative; and (*c*) a second AdoMet-initiated radical formation by abstraction of the pro-*S* hydrogen at C-6 to generate a conformationally restrained radical that subsequently captures the C-9 thiol resulting in tetrahydrothiophene ring clo-

* This work was supported in part by the Biotechnology and Biological Sciences Research Council (BBSRC). The costs of publication of this article were defrayed in part by the payment of page charges. This article must therefore be hereby marked "*advertisement*" in accordance with 18 U.S.C. Section 1734 solely to indicate this fact.

The nucleotide sequences reported in this paper have been submitted to the Swiss Protein Database under Swiss-Prot accession numbers P12996, O67104, P54967, P19206, P53557, P46396, Q9Z6L5, Q47862, P44987, O25956, P94966, P46715, O06601, P32451, O60050, P36569, and P73538.

‡ Supported by the Department of Chemistry, Edinburgh University.

§ To whom correspondence should be addressed. Tel.: 44 131 650 4712; Fax: 44 131 650 7155; E-mail: Dominic.Campopiano@ed.ac.uk (for D. J. C.) or Tel.: 44 131 650 4708; Fax: 44 131 650 7155; E-mail: r.baxter@ed.ac.uk (for R. L. B.).

[1] The abbreviations used are: AdoMet, *S*-adenosylmethionine; CV, column volume; DTT, dithiothreitol; FLD, *E. coli* Flavodoxin; FLDR, *E. coli* flavodoxin (ferredoxin) $NADP^+$ oxidoreductase; His_6, six consecutive histidine residues; ICP-AES, inductively coupled plasma-atomic emission spectroscopy; IMAC, immobilized metal affinity chromatography; IPTG, isopropyl-β,D-thiogalactopyranoside; LAM, lysine 2,3-aminomutase; LIPA, lipoic acid synthase; PFL-AE, pyruvate formate lyase-activating enzyme; ARR-AE, ribonucleotide reductase-activating enzyme; PAGE, polyacrylamide gel electrophoresis; Bis-Tris, 2-[bis(2-hydroxyethyl)amino]-2-(hydroxymethyl)propane-1,3-diol; PCR, polymerase chain reaction.

SCHEME 1.

sure (13). Recent studies indicate that a sulfur atom of the [Fe-S] cluster of biotin synthase, rather than cysteine itself, may act as the actual sulfur donor, suggesting that the [Fe-S] cluster of the enzyme must be regenerated prior to the next reaction (14). Thus biotin synthase could be regarded as both a reagent and a catalyst. It has been suggested that a NifS-like enzyme, similar to the *Azotobacter vinelandii* NifS (15), may be required for construction of the [Fe-S] cluster *in vivo* and regeneration *in vitro* but such an activity has still to be identified. NifS is a pyridoxal phosphate-dependent enzyme that catalyzes the desulfuration of L-cysteine to yield L-alanine and sulfide that has been shown to catalyze [Fe-S] cluster formation *in vitro* and *in vivo*.

The fact that *E. coli* biotin synthase is based on a core [2Fe-2S] protein with a requirement for a FLD/FLDR redox couple and AdoMet as a radical generator suggests that it belongs to the family of enzymes that include anaerobic ribonucleotide reductase-activating enzyme (ARR-AE) (16), pyruvate formate-lyase-activating enzyme (PFL-AE) (17), lysine 2,3-aminomutase (LAM) (18), and lipoic acid synthase (LIPA) (19). Even within this small group there already appears to be differences with regard to subunit composition and chemical function; biotin synthase, LIPA, and ARR-AE are dimers; LAM is a hexamer, and PFL-AE is a monomer. Biotin synthase, LIPA, and LAM generate a radical on a small molecule, whereas ARR-AE and PFL-AE generate a protein glycyl radical.

Characterization of the *E. coli* biotin synthase has been complicated by the fact that most preparations of the protein contain variable amounts of polymeric forms (mainly dimers and tetramers) with variable [Fe-S] content. The major native form of the core biotin synthase, however, appears to be a 76-kDa dimer, each monomer containing an [2Fe-2S] cluster (20). Spectroscopic studies suggest that reduction of the two [2Fe-2S] clusters in the oxidized protein dimer, an obligatory step in the mechanism, results in formation of a biotin synthase dimer containing a single [4Fe-4S] cluster in which each of the iron centers is coordinated to a thiol ligand(s) of the protein (21–23).

However, almost nothing is known about the protein residues involved in coordination to the [Fe-S] clusters of biotin synthase. Whereas the active sites have been proposed to involve the cysteine thiols of the common GXCXXXCXXCXQ motif as a "cysteine ([Fe-S] coordination) box" motif, there has been as yet no experimental evidence to support this contention (20). In this paper we describe studies on mutants of the biotin synthase protein that uniquely identify the key protein cysteine residues involved in formation of the [Fe-S] cluster.

EXPERIMENTAL PROCEDURES

Materials—Electrophoresis was carried out using a Bio-Rad Protean II minigel system (protein) and a Life Technologies, Inc., H5 system (DNA). PCR and sequencing reactions were done on a Perkin-Elmer 480 thermal cycler, and automated DNA sequencing was carried out using an ABI prism 377 DNA sequencer. An Amersham Pharmacia Biotech FPLC system and columns were used for chromatographic separations of proteins. Electrospray mass spectrometry was performed on a Micromass Platform II quadrupole mass spectrometer. UV-visible spectrophotometry was done on a Unicam UV4. Determination of metal ion concentrations were carried out using a Thermo Jarrell Ash IRIS inductively coupled plasma atomic emission spectrometer. Primers were purchased from Life Technologies, Inc., and Ready to Go PCR™ beads from Amersham Pharmacia Biotech. Pre-cast SDS-PAGE gels (10% Bis-Tris) were purchased from Novex and were used according to the manufacturer's instructions.

E. coli Strains and Plasmids—The *E. coli* strain Top 10 One Shot™ cells (F′*mcr*A D(*mrr-hsd*RMS-*mcr*BC) F80*lac*ZDM15 D*lac*X74 *deo*R *rec*A1 *ara*D139 Δ(*ara-leu*)7697 *gal*U *gal*K *rps*L *end*A1 *nup*G, Invitrogen) were used for the maintenance of plasmids and also for the initial transformation of ligation products. HMS174 (DE3) cells (F⁻ *rec*A *hsd*R(r_{K12}^- m$K12^+$) Rif^r (DE3), Novagen) were used for the overexpression of genes cloned into pET plasmids. PCOi (*bio*⁻Δ (*attλ*, *bio uvrB*) *thr*, *leu*, *thi*, *placi*) was used to prepare a biotin minus cell-free extract. The biotin auxotroph *Lactobacillus plantarum* (ATCC 8014) was used in the microbial biotin assay (24). A 1041-base pair *Nco*I/*Bam*HI fragment from pB030 (a gift from Lonza AG) containing the *bio*B gene was cloned into the same sites of pET16b (Novagen), and the resultant plasmid was called pET16b/bioB.

Mutagenesis—Site-directed mutagenesis was performed using the "mega-primer" PCR method using vector forward (BIOB PCR) and reverse (M13) oligonucleotides and the mutagenic primers (C53S, C57S, C60S, C188S and C288T) (25). The typical PCR reaction volume was 50 μl and consisted of template DNA (1 μl), forward primer (1 μM), reverse primer (1 μM), water (39 μl), and two *Taq* beads. The primers for the cysteine mutations used were C53S (5′ AAG ACC GGA GCT TCC CCG GAA GAT 3′), C57S (5′ CCG GAA GAT TCT AAA TAC TGC CCG 3′), C60S (5′ AAA TAC TCT CCG CAA ACG TCG CGC 3′), C188S (5′ GGG ATC AAA GTC TCT TCT GGC 3′), and C288T (5′ GGT CAG CAG TTT **GGT ACC** GTA 3′). The bases underlined in each primer indicate the position where the cysteine codon is replaced by one encoding a serine or in the case of C288T a threonine. The bases in bold indicate a *Kpn*I restriction site. All clones were sequenced, and the data were analyzed using ABI Prism editview software.

Preparation of Biotin Synthase Cell-free Extracts—Wild-type biotin synthase, His_6-tagged biotin synthase (from HMS174 (DE3)/pET16b/bioB and pET6H/bioB), and mutant proteins (from HMS174 (DE3)/pHC53S, pHC57S, pHC60S, pHC188S, and pHC288T) were prepared from cultures grown in 2–10 liters of 2YT media (tryptone (16 g/liter), yeast extract (10 g/liter), sodium chloride (5 g/liter), pH 7.5) containing ampicillin (100 μg/ml). Transformed cells were grown at 37 °C (shaking 250 rpm) until the $A_{600\ nm}$ = 1.0 and biotin synthase was produced by addition of IPTG to a final concentration of 1 mM. Cells (~2.5 g/liter wet weight) were harvested (5,000 × *g* for 20 min, 4 °C) after a further 4 h of growth. The cells pellets were washed by resuspension in ice-cold buffer A (20 mM Tris-HCl, pH 7.9, 0.5 M sodium chloride, 5 mM imidazole). All other cell pellets were washed in buffer B (100 mM sodium phosphate, pH 7.5). The cell pellets were lysed by intermittent sonication (30 s on, 30 s off) 4 °C for 15 min. Cellular debris was removed by centrifugation (15,000 × *g* for 30 min, 4 °C), and the supernatants were stored frozen (−20 °C) in glycerol (15%). The PCOi (*bio*B⁻) strain was grown in 2YT, and the cells washed with buffer A and cell extracts, used for augmentation in the *in vitro* assay, were prepared in a similar fashion to that described above.

Purification of Wild-type Biotin Synthase—Protamine sulfate (1%, 0.5 ml per 10 ml) was added to the cell-free extract to remove nucleic acids. After ammonium sulfate (45%) precipitation, precipitated proteins were collected by centrifugation, resuspended in buffer B, and filtered (0.45 μm) prior to being loaded onto a Q-Sepharose 26/10 high load anion exchange column (2.5 × 10 cm) which had been equilibrated with buffer B. The proteins were eluted with an increasing gradient of potassium chloride (0–1 M, 20 CV) in buffer B. The deep red fractions containing biotin synthase eluted at 300 mM salt. These were combined, brought to a final concentration of 10% ammonium sulfate, and loaded onto a phenyl-Sepharose hydrophobic interaction column (1 × 30 cm) that had been equilibrated with buffer B containing ammonium sulfate (10%). Biotin synthase was eluted with a decreasing gradient of buffer B containing ammonium sulfate (10–0%, 20 CV). Biotin synthase eluted at the end of the gradient, and these fractions were combined and filtration concentrated (Amicon PM10 membrane). The protein was purified by gel filtration on Sephacryl S-200 HR eluting with buffer B. Protein samples were diluted with glycerol (15%) and stored (−80 °C).

Purification of His_6-tagged Biotin Synthase and Mutants—Cell-free extracts were loaded directly onto a Hi-Trap™-chelating column (5 ml, Amersham Pharmacia Biotech) that had been charged with $NiSO_4$ (100 mM) and prewashed with buffer A. Proteins were eluted with a linear gradient of (5 mM to 1 M) imidazole in buffer A. Biotin synthase-containing fractions typically eluted between 120 and 150 mM imidazole. These were combined and exhaustively dialyzed against buffer B to remove imidazole and nickel salts and concentrated by ultrafiltration.

The purity and integrity of wild-type, His_6-tagged, and mutant biotin synthase forms were assessed by SDS-PAGE, mass spectrometry, and UV-visible spectrophotometry. Protein concentrations were determined by the Bradford method using bovine serum albumin as a reference (26) and by spectrophotometry using reported extinction coefficients ($\epsilon_{274\ nm} = 3.3 \times 10^4\ M^{-1}\ cm^{-1}$, $\epsilon_{330\ nm} = 1.4 \times 10^4\ M^{-1}\ cm^{-1}$, $\epsilon_{420\ nm} = 6.0 \times 10^3\ M^{-1}\ cm^{-1}$, $\epsilon_{453\ nm} = 7.1 \times 10^3\ M^{-1}\ cm^{-1}$, $\epsilon_{540\ nm} = 3.5 \times 10^3\ M^{-1}\ cm^{-1}$) (20).

Mass Spectrometry—Prior to mass spectrometry all protein samples were passed through an Aquapure reverse phase C-4 column at a constant trifluoroacetic acid concentration of 0.1% using a linear gradient of 10–100% acetonitrile in water over 40 min at a flow rate of 1 ml/min and the separation monitored at 280 nm. The total ion count of all the ions in the m/z range 500–2,000 was recorded. The mass spectrometer was scanned at intervals of 0.1 s, the scans accumulated, spectra combined, and the average molecular mass determined using MaxEnt and Transform algorithms of MassLynx software.

Sequence Alignments—Swiss-Prot and the Genomes Representation Organization data bases were used to search for amino acid sequences that were then aligned using Expasy, Clustal W, and Alscript (27).

Preparation of Apo and Holo Wild-type Biotin Synthase and Mutants—This was carried out using methods previously described (14, 20).

In Vitro Assay for Biotin Synthase Activity–In vitro biotin production was determined using the *Lactobacillus* assay (24). Incubations were carried out both aerobically and anaerobically in buffer B. A typical assay mixture contained biotin synthase or mutant protein (5 μM), potassium chloride (10 mM), dethiobiotin (50 μM), AdoMet (150 μM), $Fe(NH_4)_2(SO_4)_2$ (5 mM), NADPH (1 mM), fructose 1,6-biphosphate (5 mM), L-cysteine (500 μM), DTT (10 mM), PCOi cell-free extract (100 μl), FLD (12.5 μM), and FLDR (2 μM). The final reaction volume was typically 1 ml. The reaction was incubated at 37 °C for 2 h and then stopped by adding 100 μl of 10% trichloroacetic acid. The resulting precipitate was centrifuged, and 5 μl of the supernatant was used for bioassay.

In Vivo Assays for Biotin Synthase Activity—Transformants of HMS174 (DE3) with pET16b, pET6H, pET16b/bioB, pET6H/bioB, pHC53S, pHC57S, pHC60S, pHC188S, and pHC288T were grown in M9CA media containing dethiobiotin (5 μg/ml), glucose (0.4%), thiamine (0.8 μg/ml), $MgSO_4$ (2 mM), $CaCl_2$ (0.1 mM), and ampicillin (100 μg/ml). At $A_{600\ nm} = 1.0$ the cells were equally divided, and one sample was kept as a control and the other was induced with IPTG (1 mM). Aliquots (1 ml) of cells were removed from both control and induced samples at various time intervals. The cells were pelleted by centrifugation, and 5 μl of the supernatants were used in the bioassay as above. Supernatant from HMS174 (DE3) cells were grown in the same media minus ampicillin and used as the control.

Elemental Analyses—Inductively coupled plasma atomic emission spectroscopy (ICP-AES) was used for metal analyses. All data were interpreted using thermospec/CID software. The radiofrequency power was 1150 watts, the nebulizer flow was 30 pounds/square inch, the pump rate was 100 rpm, and the purge time was 90 s. $Fe(NO_3)_3$ (0.01–100 ppm; 180 nM to 1.8 mM) and $Ni(NO_3)_2$ (0.0001–1.0 ppm; 1.7 nM to 17 mM) solutions were used as standards. All biotin synthase samples (27 μM) and standard solutions were made up in buffer B (28). Chemical analysis for iron was carried out using the ferrozine assay as described by Stookey (29) using the standard described above. Labile sulfide analysis was determined as previously reported (20).

RESULTS

Overexpression of Biotin Synthase—To study the molecular properties of wild-type and mutant forms of biotin synthase, we overproduced the protein using the pET system. In our hands we found the purification procedure described by Sanyal *et al.* (20) both technically difficult and time-consuming, although the procedure provided ~80% pure biotin synthase. We found it impossible to reproduce the purification of biotin synthase using a cobalt column, as described by Marquet and co-workers (30). To overcome these problems, we decided to express the protein with an N-terminal polyhistidine tag. The *bio*B gene was cloned into pET6H which fused the 5′ terminus of the gene to a sequence encoding a MHHHHHHA tag. Overexpression of His_6-tagged biotin synthase was carried out in HMS174 (DE3) and gave comparable expression levels when compared with wild-type biotin synthase. Optimal yields of both proteins were obtained by aerobic cell growth in 2YT at 37 °C. By using the IMAC purification system, we were able to routinely prepare 100-mg quantities of >95% pure His_6-tagged biotin synthase from 5 liters of transformed cell culture.

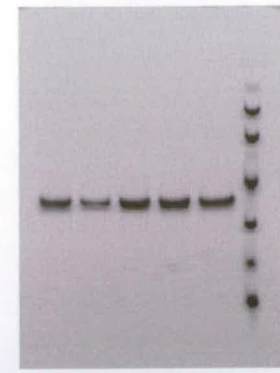

FIG. 1. **SDS-polyacrylamide gel electrophoresis analysis of His_6-tagged biotin synthase and mutants C53S, C57S, C60S, and C288T.** Protein samples were applied to a polyacrylamide gel (10% Bis-Tris, Novex) in the presence of SDS (0.1%) as follows: *1st lane*, wild-type biotin synthase; *2nd lane*, C53S; *3rd lane*, C57S; *4th lane*, C60S; *5th lane*, C288T; and *6th lane*, low molecular mass markers in kDa, 96, 64, 43, 30, 20, and 14.4 (Amersham Pharmacia Biotech). Coomassie Blue was used for staining.

Essential Cysteine Residues of Biotin Synthase—Spectroscopic studies on biotin synthase, PFL activase, and LIPA (17, 19, 31) suggest that three cysteine residues from each monomer are required to coordinate the iron in the [2Fe-2S] clusters of the oxidized dimer and that two of these are required ligands in the reduced catalytically active form. Five cysteine residues of biotin synthase (Cys-53, Cys-57, Cys-60, Cys-188, and Cys-288) were replaced separately with serine or threonine residues by site-directed mutagenesis (threonine was chosen as a replacement for Cys-288 since it enabled us to engineer a *Kpn*I restriction site into the *bioB* gene to facilitate mutant selection). Each of the mutant proteins was overproduced in *E. coli* HMS174 (DE3), and its catalytic activity was determined. Since the His_6-tagged biotin synthase showed identical *in vitro* spectroscopic parameters and catalytic activity to wild-type protein, the mutant *bioB* genes were also expressed as histidine fusion proteins. Each of the mutant proteins was purified using IMAC under identical conditions to the histidine-tagged wild-type biotin synthase except for mutant C188S, which despite numerous attempts (low temperature induction and IPTG concentrations <0.1 mM), remained intractably insoluble. Protein purity was estimated by SDS-PAGE (Fig. 1).

Preparation of Wild-type and His_6-tagged Apoenzymes and the Reconstitution of [2Fe-2S] Cluster Containing Holoenzymes—The apoenzymes of each of wild-type biotin synthase, His_6-tagged biotin synthase, and mutants were prepared anaerobically using sodium dithionite and EDTA. The samples were then desalted using a G10 gel filtration column. ICP-AES analysis and UV-visible spectroscopy confirmed the absence of iron in the proteins. The samples were then reconstituted by incubation with $FeCl_3$ and Na_2S under similar conditions to those described previously (14, 20).

Spectral Characteristics—Solutions of wild-type, His_6-tagged, and C288T biotin synthase were all reddish brown in color, and they showed virtually identical UV-visible spectra with a maximum at 274 nm, a shoulder at 330 nm, and a distinctive peak at 420 nm (see Fig. 2). The spectra of the apo forms of each of these proteins were colorless and showed no peaks at 330 or 420 nm. Upon incubation with $FeCl_3$ and Na_2S for 2 h, their spectra were identical to that of the wild-type isolate.

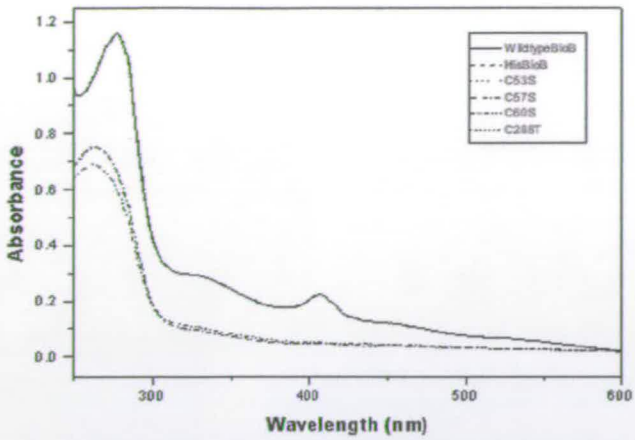

FIG. 2. **UV-visible spectra of wild-type, His_6-tagged, and mutant biotin synthases.** The spectra are from samples of all proteins (1 mg/ml) in 100 mM sodium phosphate, pH 7.5. Wild-type, His_6-tagged, and C288T biotin synthases have almost identical adsorption spectra (*upper trace, solid lines*). The three mutants (C53S, C57S, and C60S) are very similar to each other (*lower trace, dashed lines*).

The mutants (C53S, C57S, and C60S) were colorless, and their spectra showed no peaks indicative of the presence of an [Fe-S] cluster. Moreover, their spectra did not show any significant changes even after prolonged incubation with $FeCl_3$ and Na_2S.

All the mass spectrometry results were within 0.1% of the expected values for the polypeptide chains (Table I) indicating that the [Fe-S] cluster is lost under the MS conditions.

Elemental Analyses—Analyses for iron, sulfur, and nickel were carried out on all proteins using ICP-AES, the Beinert method, and the ferrozine method (29). The protein concentrations were adjusted to ~27 μM (based on a monomeric mass of 39,673 Da for His_6-tagged proteins and 38,648 Da for wild-type biotin synthase). The amount of sulfur (as S^{2-}) in His_6-tagged biotin synthase was virtually identical to that in the untagged protein and similar to the value previously reported by Sanyal *et al.* (20) for wild type. Analysis for nickel content proved that there was negligible nickel binding. Iron analysis (Table II) on the purified proteins revealed a 1:1 ratio between iron and sulfide in both unmodified and His_6-tagged biotin synthase in agreement with previously reported values (14), although it should be noted that Sanyal (20) has reported a 2:1 ratio. In order to try to increase the iron/protein ratio, the proteins were converted to their apoenzymes by incubation with sodium dithionite and EDTA, and the [Fe-S] clusters were reconstituted by incubation with $FeCl_3$ and Na_2S. In the case of the wild-type, the His_6-tagged, and C288T proteins, the protein/iron ratios increased to values comparable with those previously reported (20). The ferrozine assay gave a slightly lower iron/protein ratio than that obtained by ICP-AES (Table III).

In Vitro Assay for Biotin Production—The *in vitro* activities of all proteins were determined using the *Lactobacillus* assay. Biotin was produced by the wild-type, the His_6-tagged, and the C288T mutant but not by the three other cysteine mutants (Table IV). There was no difference in biotin production between aerobic and anaerobic incubations.

In Vivo Assay for Biotin Production—HMS174 (DE3) cells did not produce detectable levels of biotin either on their own or when transformed with pET16b and pET6H and were used as a control. To examine whether or not the His_6 tag affected biotin synthase activity, an *in vivo* assay was carried out using HMS174 (DE3) cells transformed with either pET16b/BioB or pET6H/bioB. All the cells grew in a similar fashion, and production of biotin was found to increase with cell growth. There was no difference in the cells transformed with pET16b/BioB when compared with those that were producing His_6-tagged protein indicating that the tag does not seem to affect the activity of wild-type biotin synthase. Similar experiments were carried out with the five mutant plasmids, all the clones grew as vigorously to those of the wild-type, but only the non-conserved C288T mutant produced significant amounts of biotin. Cells expressing the C53S, C57S, C60S, or C188S mutants did not produce any detectable quantities of biotin (Table V).

TABLE I
Molecular masses of the wild-type, His_6-tagged, and mutant E. coli biotin synthases measured by electrospray mass spectrometry

5-μl samples of proteins (20 μM) in trifluoroacetic acid/acetonitrile/water (0.1:50:50%) solution were used in the measurements. The instrument was calibrated with a myoglobin standard. The estimated error of the molecular mass for each protein is within 0.1%.

Protein	Expected	Actual
Wild-type biotin synthase	38,648	38,646
His_6-tagged biotin synthase	39,673	39,666
C53S	39,657	39,656
C57S	39,657	39,658
C60S	39,657	39,652
C288T	39,671	39,670

DISCUSSION

Biotin synthase has two dimeric forms that contain different types of [Fe-S] clusters. In its oxidized form the protein contains a single [2Fe-2S] cluster in each monomer unit, but on reduction this converts to a single [4Fe-4S] cluster in the dimer. EPR and Raman spectroscopy studies have provided evidence that in the oxidized [2Fe-2S] form biotin synthase has one Fe^{3+} that is coordinated to two cysteines and one Fe^{3+} that is coordinated to a cysteine and an oxygenic ligand (21, 22). In contrast, after dithionite reduction a [4Fe-4S] cluster is formed in which each iron is coordinated to a single cysteine sulfur. A possible mechanism for this interconversion has been proposed by Johnson *et al.* (22) (Fig. 3). It has been speculated that the cysteine residues of the highly conserved "cysteine box" GX-CXXXCXXCXQ motif of these proteins are involved in [Fe-S] cluster binding. This is supported by the fact that an identical motif is found in other [Fe-S] cluster proteins such as LIPA (Swiss-Prot accession number P25845) (19), ARR-AE (P39329) (32), LAM (33), the nitrogen fixation B gene product (P11067) (34), pyrrolo-quinoline-quinone synthase (Q01060) (35), PFL-AE (P09374) (17), NARA protein (P39757) (36), FNR (P03019) (37), benzylsuccinate synthase-activating enzyme (CAA05050) (38), spore photoproduct lyase (P37956) (39), molybdenum cofactor synthase (O27593) (40), and the thiamine synthase H gene product (P30140) (39). Mutational studies on PFL-AE have shown that the three cysteine residues of the cysteine box are vital for its activity (41).

Our attempts to purify wild-type biotin synthase from overexpressing clones using previously reported methods afforded protein that was ~90% pure contaminated with several high molecular weight contaminants. To circumvent this problem we elected to clone the *bio*B gene with an N-terminal His_6 tag and to purify the fusion using nickel-bound affinity chromatography. This appeared to be a safe approach since *E. coli* biotin synthase has a relatively long N-terminal sequence, which is either not present or unconserved in the ORFs of genes from other species, and the tag was unlikely to affect enzymatic activity.

A further significant result was that the activity of the N terminus His_6-tagged biotin synthase proved indistinguishable from that of the wild-type protein. The His_6 tag allows purification of much larger quantities of homogeneous *E. coli* biotin synthase than previously available. Typically, protein of >95%

TABLE II
ICP-AES analysis on wild-type biotin synthase, His_6-tagged biotin synthase, and the mutant proteins
Protein samples (27 μM) and standards ($Fe(NO_3)_3$) were in 100 mM sodium phosphate, pH 7.5.

Protein	[Fe] in protein[a]	Protein/iron ratio	[Fe] in apoenzyme[b]	Apoenzyme: iron ratio	[Fe] in holoenzyme[c]	Holoenzyme/iron ratio
	μM		μM		μM	
Wild-type	26.0	1:096	2.9	1:0.11	37.0	1:1.37
His_6-tagged	26.0	1:0.96	2.9	1:0.11	37.0	1:1.37
C53S	3.6	1:0.13	1.8	1:0.07	12.8	1:0.47
C57S	5.7	1:0.21	1.7	1:0.06	7.4	1:0.27
C60S	5.8	1:0.21	1.7	1:0.06	12.0	1:0.44
C288T	20.8	1:0.77	1.2	1:0.04	43.0	1:1.59

[a] Total concentration of iron in as-purified protein.
[b] Total concentration of iron in the apoenzyme.
[c] Total concentration of iron in the reconstituted holoenzyme.

TABLE III
Results of the ferrozine iron assay
Protein samples (27 μM) and standards ($Fe(NO_3)_3$) were in 100 mM sodium phosphate, pH 7.5.

Protein	Iron concentration	Protein/iron ratio
	μM	
Wild-type biotin synthase	18.5	1:0.68
His_6-tagged biotin syntase	19.3	1:0.72
C53S	2.6	1:0.09
C57S	2.0	1:0.07
C60S	2.9	1:0.11
C288T	11.9	1:0.44

TABLE IV
In vitro biotin production
Biotin production was measured using the *Lactobacillus* assay in the presence of biotin synthase or mutant protein (5 μM), potassium chloride (10 mM), dethiobiotin (50 μM), AdoMet (150 μM), $Fe(NH_4)_2(SO_4)_2$ (5 mM), NADPH (1 mM), fructose 1,6-biphosphate (5 mM), L-cysteine (500 μM), DTT (10 mM), PCO_1 cell free extract (100 μl), FLD (12.5 μM), and FLDR (2 μM). The reaction mixture was incubated for 2 h at 37 °C. +, biotin produced, −, no biotin production.

Protein	Biotin produced	Biotin produced by apoenzyme	Biotin produced by holoenzyme
	(in vitro)		
Wild-type	+	+	+
His_6-tagged	+	+	+
C53S	−	−	−
C57S	−	−	−
C60S	−	−	−
C288T	+	+	+

TABLE V
In vivo production of biotin
Biotin production was measured using the *Lactobacillus* assay as described under "Experimental Procedures." +, biotin produced, −, no biotin production.

Protein	Biotin produced
	(in vivo)
Wild-type	+
His_6-tagged	+
C53S	−
C57S	−
C60S	−
C188S	−
C288T	+

homogeneity can be isolated in a single chromatographic operation.

Metal analyses on both the wild-type and the His_6-tagged protein revealed that they contained the same amount of iron as that reported by Marquet and co-workers (14) but less than that reported by Sanyal *et al.* (20). This is possibly a result of the high protein expression levels. Shortage of free intracellular Fe^{2+} and/or the fact that the enzyme involved in cluster

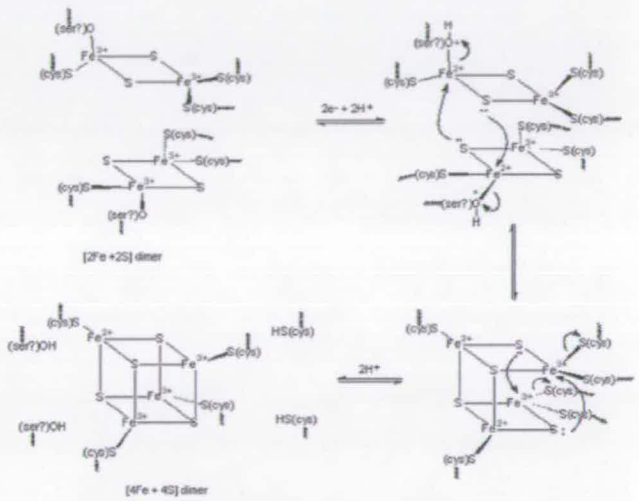

FIG. 3. **Proposed mechanism for [Fe-S] cluster interconversion.** Modified from Johnson *et al.* (22).

formation in the cell is expressed at wild-type levels would lead to a proportion of the biotin synthase population being formed with incomplete clusters. In order to increase the iron content of biotin synthase, the apo-enzyme was prepared anaerobically by treatment of the proteins with sodium dithionite and EDTA, and the [2Fe-2S] cluster was reconstituted by incubation with $FeCl_3$ and Na_2S. Although the concentration of biotin synthase with intact [2Fe-2S] clusters was significantly increased by this procedure, both forms produced equal amounts of biotin (0.2 mol biotin/mol protein/h) which is in agreement with reported values (8, 12, 20). This suggests that there is sufficient iron and sulfide in the assay mixture to reconstitute the cluster *in situ*. Clearly, biotin synthase is not acting as a true catalyst, and one reasonable explanation for this is that an unknown cofactor(s) (possible sulfur donor) is missing from the reaction mixture.

Sequence similarity searches reveal that there at least 20 known species of bacteria, yeasts, and plants that contain a *bio*B gene sequence similar to that from *E. coli*. To date, biotin synthase from *Bacillus sphaericus* (42), *Arabidopsis thaliana* (43), *Saccharomyces cerevisiae* (44), and *E. coli* (20) have been cloned, overexpressed, and purified. Sufficient complementation analysis has been carried out on *Methylobacillus, Bacillus flavum* (45), *Bacillus subtilis* (46), *Erwinia herbicola* (47), and *Serratia marcescens* (48) to confirm that they also express active biotin synthases. Sequence alignment reveals a number of conserved regions (Fig. 4). There are 25 completely conserved residues, four of which are cysteine. Three of these (Cys-53, Cys-57, and Cys-60) lie in the 15-residue cysteine box motif (K(S/T)GXCXE(D/N)CX(Y/F)CXQS), and the fourth (Cys-188 in the *E. coli* sequence) is remote.

FIG. 4. **Sequence alignment of 17 known biotin synthases.** The conserved residues are *boxed* in *gray* and the two extended conserved motifs *outlined* in *black*. The *black arrows* show the residues mutated in this study, and the residue numbering is that of the *E. coli* sequence. (The Swiss-Prot accession numbers from the top are P12996, O67104, P54967, P19206, P53557, P46396, Q9Z6L5, Q47862, P44987, O25956, P94966, P46715, O06601, P32451, O60050, P36569, and P73538). The sequence alignment was carried out using Expasy and ClustalW, and the data were formatted using Alscript.

To determine which of the cysteine residues are involved in stabilizing the [2Fe-2S] and [4Fe-4S] forms of biotin synthase, single point mutations were made of all five cysteine residues (Cys-53, Cys-57, Cys-60, Cys-188, and Cys-288) to either serine or threonine. The choice of cysteine substitution by hydroxylated residues was made to preserve as much as possible the H-bonding character and the side chain geometry of the original cysteine residues. All the mutant proteins were expressed as His_6 tag fusions and purified using IMAC. The molecular weights of all the polypeptides were verified by mass spectrometry (Table I), and the purified proteins were characterized by UV-visible spectrophotometry (Fig. 2), nickel, iron, and sulfur analyses (Tables II and III), and *in vivo* and *in vitro* assays for biotin production (Tables IV and V).

Native biotin synthase, His_6-tagged biotin synthase, and the His_6-tagged non-conserved mutant C288T all had similar UV-visible spectrophotometric characteristics that were indicative of intact [2Fe-2S] cluster formation. All of these proteins, along with their apo-proteins and reconstituted holo-proteins, were active both *in vitro* (Table IV) and *in vivo* (Table V). In contrast, C53S, C57S, and C60S were all colorless, and their absorption spectra showed no indication of the presence of [2Fe-2S] clusters (Fig. 2) indicating that these residues are absolutely vital for [Fe-S] cluster formation which is in turn crucial for activity. C188S proved to be insoluble and could only be characterized *in vivo*. The fact that only three cysteine residues appear to be needed for [2Fe-2S] cluster binding (22) and that the C53S, C57S, and C60S mutants are inactive suggest that Cys-188 may be required for correct folding of the protein. Attempts to induce [Fe-S] cluster formation by incubation of these mutants with excess reagents did not result in any significant increase of iron binding.

The only cysteine mutant of *E. coli* biotin synthase that was catalytically active and could support formation of a [2Fe-2S] cluster was C288S, the mutant of the non-conserved cysteine residue, showing that the presence of C288 is not essential for folding, [2Fe-2S] and [4Fe-4S] cluster formation, or for activity. In contrast, all the conserved residues Cys-53, Cys-57, and Cys-60 of the cysteine box are proven to be absolutely crucial for both the formation of the [2Fe-2S] cluster and the activity of the enzyme. These results are consistent with recent mutational studies on PFL-AE where it was also found that mutations of cysteine residues in the cysteine box abolish metal binding (41).

In the absence of crystallographic evidence, this work is a step toward the definition of the essential protein residues involved in the mechanism of [Fe-S] cluster formation in biotin synthase and the relevance of these to the catalytic action of the enzyme. The inference of spectroscopic studies on *E. coli* biotin synthase is that a hydroxylated residue is also involved in the initial [2Fe-2S] cluster formation (22) and here the conserved cysteine box residues Thr-50 and Ser-63 are obvious candidates. Another region in the protein that is completely conserved is the sequence Tyr-150, Asn-151, His-152, Asn-153, and Leu-154 which is also found in lipoic acid synthase (13) (see Fig. 4). Biotin synthase mutants at sites within these sequences are the subject of current studies. We have recently described the overexpression, purification, and redox characteristics of the flavoprotein components of the *E. coli* biotin synthase system, FLD, and FLDR (49) and the fact that it is now possible to obtain relatively large quantities of these, and functional, homogeneous *Bio*B protein should facilitate exam-

ination of the protein-protein and protein-cofactor interactions involved in the redox chemistry of the biotin synthase complex.

Acknowledgments—We thank Dr. S. P. Webster and Dr. L. Jiang for mass spectrometry; N. Preston for DNA sequencing; and Dr. M. Fuhrmann (Lonza AG) for pB030.

Addendum—Since the acceptance of this manuscript Hewitson *et al.* (Hewitson, K. S., Baldwin, J. E., Shaw, N. M., and Roach, P. L. (2000) *FEBS Lett.* **466,** 372–376) have published the results of a similar study on *E. coli* biotin synthase. They describe the characterization of three biotin synthase mutant enzymes C53A, C57A, and C60A. All three mutant enzymes were inactive in *in vitro* dethiobiotin to biotin conversion assays but are reported to exhibit the characteristic UV-visible spectrum of a $[2Fe\text{-}2S]^{2+}$ cluster, in contrast to the C53S, C57S, and C60S mutants described here. The exact nature of these differences awaits further structural investigation and highlights the complexity of the biotin synthase system.

REFERENCES

1. Otsuka, A., Buonocristiani, M. R., Howard, P. K., Flamm, J., Johnson, C., Yamomoto, R., Uchida, K., Cook, C., Ruppert, J., and Matzuki, J. (1988) *J. Biol. Chem.* **263,** 19577–195785
2. Alexeev, D., Alexeeva, M., Baxter, R. L., Campopiano, D. J., Webster, S. P., and Sawyer, L. (1998) *J. Mol. Biol.* **284,** 401–419
3. Kack, H., Sandmark, J., Gibson, K., Schneider, G., and Lindqvist, Y. (1999) *J. Mol. Biol.* **291,** 857–876
4. Alexeev, D., Bury, S. M., Boys, C. W. G., Sawyer, L., Ramsey, A. J., Baxter, H. C., and Baxter, R. L. (1994) *J. Mol. Biol.* **235,** 774–776
5. Sanyal, I., Gibson, K. J., and Flint, D. H. (1996) *Arch. Biochem. Biophys.* **326,** 48–56
6. Ifuku, O., Koga, N., Haze, S., Kishimoto, J., and Wachi, Y. (1994) *Eur. J. Biochem.* **224,** 173–178
7. Birch, O. M., Fuhrmann, M., and Shaw, N. M. (1995) *J. Biol. Chem.* **270,** 19158–19165
8. Méjean, A., Tse Sum Bui, B., Florentin, D., Ploux, O., Izumi, Y., and Marquet, A. (1995) *Biochem. Biophys. Res. Commun.* **217,** 1231–1237
9. Baxter, R. L., Camp, D. J., Cotts, A., and Shaw, N. (1992) *J. Chem. Soc. Perkin Trans.* **1,** 255–258
10. Marti, F. B. (1983) *Zur biosynthese von biotin: Einsatz von Vorlaufern mit chiraler Methylgruppe.* Ph.D. thesis, Edigenossischem Technischen Hochschule, Zurich
11. Parry, R. J. (1980) *Tetrahedron Lett.* **21,** 4783–4786
12. Guianvarc'h, D., Florentin, D., Tse Sum Bui, B., Nunzi, F., and Marquet, A. (1997) *Biochem. Biophys. Res. Commun.* **236,** 402–406
13. Marquet, A., Florentin, D., Ploux, O., and Tse Sum Bui, B. (1998) *J. Phys. Org. Chem.* **11,** 529–535
14. Tse Sum Bui, B., Florentin, D., Fournier, F., Ploux, O., Méjean, A., and Marquet, A. (1998) *FEBS Lett.* **440,** 226–230
15. Zheng, L., White, R. H., Cash, V., and Dean, D. (1994) *Biochemistry* **33,** 4714–4720
16. Mulliez, E., Fontecave, M., Gaillard, J., and Reichard, P. (1993) *J. Biol. Chem.* **268,** 2296–2299
17. Broderick, J. B., Duderstadt, R. E., Fernandez, D. C., Wojtuszewski, K., Henshaw, T. F., and Johnson, M. K. (1997) *J. Am. Chem. Soc.* **119,** 7396–7397
18. Leider, K. W., Booker, S., Ruzicka, F. J., Beinert, H., Reed, G. H., and Frey, P. A. (1998) *Biochemistry* **37,** 2578–2585
19. Ollangier-de Choudons, S., and Fontecave, M. (1999) *FEBS Lett.* **453,** 25–28
20. Sanyal, I., Cohen, G., and Flint, D. H. (1994) *Biochemistry* **33,** 3625–3631
21. Duin, E. C., Lafferty, M. E., Crouse, B. R., Allen, R. M., Sanyal, I., Flint, D. H., and Johnson, M. K. (1997) *Biochemistry* **36,** 11811–11820
22. Johnson, M. K., Staples, C. R., Duin, E. C., Lafferty, M. E., and Duderstadt, R. E. (1998) *Pure Appl. Chem.* **70,** 939–946
23. Begley, T., Xi, J., Kinsland, C., Taylor, S., and McLafferty, F. (1999) *Curr. Opin. Chem. Biol.* **3,** 623–629
24. DeMoll, E., and Shive, W. (1986) *Anal. Biochem.* **158,** 55–58
25. Sarker, G., and Sommers, S. S. (1990) *BioTechniques* **8,** 404–407
26. Bradford, M. M. (1976) *Anal. Biochem.* **72,** 248–254
27. Barton, G. J. (1993) *Protein Eng.* **6,** 37–40
28. Harris, D. C. (1948) *Quantitative Chemical Analysis,* pp. 513–532, W. H. Freeman & Co., New York
29. Stookey, L. L. (1970) *Anal. Chem.* **42,** 779–781
30. Tse Sum Bui, B., and Marquet, A. (1997) *Methods Enzymol.* **279,** 356–362
31. Busby, R. W., Schelvis, J. P. M., Yu, D. S., Babcock, G. T., and Marletta, M. A. (1999) *J. Am. Chem. Soc.* **121,** 4706–4707
32. Ollangier, S., Meier, C., Mulliez, E., Gaillard, J., Schuenemann, V., Trautwein, A., Mattioloi, T., Lutz, M., and Fontecave, M. (1999) *J. Am Chem. Soc.* **121,** 6344–6350
33. Frey, P. A., and Reed, G. H. (1993) *Adv. Enzymol. Relat. Areas Mol. Biol.* **66,** 1–39
34. Joerger, R. D., and Bishop, P. E. (1988) *J. Bacteriol.* **170,** 1475–1487
35. Liu, S. T., Lee, L. Y., Tai, C. Y., Hung, C. H., Chang, Y. S., Wolfram, J. H., Rogers, R., and Goldstein, A. H. (1992) *J. Bacteriol.* **174,** 5814–5819
36. Glaser, P., Danchin, A., Kunst, F., Zuber, P., and Nakano, M. (1995) *J. Bacteriol.* **177,** 1112–1115
37. Shaw, D. J., and Guest, J. R. (1982) *Nucleic Acids Res.* **10,** 6119–6130
38. Leuthner, B., Leutwein, C., Schulz, H., Horth, P., Haehnel, W., Sclitz, E., Schagger, H., and Heider, J. (1998) *Mol. Microbiol.* **28,** 615–628
39. Fajardo-Cavazos, P., Salazar, C., and Nicholson, W. L. (1993) *J. Bacteriol.* **175,** 1735–1744
40. Smith, D. R., Doucette-Stamm, L. A., Deloughery, C., Lee, H. M., Dubois, J., Aldredge, T., Bashirzadeh, R., Blakely, D., Cook, R., Gilbert, K., Harrison, D., Hoang, L., Keagle, P., Lumm, W., Pothier, B., Qui, D., Spadafora, R., Vicare, R., Wang, Y., Weizerbowski, J., Gibson, R., Jiwani, N., Caruso, A., Bush, D., Safer, H., Patwell, D., Prabhakar, S., McDougall, S., Shimer, G., Goyal, A., Pietrovski, S., Church, G. M., Daniels, C. J., Mao, J. I., Rice, P., Nolling, J., and Reeve, J. N. (1997) *J. Bacteriol.* **179,** 7135–7155
41. Kulzer, R., Pils, T., Kappl, R., Huttermann, J., and Knappe, J. (1998) *J. Biol. Chem.* **273,** 4897–4903
42. Florentin, D., Bui, B., Marquet, A., Ohshiro, T., and Izumi, Y. (1994) *C. R. Acad. Sci.* **317,** 485–488
43. Baldet, P., Alaban, C., and Douce, R. (1997) *FEBS Lett.* **419,** 206–210
44. Flint, D. H., and Allen, R. M. (1997) *Methods Enzymol.* **279,** 349–356
45. Serebriiskii, I. G., Vassin, V. M., and Tsygankov, Y. D. (1996) *Gene (Amst.)* **175,** 15–22
46. Bower, S., Perkins, J. B., Rogers, Y., R, Howitt, C. L., Raiham, P., and Pero, J. (1996) *J. Bacteriol.* **178,** 4122–4130
47. Wu, C. H., Chen, H. Y., and Shiuan, D. (1996) *Gene (Amst.)* **174,** 251–258
48. Sakurai, N., Imai, Y., Masuda, M., Komatsubara, S., and Tosa, T. (1993) *Appl. Environ. Microbiol.* **59,** 2857–2863
49. McIver, L., Leadbeater, C., Campopiano, D. J., Baxter, R. L., Daff, S. N., Chapman, S. K., and Munro, A. W. (1998) *Eur. J. Biochem.* **257,** 577–585

Appendix III

Conferences and Courses Attended

1995

Radiation Protection Course

First Aid Course

Departmental Postgraduate Lectures (1995)

24th Royal Society of Chemistry - Perkin Division (Glasgow 18.12.95)

1996

Departmental Postgraduate Lectures (1996)

Perkin Symposium (26.03.96)

Structures - form and function (12.03.96)

Promega Conference (12.06.96)

European Peptide Symposium (8 - 13.09.96)

Romanes Lecture

Walker Memorial Lecture

Ames Symposium

25th Royal Society of Chemistry - Perkin Division (Edinburgh 12.96)

1997

Departmental Postgraduate Lectures (1997)

Oxidases (25.03.97)

Firbush (04.06.06.97)

17th International Congress of Biochemistry and Molecular Biology including American Society for Biochemistry and Molecular Biology

(San Francisco 24-29.08.97) Poster presented

26th Royal Society of Chemistry - Perkin Division (Strathclyde 12.97)

Walker Memorial Lecture

Ames Symposium

SET Mentoring Programme

Scottish Protein Structure Group Meeting (Edinburgh 15.11.97)

1998

Departmental Postgraduate Lectures (1998) Oral presentation given (27.04.98)

Biochemistry Meeting (Southampton 31.03.98 - 03.04.98) Poster presented

Bio-inorganic Firbush Meeting (10-12.06.98) Oral presentation given

Walker Memorial Lecture (John- Marie Lehn)

Presentation skills workshop

Presenting a positive image

Thesis writing workshop

Biochemistry Society Meeting (Leicester 21- 23.09.98)

27th Royal Society of Chemistry - Perkin Division (St. Andrews 12.98) Poster presented

1999

Departmental Postgraduate Lectures (1999)

Scottish Protein Meeting (Glasgow 13.3.99)

13th International Flavins Conference (Constance 28.8 –4.9.99) Poster presented

RSC Bio-Organic Meeting (Oxford 16-18.12.99) Oral presentation given. Prize received for Best Oral Presentation

2000

Scottish Protein Meeting (Dundee 26.02.00) Oral presentation given